

# **OPTIMAL LOCATION AND SIZING OF FACTS DEVICES FOR REACTIVE POWER COMPENSATION IN A MULTI-BUS POWER SYSTEM**

*The Thesis is Submitted in Partial Fulfillment of the Requirements  
for the Degree of*

**MASTER OF ENGINEERING  
IN  
ELECTRICAL ENGINEERING**

**JADAVPUR UNIVERSITY**

*Submitted By*

**NIMA SANGAY SHERPA**

Roll No.: 002010802025

Examination Roll No.: M4ELE22025B

Registration No.: 154015 of 2020-21

*Under the Supervision of*  
**Madhumita Mandal**  
Assistant Professor

**DEPARTMENT OF ELECTRICAL ENGINEERING  
FACULTY OF ENGINEERING & TECHNOLOGY  
JADAVPUR UNIVERSITY  
Kolkata-700032  
2020-2022**

# **CERTIFICATE**

This is to certify that this thesis entitled “**Optimal Location and Sizing of FACTS devices for Reactive Power Compensation for Multi-Bus Power System**” which is submitted by **Nima Sangay Sherpa** (Registration No. 154015 of 2020-2021, Examination Roll No. **M4ELE22025B**), in partial fulfillment of the requirement for the degree of Master of Engineering in Electrical Engineering, offered by Department of Electrical Engineering of Jadavpur University, Kolkata-700032 during the academic year 2020-2022, is the record of the student’s own work carried by him under the supervision of Madhumita Mandal.

---

**Madhumita Mandal**  
Assistant Professor  
Electrical Engineering Department  
Jadavpur University

## **COUNTERSIGNED**

---

**Prof. (Dr.) Saswati Mazumdar**  
Head of the Department  
Electrical Engineering Department  
Jadavpur University

---

**Prof.(Dr) Bhaskar Gupta**  
Dean of Faculty of Engineering  
and Technology  
Jadavpur University

# **CERTIFICATE OF APPROVAL**

The foregoing thesis is hereby approved as a creditable study of an engineering subject and presented in a manner satisfactory to warrant acceptance as pre-requisite to the degree for which it has been submitted. It is understood that by this approval the undersigned do not necessarily endorse or approve any statement made, opinion expressed or conclusion drawn there in but approve the thesis for which it is submitted.

Committee on Final Examination for Evaluation of Thesis

-----

-----

-----

-----

*(Signature of the Examiners)*

# DECLARATION

I certify that

1. The work contained in the thesis is original and has been done by myself under the general supervision of my supervisor(s).
2. The work has not been submitted to any other institute for any degree or diploma.
3. I have followed the guidelines provided by the institute in writing the thesis.
4. I have conformed to the norms and guidelines given in the Ethical Code of Conduct of the Institute and University.
5. Whenever I have used materials (data, theoretical analysis, and text) from other sources, I have given due credit to them by citing them in the text of the thesis and giving their details in the references.
6. Whenever I have quoted written materials from other sources, I have put them under quotation marks and given due credit to the sources by citing them and giving required details in the references.

Name : **Nima Sangay Sherpa**

Examination Roll No. : **M4ELE22025B**

Signature :

Date :

Place :

# ACKNOWLEDGEMENT

I take this opportunity to express my profound gratitude and deep regards to my supervisor, **Madhumita Mandal**, for their exemplary guidance, monitoring and constant encouragement throughout the course of this thesis. The blessing, help and guidance given by them time to time will carry me a long way in the journey of life on which I am about to embark.

I am indebted to Prof.(Dr) Saswati Majumdar ,Head ,Department of Electrical Engineering, Jadavpur University, for her kind help and co-operation extended during this thesis work. I am also thankful to Prof. (Dr.)Bhaskar Gupta ,Dean of Faculty of Engineering and Technology for his kind help and co-operation during this thesis work.

Also special thanks to Nibir Baran Roy, Romio Atha and Bibudh Mitra and all my friends for their ideas and moral support during the course of study.

I would like to express my heartiest appreciation to my parents, sisters and brothers and all my family members for their love and active support and encouragement throughout the endeavor.

Date:

Electrical Engineering Department  
Jadavpur University  
Kolkata-700032

---

Nima Sangay Sherpa

Dated:

# ABSTRACT

Globally, the electrical supply industry is undergoing a profound transition. Among the factors responsible for such a radical shift are market pressures, the scarcity of natural resources, and the rising need for high-quality energy delivery. The phrase "quality of delivery" refers to the capacity of the several parts, namely generation, transmission, and distribution, to supply the good (electric power) to any point of consumption in the quantity and quality demanded by the customer. In the hierarchy of electric power systems, it is recognized that well-designed power stations provide quality electricity since the system voltages are almost sinusoidal. Power system operators' primary objectives include preventing voltage breakdown and ensuring the stability of the power system. Flexible AC transmission systems (FACTS) are cutting-edge technologies that can increase power system stability, improve voltage profile, and raise real power transfer by controlling various power system parameters like impedance, voltage, and angle.

Nevertheless, to maximize benefits and effectively control power flow, FACTS must be allocated and sized in the power system network. The implementation of series and shunt compensation devices, such as "Thyristor controlled series Capacitor (TCSC), Static VAR Compensator (SVC), and Static synchronous compensator (STATCOM)", as well as the impact of equality and inequality constraints, are discussed in this research work. Discrete –Continuous Particle Swarm Optimization (PSO) and Squirrel Search Algorithm (SSA) are used in this work to provide the best possible strategic allocation and sizing of FACTS Devices. Suggested approach has been tested on the IEEE-30 bus system. Real power losses and reactive power losses have significantly decreased as a result.

# **TABLE OF CONTENT**

|  |       |
|--|-------|
| Title Sheet .....                                      | (i)   |
| Certificate.....                                       | (ii)  |
| Certificate of Approval .....                          | (iii) |
| Declaration .....                                      | (iv)  |
| Acknowledgement .....                                  | (v)   |
| Abstract.....  | (vi)  |
| Table of Content .....                                 | (vii) |
| List of Tables .....                                   | (ix)  |
| List of Figures .....                                  | (xii) |
| List of Abbreviations .....                            | (xiv) |
| List of Symbols .....                                  | (xv)  |
| CHAPTER 1 .....  | 1     |
| 1.1 BACKGROUND .....                                   | 1     |
| 1.2 FACTS APPLICATION TO PQ PROBLEM.....               | 3     |
| 1.3 SERIES COMPENSATION .....                          | 5     |
| 1.4 SHUNT COMPENSATION.....                            | 6     |
| 1.5 PROBLEMS ASSOCIATED WITH SERIES COMPENSATION ..... | 7     |
| 1.6 FACTS CONTROLLERS FOR POWER SYSTEM .....           | 7     |
| 1.7 SERIES CONNECTED CONTROLLERS.....                  | 8     |
| 1.7.1 TCSC.....  | 8     |
| 1.8 SHUNT CONNECTED CONTROLLERS.....                   | 9     |
| 1.8.1 STATIC SYNCHRONOUS COMPENSATORS.....             | 9     |
| 1.8.2 STATIC VAR COMPENSATOR.....                      | 10    |
| 1.9 OBJECTIVE OF THE RESEARCH.....                     | 10    |
| 1.10 THESIS ORGANIZATION.....                          | 11    |
| 1.11 SUMMARY .....                                     | 11    |
| CHAPTER 2 .....  | 12    |
| 2.1 INTRODUCTION .....                                 | 12    |
| 2.2 POWER SYSTEM SECURITY ENHANCEMENT .....            | 12    |
| 2.4 POWER SYSTEM LOADABILITY IMPROVEMENT.....          | 17    |
| 2.5 SUMMARY .....                                      | 27    |
| CHAPTER 3 .....  | 27    |
| 3.1 OBJECTIVE .....                                    | 29    |
| 3.2 INTRODUCTION .....                                 | 29    |

|  |           |
|--|-----------|
| 3.3 OPTIMAL POWER FLOW .....                 | 32        |
| 3.3.1 Objective functions .....              | 32        |
| 3.4.1 Modeling of TCSC .....                 | 35        |
| 3.4 .1STATIC VAR COMPENSATOR .....           | 36        |
| 3.4.1 SVC Equivalent Susceptance Model ..... | 36        |
| 3.4.2 Modeling of SVC .....                  | 37        |
| 3.4.3 Modelling of STATCOM.....              | 38        |
| <b>3.5 FACTS Optimal Allocation .....</b>    | <b>39</b> |
| 3.6 Particle swarm optimization.....         | 39        |
| 3.7 SQUIRREL SEARCH ALGORITHM .....          | 41        |
| 3.8 SUMMARY .....                            | 47        |
| CHAPTER 4 .....                              | 48        |
| 4.1 SIMULATION RESULT .....                  | 48        |
| 4.2 EXPERIMENTAL ANALYSIS .....              | 49        |
| 4.3 SUMMARY .....                            | 83        |
| CHAPTER 5 .....                              | 84        |
| 5.1 CONCLUSION.....                          | 84        |
| 5.2 FUTURE WORK.....                         | 85        |
| Reference .....                              | 86        |
| Appendix.....                                | A         |



## **LIST OF TABLES**

| <b>TABLE NO.</b> | <b>TITLE</b>   | <b>PAGE NO.</b> |
|------------------|--|-----------------|
| .                | .  | .               |
| 4.1              | Load flow results of IEEE30bus system without FACTS devices(Voltage magnitude and phase angle) | 49              |
| 4.2              | Load flow results of IEEE30bus system without FACTS devices                                    | 50              |
| 4.3              | Line losses without FACTS devices  | 51              |
| 4.4              | Voltage magnitude and phase angle after placement STATCOM                                      | 52              |
| 4.5              | PSO STATCOM CASE 1   | 52              |
| 4.6              | Line lossess after placement of STATCOM CASE1  | 53              |
| 4.7              | PSO STATCOM CASE2  | 55              |
| 4.8              | Line lossess after placement of STATCOM CASE2  | 56              |
| 4.9              | Voltage magnitude and phase angle after placement TCSC   | 57              |
| 4.10             | PSO TCSC CASE 1  | 58              |
| 4.11             | Line lossess after placement of TCSC CASE1   | 60              |
| <b>4.11.1</b>    | <b>PSO TCSC CASE 2</b>   | <b>60</b>       |
| <b>4.11.2</b>    | <b>Line lossess after placement of TCSC CASE2</b>  | <b>61</b>       |
| 4.12             | Voltage magnitude and phase angle after placement SVC  | 62              |

|  |    |
|--|----|
| 4.13 PSO SVC CASE 1  | 63 |
| 4.14 Line lossess after placement of SVC CASE1                           | 64 |
| 4.15 PSO CASE 2  | 65 |
| 4.16 Line lossess after placement of SVC CASE2                           | 66 |
| 4.17 Voltage magnitude and phase angle after placement STATCOM SSA CASE  | 68 |
| 4.18 SSA STATCOM CASE1   | 68 |
| 4.19 Line lossess after placement STATCOM SSA CASE1                      | 69 |
| 4.20 SSA STATCOM CASE2   | 70 |
| 4.21 Line lossess after placement STATCOM SSA CASE2                      | 71 |
| 4.22 Voltage magnitude and phase angle after placement TCSC              | 72 |
| 4.23 SSA TCSC CASE 1   | 73 |
| 4.24 Line lossess after placement TCSC SSA CASE1                         | 74 |
| 4.25 SSA TCSC CASE 2   | 75 |
| 4.26 Line lossess after placement TCSC SSACASE 2                         | 76 |
| 4.27 Voltage magnitude and phase angle after placement SVC SSA CASE      | 77 |
| 4.28 SSA SVC CASE1   | 78 |
| 4.29 Line lossess after placement SVC SSA CASE1                          | 79 |
| 4.30 SSA SVC CASE 2  | 80 |
| 4.31 Line lossess after placement SVC SSACASE 2                          | 81 |
| 4.32 Comparisons for results obtained from both algorithms for SATATCOM  | 82 |
| 4.33 Comparisons for results obtained from both algorithms for TCSC CASE | 83 |
| 4.34 Comparisons for results obtained from both algorithms for SVC CASE  | 84 |

## **LIST OF FIGURES**

| <b>FIGURE NO.</b> | <b>TITLE</b>   | <b>PAGE NO.</b> |
|-------------------|--|-----------------|
| 1.1               | Power quality disturbance in power system                | 2               |
| 1.2               | Types of FACTS devices                                   | 4               |
| 2.1               | Overview of Major FACTS-Based Devices                    | 13              |
| 2.2               | SVC building blocks and voltage / current characteristic | 14              |
| 2.3               | Principle setup of a TCSC                                | 16              |
| 2.4               | Principle configuration of a UPFC                        | 18              |
| 3.1               | General classification of FACTS                          | 31              |
| 3.2               | Configuration of a TCSC                                  | 35              |
| 3.3               | Equivalent TCSC structure                                | 35              |
| 3.4               | Voltage- Current Characteristics of SVC                  | 37              |
| 3.5               | Similar circuit for STATCOM                              | 38              |
| 3.6               | Flowchart of PSO algorithm                               | 41              |
| 3.7               | Flying squirrel landing on a tree                        | 42              |
| 3.8               | Standard squirrel search algorithm's process             | 42              |
| 4.1               | Convergence curve of PSO STATCOM case1                   | 53              |
| 4.2               | Convergence Curve of PSO STATCOM case 2                  | 55              |
| 4.3               | Convergence Curve Of PSO TCSC case1                      | 58              |
| 4.4               | Convergence curve of PSO TCSC case 2                     | 60              |
| 4.5               | Convergence curve of PSO SVCcase 1                       | 63              |
| 4.6               | Convergence curve of PSO SVC case 2                      | 65              |
| 4.7               | Convergence curve of STATCOM SSA case 1                  | 67              |

|      |  |    |
|------|--|----|
| 4.8  | Convergence curve of STATCOM SSA case2 | 68 |
| 4.9  | Convergence curve of STATCOM SSA case2 | 70 |
| 4.10 | Convergence curve of TCSC SSA case1    | 73 |
| 4.11 | Convergence curve of TCSC SSA case2    | 75 |
| 4.12 | Convergence curve of SVC SSA case1     | 78 |
| 4.13 | Convergence curve of SVC SSA case2     | 80 |

## **LIST OF ABBREVIATIONS**

|         |   |  |
|---------|---|--|
| TCSC    | - | Thyristor Controlled Series Capacitors   |
| STATCOM | - | Static Synchronous Compensator           |
| SVS     | - | Static Var System                        |
| FACTS   | - | Flexible AC Transmission Systems         |
| PSO     | - | Particle Swarm Optimization              |
| SSA     | - | Squirrel Search Algorithm                |
| PQ      | - | Power Quality                            |
| EHV     | - | Extra High Voltage                       |
| UPFC    | - | Unified Power Flow Controllers           |
| SSSC    | - | Static Synchronous Series Comparator     |
| IPFC    | - | Inter Line Power Flow Controller         |
| TSSC    | - | Thyristor Switched Series Capacitor      |
| TCSR    | - | Thyristor Controlled Series Reactor      |
| TSSR    | - | Thyristor Switched Series Reactor        |
| SSG     | - | Static Synchronous Generator             |
| BESS    | - | Battery Energy Storage System            |
| SMES    | - | Super Conducting Magnetic Energy Storage |
| TCR     | - | Thyristor Controlled Reactor             |
| TSR     | - | Thyristor Switched Reactor               |
| TSC     | - | Thyristor Switched Capacitor             |
| TCBR    | - | Thyristor Controlled Braking Resistor    |
| GA      | - | Genetic Algorithm                        |
| SSA     | - | Salp Swarm Algorithm                     |
| SSR     | - | Sub-Synchronous Resonance                |

|       |   |   |
|-------|---|---|
| ATC   | - | Available Transfer Capability           |
| CSC   | - | Controlled Series Capacitor             |
| SVC   | - | Switched Variable Capacitor             |
| IPFC  | - | Interline Power Flow Controller         |
| FPA   | - | Flower Pollination Method               |
| PLI   | - | Power Loss Index                        |
| PGSA  | - | Plant Growth Simulation Algorithm       |
| DSA   | - | Direct Search Algorithm                 |
| TLBO  | - | Teaching Learning-Based Optimization    |
| CSA   | - | Cuckoo Search Algorithm                 |
| ABC   | - | Artificial Bee Colony                   |
| OPF   | - | Optimal Power Flow                      |
| IDE   | - | Improved Differential Evolution         |
| MOOPF | - | Multiobjective Optimum Power Flow       |
| ICA   | - | Imperialist Competitive Algorithm       |
| DE    | - | Differential Evolution                  |
| CoDE  | - | Composite Differential Evolution        |
| CSA   | - | Cuckoo Search Algorithm                 |
| SLUF  | - | Subtracting The Line Utilization Factor |
| LDC   | - | Load Duration Curve                     |
| SQP   | - | Sequential Quadratic Programming        |
| FA    | - | Firefly Algorithm                       |
| KSA   | - | Kingdom Of Saudi Arabia                 |
| ABC   | - | Artificial Bees Colony                  |
| DLUF  | - | Disparity Line Usage Factor             |
| MVA   | - | Mega Voltage Ampere                     |
| AHP   | - | Analytical Hierarchy Process            |
| IGSA  | - | Improved Gravitational Search Algorithm |

|      |   |                                     |
|------|---|-------------------------------------|
| ORPD | - | Optimal Receptive Power Dispatch    |
| APC  | - | Active Power Conditioner            |
| IDFA | - | Improved Discrete Firefly Algorithm |
| NR   | - | Newton-Raphson                      |
| SBX  | - | Simulated Binary Crossover          |
| FVSI | - | Fast Voltage Stability Index        |
| VCPI | - | Voltage Collapse Proximity Index    |
| SSR  | - | Sub Synchronous Resonance           |
| PMU  | - | Phasor Measurement Unit             |

## LIST OF SYMBOLS

|                          |   |   |
|--------------------------|---|---|
| $\theta$ and $\emptyset$ | - | transmitting and receiving end bus angles |
| $\beta$ and $\alpha$     | - | constant with the value 1.5               |

# **CHAPTER 1**

## **INTRODUCTION**

### **1.1 BACKGROUND**

Electric power networks have seen a constant rise in power consumption over the last 20 years without a corresponding growth of the transmission and generating capabilities. Due to this disparity, systems are now more susceptible to voltage disturbances, and instabilities have been seen in power networks all around the globe. Due to the constant increase in demand for electric power, most of which must be carried across vast distances, global transmission networks are constantly changing. Power Quality (PQ) requires a high level of engineering expertise in the decrease of power system load losses and proficiency improvement. Due to the ease of culture and the complexity of control systems, PQ difficulties have emerged as one of the most pressing challenges for power electronic engineers. Therefore, PQ is becoming prevalent and critical importance for power industry. The most crucial intention of electric utility companies is to offer their customers with incessant sinusoidal voltage of firm magnitude. It has been planned out what impact induction generators will have on the PQ characteristics of the grid, namely “voltage, frequency, power factor, harmonics, and reactive power”. Customers are impacted by any PQ issues with voltage, current, or frequency aberrations. PQ concerns have drawn considerable attention from utilities and consumers as a consequence of the use of many types of legally acceptable electronic devices. The most important PQ discrepancies are often caused by “short circuits, harmonic distortions, notching, flickers, voltage sags, voltage swells, and transients related to load switching”. Figure 1.1 depicts the power quality disturbance in power system.

The investigation of voltage stability has gained significance as a result of several recorded instances of voltage collapse in France, Japan, and other countries. Voltage collapse is caused by a number of circumstances, including a rise in transmission line load, a restriction on reactive power, a transformer with an on-load tap change feature, and dynamic load characteristics. The power transmission capability of an “EHV (Extra High Voltage)” line is determined by Conductor thermal limit, steady state and transient stability limit [1].

The conductor's thermal limit is often far before the stability limit is achieved for long distance transmission lines. Therefore, by raising the stability



limit up to the extent of the conductor's thermal limit, the capacity of a transmission line to transmit power may be improved. The majority of approaches is excessively costly and only slightly raises the stability limit. The most appealing thrust areas of study are the series and shunt compensation approaches. Reactors, capacitors, and thyristors are employed in parallel in Static VAR Systems (SVS) to regulate the production of reactive power. In reaction to shifting system circumstances, an SVS has the capacity to quickly and continuously change the reactive power output. As a result, they are often used to control reactive power in order to stabilize the system voltage.

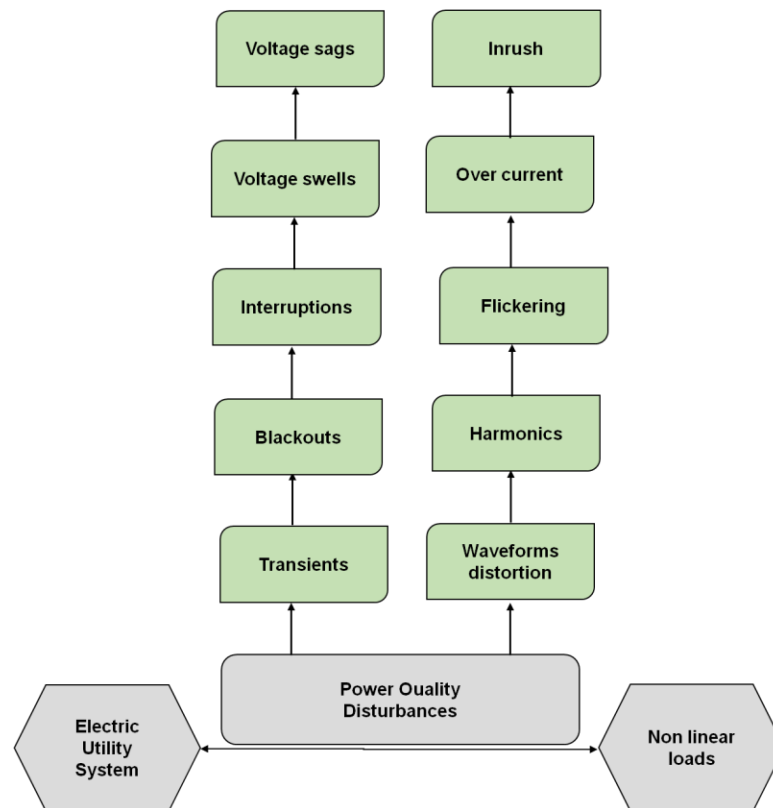


**Figure 1.1 Power Quality Disturbances in Power System**

Series Compensation, on the other hand, is often employed in extra high voltage transmission lines to account for the series inductive reactance. Recently series compensations are being used in the distribution network. Moreover, these are also proposed to be used in are furnace feeding network for increased industrial production. Series compensations offer the best and most economical solution to voltage fluctuations at welding machine terminal [2].

Furthermore, the existing atmosphere makes it more difficult to operate electricity systems. The causes of this are deregulation issues, which demand open access power delivery within and between regions, facilitate interconnected competitive generation, offer limited to no market-based rewards for transmission investment, and elevate issues related to dependability, protection, and consistency. The "open access" rule, which requires services to accept the producing load sources at any position in the present transmission network in order to promote competition, was carried about by deregulation. The transmission owners are faced with a difficulty as a result of this "open access" structure: they must continuously maintain system security while attempting to reduce expensive power flow congestion in transmission corridors. Cost-effective solutions must be taken into account for voltage security or congestion issues throughout the design and analysis phase.

Traditional approaches to the problem of congestion voltage security included constructing better, expensive transmission lines that frequently run into resistance from the public or employing mechanically switched capacitor banks, which had few advantages for dynamic performance due to the switching time frequency. With the objective of creating new tools or technologies to manage the flow of power and enable more effective use of current power generating and transmission power plants, these developments have generated significant research interest in "Flexible AC transmission Systems (FACTS)".

## **1.2 FACTS APPLICATION TO PQ PROBLEM**

FACTS are designed to overcome the current restrictions in mechanically regulated AC power transmission systems. It is comparable to high voltage DC and associated thyristor advances. Due of their low cost and higher impact on power supplies, these gadgets are receiving greater attention. The cost effectiveness of these devices results from the massive development of high power electronic circuits. Power flow management is encouraged by the deregulation of the power business and the rising strain on electricity networks to transport power at a lower cost. Due to problems in the competitive power market, such as congestion management, increased security, the system's current transfer capabilities, and transmission price, the free and fair exchange of energy is significantly constrained. Further, the cost of these devices also demands the determination of the location where the device has to be placed. FACTS devices employ the same strategies and concepts that are used to face the power quality issues but they differ only in their objectives and location of placement. FACTS form a new field in power system control engineering that

makes use of power electronic devices and they are the latest technology that is available in automatic control. The two important aims of FACTS are as follows:

- To enhance the transmission capacity of lines.
- To electronically and statically manage the flow of power over the selected transmissions without requiring any kind of operator's action, mechanical treatment and the conventional breakers switching.

Numerous power system steady state control issues, including “voltage regulation, power flow management, and transfer capability enhancement”, have found answers thanks to the widespread usage of FACTS devices. Using power electronics in transmission systems, FACTS technology effectively reduces voltage sag in power networks by managing and regulating electric variables including current, voltage, and impedance. Power electronic equipment that operates at different voltage levels is now extensively employed thanks to the swift growth of the field.

FACTS have shown to be an economical, eco-friendly solution for a variety of power system problems. A FACT has offered utilities the choice to postpone the building of new transmission lines by boosting the capacity of existing lines and compensating the system voltage. “Static VAR compensators (SVC), Thyristor Controlled Series Capacitors (TCSCs), Static Synchronous Compensator (STATCOM), and Unified Power Flow Controllers (UPFC)” are some of the numerous types of FACTS controllers that are available [3]. The many categories of FACTS devices are shown in Figure 1.2.

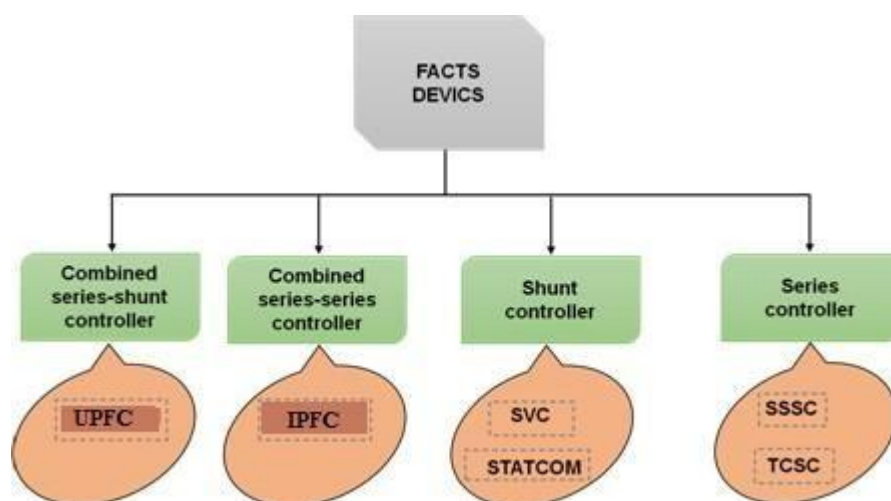


**Figure 1.2 Types of FACTS devices**

### 1.3 SERIES COMPENSATION

Recent decades have witnessed an incredible growth rate of production/consumption of electrical energy. This has amplified the complexity of power systems with increasing need for transmitting large amounts of power over long distances in EHV and UHV voltage range. One of the major problems associated with responding to this demand is the stability of these complex power systems because they require a comprehensive survey taking into account different aspects. Several measures have been taken to improve the stability of power systems:

- lowering the generating transformers' reactance
- expanding the parallel lines/sections
- Using series and shunt compensation on multiple conductor lines
- Making use of series capacitors with EHV lines.

Series capacitors provide a powerful, useful, and affordable way to increase the stability limits and enable lines to carry more power. The series capacitors are also highly beneficial in terms of voltage control, reactive power balancing, lowering transmission losses, load distribution, etc. The ratio of the capacitive reactance of the series capacitor to the overall reactance of the series line serves as a general indicator of the quantity of series capacitance employed in lengthy EHV lines. However, the position of the series compensation throughout the length of the line affects the net transfer impedance with series capacitor installation [4].

Moreover to series compensation, shunt compensation is also provided on these lines because of its ability to compensate the capacitive effect of generation on line and provide an economical technical means to control the voltage rise. Additionally, the series capacitors artificially lower the line's series reactance in order to raise the system's stability limit. The best locations for reactors and capacitor banks, as well as the most effective compensation plans for the number of intermediate stations, must all be determined when planning for long-distance transmission.

Given the above considerations, in the present work, a comparative study is done using maximum receiving end power [ $P_{R(max)}$ ], compensation efficiency criterion for the various systems of the series shunt compensation for a 400kV line under study. The optimal series compensation value for each

scheme is determined. The performances of various schemes are evaluated by deriving the generalized expressions for maximum receiving end power in terms of generalized line constants, capacitive reactance used and receiving end/sending end voltages.

In India, we have a large transmission network with many long 220kV lines in operation and a number of 400kV lines have been added/are being added. Many upper-thermal power stations, being connected to the system, call for effective evaluation of power requirements. Series compensation schemes are suitably planned for new 400kV lines, as also for existing 220kV, over 400km net in operation. Since uncompensated network suffers from significant reactive losses, poor voltage profile causes insufficient exploitation of power transfer capability, suitable series compensation is appropriate to a large extent to reduce the above deficiencies [5].

In fact, series compensation is the ideal solution to increase the transfer capability of power transmission lines such as those of 400kV long transmission lines; this increase can be almost 100% by the installation of 40-45% to compensate with the additional expenditure of 20% only. Given these advantages, series compensation is strongly recommended for the Indian conditions.

#### **1.4 SHUNT COMPENSATION**

It is understood that with the proper reactive shunt compensation, the steady state transmittable power may be raised and the voltage profile along the line can be managed. The goal of this reactive compensation is to alter the electric transmission line's inherent properties so that they are more compatible with the current load demand. As a result, in light load situations, shunt connected, fixed, or mechanically switched reactors are used to reduce line surge, whereas to maintain voltage levels under high load conditions, capacitors with shunt connections, fixed positions, or mechanical switches are used. The basic issue is to increase the transmittable power using perfect shunt coupled VAR compensation in order to provide power electronics-based compensation control solutions to fulfill the specific compensation target. To achieve this, the system's stability and steady state transmission properties must both be improved. Voltage control employs VAR compensation:

- For a line segment, at the midpoint (or a nearby intermediate),
- To avoid voltage instability, provide support at the end of the (radial) line.,
- Diffuse power oscillations to enhance transient stability

- For power oscillation damping

Reactive shunt compensators' functional specifications for enhanced power transmission, voltage transient stability, and oscillation damping are as follows:

- Under all operating circumstances, including significant disturbances, the compensator must be operating in synchronous operation with the AC system at the compensated bus. Additionally, upon fault clearance, the compensator must be able to restore synchronism promptly.
- As system circumstances may dictate, the compensator must be able to modify the bus voltage in order to priorities power oscillation dampening, enhanced transient stability, and voltage support.
- The ideal placement for VAR compensation on a transmission line linking two systems is in the center, but for a radial feed to a load, the ideal site is at the load end [6].

When linked to a source of AC power, capacitors produce reactors (inductors) that squander reactive power. For (roughly) regulated VAR generation absorption of AC power transmission, they have been employed in conjunction with mechanical switches. Over- or under-excited rotating synchronous machines were used to generate or absorb continuously changing VARs for dynamic system compensation, but subsequently, saturating reactors in combination with fixed capacitors were used. The use of series compensation leads to a number of advantages as regards power transfer capability, system stability, voltage regulation etc.

## **1.5 PROBLEMS ASSOCIATED WITH SERIES COMPENSATION**

A few issues are also brought on by the usage of series compensation. Some of these are:

- Sub-synchronous resonance
- Ferro-resonance
- Line protection
- High frequency voltage

## **1.6 FACTS CONTROLLERS FOR POWER SYSTEM**

The term "FACTS technology" does not refer to a single high power controller, but rather to a group of controllers that can be used independently or in conjunction with one another to control one or more of the interrelated system parameters that control the operation of power systems, such as series line

impedance, shunt impedance, current, voltage, phase-angle, etc.

In general, 4 different kinds of FACTS controllers may be distinguished [3]:

- Series Connected controllers.
- Shunt Connected controllers.
- Combined Series-Shunt connected controllers
- Combined series-series controllers

## **1.7 SERIES CONNECTED CONTROLLERS**

Power flow in a line may be greatly controlled by variable series compensation, which also enhances stability. With series compensation, it is possible to arbitrarily reduce the total effective series transmission impedance from the sending to the receiving end. By efficiently using oscillation damping, this ability to restrict the flow of power may be utilized to raise the limit of transient stability.

A series FACTS control may regulate the flow of current by adjusting impedance, phase angle, or series injection of voltage. As a result, the series controller might be a variable source with changeable impedance, such as a capacitor, reactor, or power electronics, to meet the required demand. However, the majority of series controllers inject changing voltage in parallel with the line. When current flows via changing impedance, a series voltage is injected. Only variable reactive power is supplied or consumed by the series controller as long as voltage is in quadrature with the line current. Real power will also be included in any other phase relationships. Controllers that are linked in series include: “Static Synchronous Series Compensator (SSSC), Inter line Power Flow Controller (IPFC), Thyristor Controlled Series Capacitor (TCSC), Thyristor Switched Series Capacitor (TSSC), Thyristor Controlled Series Reactor (TCSR), Thyristor Switched Series Reactor (TSSR)”.

### **1.7.1 TCSC**

We employed a series device called a thyristor controlled series capacitor in our study. A TCSC is a capacitive reactance compensator that uses a series capacitor bank that has been switched by a reactor controlled by a thyristor to provide a smooth variable series capacitive reactance. The TCSC is built on thyristors and lacks gate turn-off functionality. It serves as a replacement for the SSSC (described above) and is an essential FACTS controller. A series capacitor is used to link a variable reactor, such as the 4

TCR. The reactor stops conducting when the TCR firing angle reaches 180 degrees, and the series capacitor reaches its typical impedance. There is a rise in capacitive impedance when the firing angle is advanced below 180 degrees.

On the other hand, the reactor becomes entirely conducting when the TCR firing angle turns 90 degrees, and the overall impedance ends up being inductive. Since the reactor is intended to have significantly lower impedance than a series capacitor, to achieve higher performance, the TCSC may consist of a single big unit or numerous smaller capacitors of equal or various sizes.

## **1.8 SHUNT CONNECTED CONTROLLERS**

Shunt controllers, like series controllers, may have changeable sources, variable impedances, or a mix of these. All shunt controllers, in theory, introduce current into the system. A variable current injection into the line results even from varying shunt impedance. The amount of variable reactive power it produces or uses depends on whether the injected current is in quadrature phase with the line voltage. Real power exchange will also be present in any other phase connection.

The line was separated into two segments by placing the shunt compensator in the midst of a row. At this point, the voltage may be regulated to have the same value at both ends of the line, which has the benefit of increasing the maximum transmission power. It is possible to avoid voltage instability brought on by changes in load, generation, or outages by placing a shunt compensator at the end of a line that is parallel to a load. Transient stability may be improved and effective power oscillation damping occurs because the compensation shunt has the capacity to alter the power flow in the system by modifying the value of the shunt compensation, applied during/after disturbance. As a result, the transmission line's tension dampens power oscillations by compensating for the disturbed machine's swings. Various kinds of shunt coupled controllers include: “Static Synchronous Compensator (STATCOM), Static Synchronous Generator (SSG), Battery Energy Storage System (BESS), Super conducting Magnetic Energy Storage (SMES), Static VAR Compensator (SVC), Thyristor Controlled Reactor (TCR), Thyristor Switched Reactor (TSR), Thyristor Switched Capacitor (TSC), Static VAR Generator or Absorber, Static VAR system (SVS) and Thyristor Controlled Braking Resistor (TCBR)”.

### **1.8.1 STATIC SYNCHRONOUS COMPENSATORS**

A static synchronous generator functions as a branch-connected static VAR compensator that allows for the regulation of either an inductive or



capacitive output current regardless of the AC system voltage. A FACTS controller core is called STATCOM. Its foundation may be based on the converter's output voltage or current. The voltage source converter seems to be the most desired from an economic standpoint, and it often serves as the foundation for presentations of most converter FACTS controllers. For the voltage source converter, the bus capacitor voltage is automatically changed as necessary to serve as a source of voltage converter, and the AC output voltage is so precisely regulated that it is just ideal for the required current flow for each AC voltage. Thus, STATCOM may be developed to function as an active filter to take in the system harmonics.

### **1.8.2 STATIC VAR COMPENSATOR**

A Static VAR generator or absorber with a shunt connection whose output may be adjusted to exchange capacitive or inductive current in order to maintain or regulate certain electrical power system characteristics (typically busbar voltage). This often refers to a thyristor-controlled, thyristor-switched, reactor, capacitor, or any combination of these devices. SVC relies on thyristors but lacks the ability to switch off the gate. SVC is often seen by some as a less expensive alternative to STATCOM, although this may not always be the true if the needed performance is considered instead of simply the MVA size.

## **1.9 OBJECTIVE OF THE RESEARCH**

FACTS controllers' primary goal is to increase transient, voltage, and small-signal system stability so that the AC transmission system is more dependable or more power may be delivered over crucial pathways.

- An appropriate system model is created that appropriately depicts the system's steady state behavior.
- By placing the series and shunt compensation at various points along the transmission system, the technique has been tested to increase steady state stability of power system. The best location of the series shunt capacitor with respect to the SVS (Static VAR System) location has been determined to improve the steady state dynamic voltage stability over a wide range of load variations.
- The quantity of series compensation to be utilized has also been decided, as has the position of the series compensation/shunt compensation that is best.

## **1.10 THESIS ORGANIZATION**

Five chapters make up this thesis. Following is how the thesis is structured:

Chapter 1 provides a summary and the key information regarding the research effort. It offers details on power system, covering both positive and negative aspects. The foundations of data anonymization are covered. The scope of this research effort and the description of the issue are made clear. It is also predicted what this study's goal is. The objectives and research study are described.

Chapter 2 summarizes the pertinent research investigations carried out by various researchers. There are offered data about prior research studies and evaluations.

Chapter 3 describes the optimal location and sizing of FACTS devices using PSO and SSA algorithm.

Chapter 4 concludes with the important findings from the suggested work presented. This chapter also makes further suggestions on how to revamp its performance analysis for improved outcomes.

Chapter 5 evaluates the thesis' success in achieving its objectives and provides some recommendations for enhancing the next work.

## **1.11 SUMMARY**

In this chapter, the use of FACTS devices in the power system, series and shunt compensators, series and shunt connected controllers, an explanation of the issue, and objectives are all covered. The thesis's organization has been touched up on.

## **CHAPTER 2**

### **LITERATURE SURVEY**

#### **2.1 INTRODUCTION**

Numerous academic articles have been written on potential issues in the electricity system. All relevant scholarly works to which this thesis contributes have been cited. The results of the comprehensive literature review are organized in the following sections.

#### **2.2 POWER SYSTEM SECURITY ENHANCEMENT**

Generally, power systems are planned and operated in such a way that they should remain secure under all conditions. With the deregulation of the electricity market, the conventional concepts and practices of power systems are changed. This led to the introduction of Flexible AC Transmission System (FACTS) devices. These are able to modify voltage, phase angle, impedance and the power flows at particular points in power systems. They control the power flows in the network and reduce the flows in heavily loaded lines which results in low system losses, improved stability, and security of network and reduced cost of production. Due to high capital investment, it is necessary to locate FACTS devices optimally in a power system. For this purpose, evolutionary computations such as Genetic Algorithm (GA) and Squirrel Search Algorithm (SSA) are used nowadays for their global optimality, probabilistic nature, independent searching space, and robustness to solve problems which require optimal solutions. Reactive power and impedance manipulation by network components are the fundamental building blocks. In Figure 2.1, we see a selection of common devices labeled as either generally recognized or FACTS. The FACTS side lacks clarity in its classification of "dynamic" and "static." The rapid tunable nature of power semiconductor-based FACTS-devices is emphasized by the name "dynamic." This is a major difference from more commonplace gadgets. The word "static" is used to indicate that the gadgets lack dynamic controllability thanks to the absence of moving features like mechanical switches. As a result, most FACTS-devices can function both passively and actively [4].

#### **2.3 IMPACT OF FACTS DEVICES ON STEADY STATE AND DYNAMIC PERFORMANCE OF POWER SYSTEM**

Researchers have suggested the following effects of FACTS devices for improving a power system's steady state and dynamic performance:

A technique of calculating the reactive power margins for a certain set of load

buses in a power system was put out by Chevalier and Hines [7]. As the answer to an optimization issue with load growth as the goal, the collapse point is established.

A technique of calculating the reactive power margins for a certain set of load buses in a power system was put out by Małkowski et al. [8]. As the answer to an optimization issue with load growth as the goal, the collapse point is established.

Fuzzy set theory is created for the post contingent values are first stated in a fuzzy set notation, as mentioned by Chinda and Rao [9].

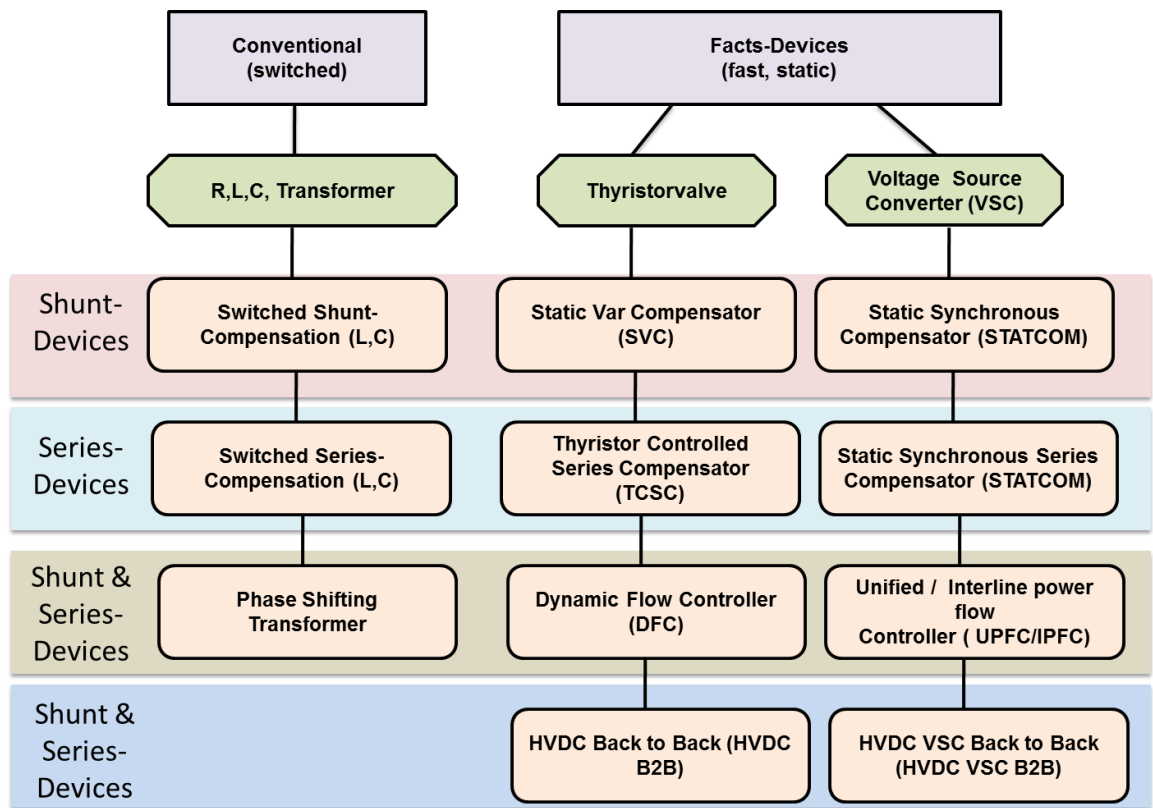


**Figure 2.1 Overview of Major FACTS-Based Devices**

The formulation of a Poolco model appropriate for power system planning was provided by Ansari pour et al. [10]. The approach immediately permits the computation of spot pricing and a bid-based dispatch with just minor changes to the software used in traditional power systems.

The authors, Sewdien et al. [11], static and dynamic methods for analyzing the voltage stability of power networks. To better comprehend the demands of modeling and to explain the phenomena of voltage instability, the results of

time domain simulations are given using a small test system.

Atchison et al. [12] spoke about the approach power system synchronous in Taiwan's primary reasons contingency ranking. Numerous techniques are investigated to examine the voltage collapse phenomena in the suggested approach to voltage collapse in a power system.

A systematic approach of worst-case detection using Genetic Algorithm (GA) and Nonlinear Programming methods was described by Zhang et al. [13]. The approach conducts feasibility checks on VAR disturbance situations, generator reactive limitations, and voltage restrictions at regulated bus bars during optimization in order to provide an accurate and trustworthy estimate. Generally speaking, the SVC is made up of thyristor switched capacitors (TSC) and thyristor controlled reactors (TSR / TCR). Figure 2.2 demonstrates that reactive power may be varied by matched control of several branches.

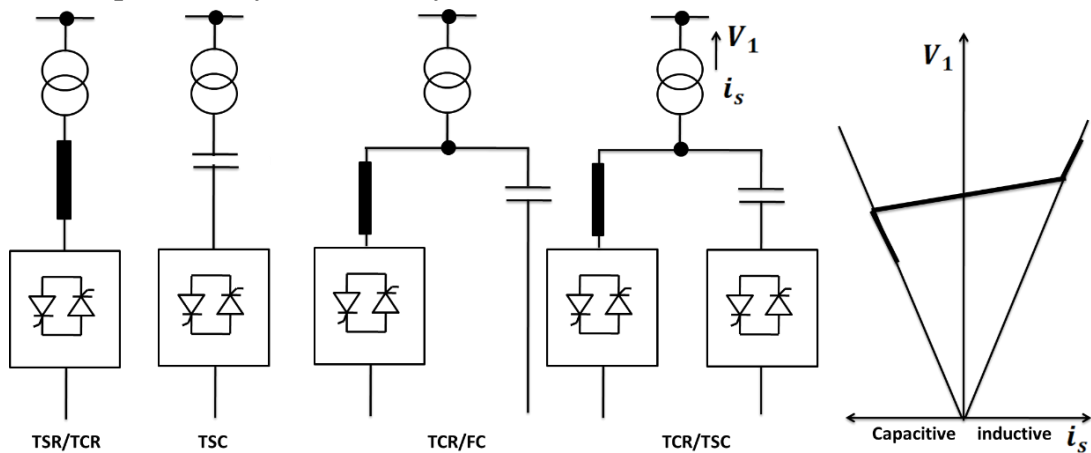


**Figure 2.2. SVC building blocks and voltage / current characteristic**

The equal area criteria has been used to construct a theory for studying power system damping augmentation by use of static var compensators (SVCs). Baadji et al. [14] discusses several basic concerns, including the impact of SVCs on power systems, how to operate an SVC to increase system damping, and the distinctions between continuous and discontinuous control of SVC reactive power.

Power flow regulation in electric power systems was the focus Mohamed et al. [15] Research. They used phase shifters and controlled series power capacitors. In this study, models that can be included into power flow plans are built and examined.

The effect of different FACTS devices on the behavior of power systems is

systematically and impartially compared using the notion of security areas. Kuthadi et al. [16] explore the use of scalar metrics of the steady-state performance of a power system with FACTS devices to evaluate this influence.

Using unified power flow controllers, thyristor controlled phase shifting transformers, and thermistor controlled series capacitors, Rawat and Tamta [17], examined how power system dynamics may be improved. This research analyses models that may be used in dynamic simulation programmed to examine angle stability.

According to Dash et al. [18] proposal, Flexible AC Transmission System (FACTS) devices should be modeled for power flow studies, and this modeling should play a part in the investigation of FACTS devices for power flow control.

From a broad perspective of nonlinear system, Birchfield and Overbye [19] proposed a novel technique of a power flow calculation taking into account FACTS devices. In the discussion, the UPFC's power flow control range in a power system is used.

Adetokun et al. [20] provide a method for determining the critical modes of voltage support using shunt FACTS devices. Understanding the system's modes close to the breaking point allows us to calculate the critical modes research evaluates the effect of adding static VAR compensators to a 1380 bus model of the BC Hydro system to test the suggested technique.

The fundamental ideas of the suggested generalized P and Q controller were described by Alhejji et al. [21], who also made comparisons to more traditional, but related, power flow controllers. Transmission systems may benefit from the use of Thyristor Controlled Series Capacitors (TCSC) to fix some types of dynamical errors. When huge electrical networks are unified, damping initially increases. Secondly, it can get around Sub-Synchronous Resonance (SSR), a problem caused by the interaction between big heat generators and series compensated transmission networks. The basic layout of a TCSC diagram is seen in figure 2.3.

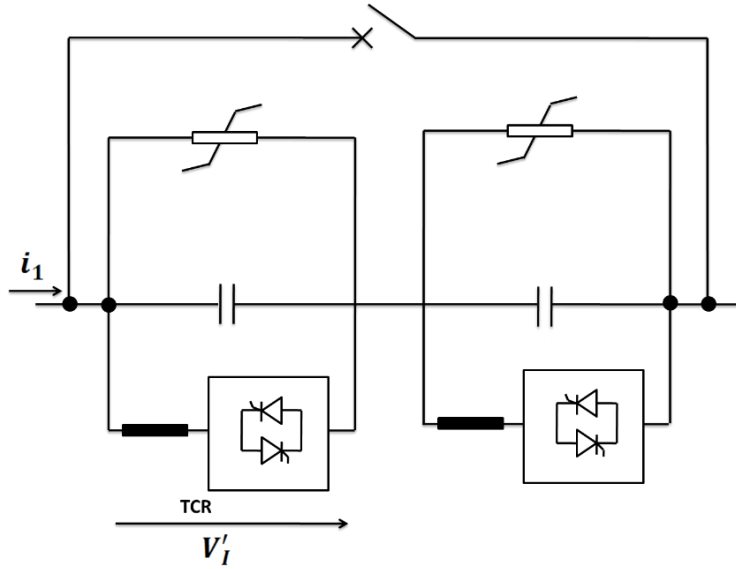


**Figure 2.3. Principle setup of a TCSC**

The impact of SVC and TCSC on the system's “Available Transfer Capability (ATC)” is shown in detail by Raj and Bhattacharyya [22]. ATC is calculated using many different voltage collapse methods.

Together, the TCSC and SVC installation have been the subject of research by Jiang et al. [23] in order to achieve optimal power system performance. The TCSC and SVC control method is derived using a nonlinear design approach called Direct Feedback Linearization.

Damping management of electrometrical oscillations in large-scale systems is a complex topic, and Abdullah et al. [24] provided effective techniques for the solution of two significant challenges in this field. The suggested method allows for the identification of generators best suited for installation of power system stabilizers and, similarly, buses most suited for placement of static VAR compensators to dampen important modes of oscillation.

Meena et al. [25] detail how controlled reactive power compensation may be used to dampen oscillations in a power system. In the context of weakly connected networks, this is of special relevance. Two types of reactive power components that may be adjusted are compared here: the Controlled Series Capacitor (CSC) and the Switched Variable Capacitor (SVC) (Static VAR Compensator)

## 2.4 POWER SYSTEM LOADABILITY IMPROVEMENT

The electrical power business has undergone significant change in tandem with the introduction of FACTS technology. Improvements in system transmission capacity and power flow management flexibility and speed may result from the use of FACTS.

Ahmed et al. [26] have modeled and simulated SVC and TCSC to determine their maximum loadability point. To counteract the inductive reactance of the line, TCSC is wired in series with the conductors. With the use of Thyristor-controlled components, the SVC may be made to either produce or consume reactive power.

In power flow research, Unified Power Flow Controller behavior has been investigated by Bhandakkar and Mathew [27]. Reports indicate that the UPFC may regulate all three variables concurrently or in any combination, so long as operational restrictions are not exceeded. This includes active power control, reactive power control, and adaptive voltage magnitude control.

In the field of computational intelligence research, population-based, cooperative, and competitive stochastic search algorithms have recently gained a lot of traction. Particle swarm optimization and other well-known search techniques, such as the Genetic Algorithm, are successfully used to efficiently and effectively tackle complicated problems. Dash et al. [18] used genetic algorithms to determine the best position for many types of FACTS devices. By addressing this issue, the optimal position, the temperature limit of the lines, and the voltage limit of the buses were considered as constraints.

Singh et al. [28] proposed a novel method for the installation of FACTS devices in open power markets. Using an actual power flow performance index, the ideal position for FACTS devices has been reported in this study in order to lower manufacturing costs as well as device costs.

Singh and Kumar [29] reported using a hybrid GA method to determine the best power flow in a power system that uses FACTS devices.

Ahmad and Sirjani [30] used multiple UPFC and evolutionary programming to improve power transmission networks. To change the phase of the series voltage, the DC-circuit permits an active power dialogue between a shunt and a series transformer. As can be seen in figure 2.4, the voltage and power flow in this configuration are fully adjustable. The Thyristor Bridge is what the series



converter needs to feel secure. Limiting real-world applications where voltage and power flow management are both crucial is the fact that a UPFC is getting rather unique treatment due to the high demands placed on Voltage Source Converters and the security.

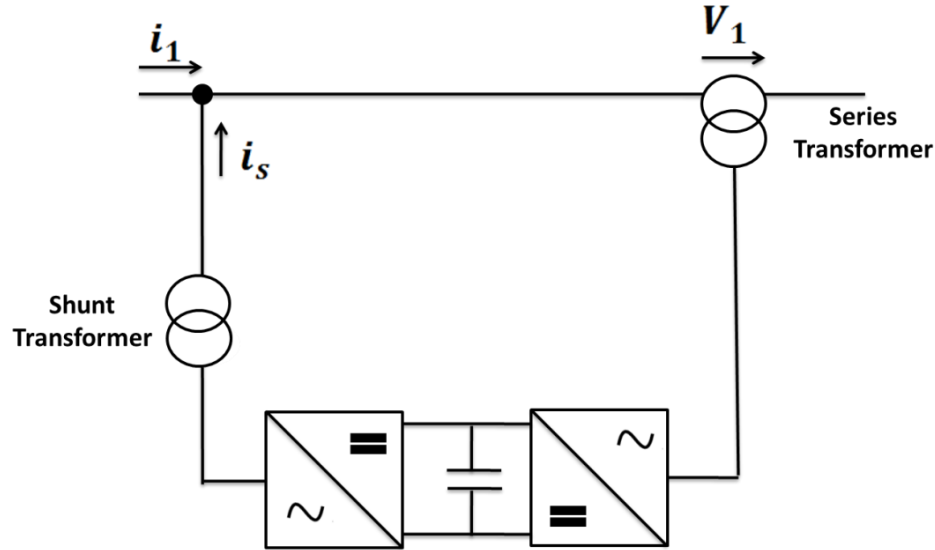


**Figure 2.4. Principle configuration of a UPFC**

In order to reduce the cost of the generator fuel while using multi-type FACTS devices for optimum power flow regulation, Gupta et al. [31] presented a hybrid Tabu search and simulated annealing method.

On the best place for the Unified power flow controller in the electrical power system, Hassan et al. [32] have worked. Using the steady state injection model of UPFC, continuous power flow method, and OPF technique, the ideal position of UPFC to reduce the generation cost function and the investment cost on the UPFC device is identified in this study.

Dash et al. [18] examined the PSO Technique for optimum placement of FACTS Devices taking system loadability and installation cost into consideration. Amouzgar et al. (2020) proposed Modified SBX and Adaptive Mutation for Real world single goal optimization.

Qiu et al. [33] examined the reliability of local approximations of the loadability surface for power systems. For the purpose of maximizing power system loadability, Kotsampopoulos et al. (2019) investigated the multi-objective optimum positioning of FACTS shunt-series controllers.

Nomula and Ganesh [34] recently worked on the best positioning of

many FACTS device types to increase the loadability of the power system using a general graphical user interface.

To maintain voltage dependability in power transmission systems, Simon et al. [35] have predicted an innovative approach to enhancing FACTS devices. The PSO method is used to optimize the gravitational consistent and boost the GSA's searching performance in the suggested improvement. The suggested algorithm is a practical method for determining where and how large the FACTS controllers should be placed. Based on the voltage crumple rating and moreover the power loss of the framework, the ideal placements and power assessments of the FACTS devices are resolved. In this case, they use the unified power flow controller (UPFC) and the interline power flow controller (IPFC) from the FACTS system to evaluate how well the suggested method works in practice (IPFC). The suggested approach is implemented in MATLAB, where its performance is evaluated in comparison to the state-of-the-art GA-GSA hybrid method. They test the suggested method with the standard IEEE 30 transport configuration using two FACTS devices, including the UPFC and the IPFC.

According to Hernández [36], it is crucial for professionals and industries to develop a versatile and dependable power framework planning strategy under basic conditions in order to reduce the likelihood of power outages. In this research, we discuss the foundational stage of this functional approach, which involves addressing the security of the smart grid power system management by using Gray Wolf Optimizer in conjunction with a pattern search algorithm. The primary goal of this suggested organizing method is to protect the reasonable power infrastructure against blackouts caused by the unknowable failure of power-generating units or critical transmission networks. The suggested method's viability and efficiency are tied to the IEEE 30-Bus test framework. The results are encouraging, and they show that the suggested method is effective in practice for ensuring system security in common situations.

According to the research of Gupta et al. [37], the voltage profile on the load buses of a power framework is a key element in ensuring the safety of the system and keeping a safe distance from a voltage collapse. This research presents a new technique for distributing FACTS devices in the most optimum locations and enhancing their properties. Results from testing the algorithm's implementation on IEEE standard 14, 30, and 57 bus architectures are compared to those obtained using PSO and GA algorithms. The results make sense, and they successfully draw attention to the most salient features and

aspects of the algorithm.

According to Martins et al. [38], the Flower Pollination Method (FPA) is a new and effective algorithm that is recommended for the best capacitor allocations and size in various circulation frameworks. First, Power Loss Index (PLI) is advised for the majority of candidate buses for adding capacitors. The obtained results from the proposed algorithm are compared to those from other algorithms, such as Genetic Algorithm (GA), Particle Swarm Optimization (PSO), Plant Growth Simulation Algorithm (PGSA), Direct Search Algorithm (DSA), Teaching Learning-Based Optimization (TLBO), Cuckoo Search Algorithm (CSA), Artificial Bee Colony (ABC), and Harmony Search Algorithm (HSA), to emphasise its advantages. Additionally, the results are known to support the suitability of the suggested algorithm to reduce losses and overall costs, as well as to enhance the voltage profile and net setting apart for various disseminating frameworks.

A knowledge-based approach to understanding the Optimal Power Flow (OPF) problem that enables Flexible AC Transmission System has been put out by Khare et al. [39]. FACTS is crucial to the long-term stability and control of power systems' elements. This section focuses on the research of the unrelenting state control that determines the ideal position of FACTS devices and the values associated with them in transmission lines. This section demonstrates an enhanced differential evolution (IDE) method to handle the OPF problem in order to determine the best FACTS solution. It is really appropriate to address the OPF issue in this way. On a framework for an IEEE 30-bus 41-transmission line, the suggested technique is tested. Results show that the suggested methodology may reduce dynamic power transmission loss by more and provides better union execution than the existing methods.

Basu et al. [40] have introduced a genetic algorithm, a non-conventional optimization approach, to find the best placement, kind, and size of FACTS devices to regulate line currents, keep bus voltage where it needs to be, and cut down on energy waste. The goals are to maximize voltage stability and static security margins while reducing losses. Optimal placement of FACTS controllers during line outages is also used for congestion management. As a simulation tool, MATLAB code has been created. Evaluations are performed on an IEEE 30 bus system with varying loading circumstances using two steady-state FACTS devices (a SVC and a TCSC), and the findings validate the efficacy of the proposed method in determining the best possible site for power system stability.

There has been a brief overview of quick and flexible management of power flow in transmission lines presented by Nguyen and Mohammadi [41]. The performance of the SVC, TCSC, and UPFC FACTS controllers have been compared and contrasted. It has also been determined how FACTS may be used to power systems.

Using an adaptive clonal selection technique, Akbari et al. [42] have proposed a solution to the multi objective optimum power flow (MOOPF) issue. It lessens the difficulty, the expense, and the loss of transmission in FACTS devices, as well as the L-index (a measure of voltage stability). To locate and control the Pareto optimum front, ACSA makes advantage of non-dominated sorting and crowding distance. UPFC, IPFC, and GUPFC are only some of the FACTS devices that may be taken into account while pursuing multi-objective optimization. The MOACSA was evaluated using the industry-standard IEEE 30-bus test system and FACTS components. Standard algorithms like NSGA-II, MOPSO, and MODE are put through their paces and compared to the results produced using the new MOACSA method.

In order to solve the FACTS optimization problem in power systems, Jordehi [43] have provided a detailed overview of the numerous heuristic approaches currently in use. It begins by categorizing FACTS optimization techniques into four broad categories, before further subdividing heuristic techniques into distinct groupings and providing in-depth discussions of the features, benefits, and drawbacks of each. Some suggestions for further study in this area will be provided as a conclusion.

Computer-based intelligence algorithms, as described Morshed and Fekih [44], might improve the loadability of pool and hybrid models in a reorganized power system by determining where FACTS devices should be placed and how they should be operated. They employed and compared the techniques Particle Swarm Optimization (PSO), Differential Evolution (DE), and Composite Differential Evolution (CoDE). The research takes into account the Thyristor Controlled Series Compensator, the Static VAR Compensator, and the Thyristor Controlled Phase Shifting Transformer. To do this, AC load flow equations are used together with limitations on actual and reactive power generation, transmission line flow, bus voltage magnitude, and FACTS device configuration. The AC distribution factor with slack bus contribution is used to simulate bilateral transactions in the hybrid model's secured bilateral transaction matrix.

A multi-objective framework has been presented for congestion management by Salkuti and Kim [45]. Operating cost, voltage, and transient stability margins are all optimised. Utilizing locational margin pricing, this architecture strategically places FACTS devices in heavy traffic areas and modifies their layout accordingly. The effectiveness of the suggested technique is confirmed by testing results on the well-known New-England test system, which are detailed at length.

To improve the efficiency of the interline power flow controller (IPFC) in multiline transmission, Radhakrishnan and Gopalakrishnan [46] have introduced a novel system based on the cuckoo search algorithm (CSA). As a result, there is far less congestion on the lines carrying data. Subtracting the line utilization factor (SLUF) from the CSA-based optimal tuning yields the ideal location of IPFC. Through fine-tuning the multi-objective function, CSA determines the best place from which to reduce transmission line congestion. Different loading situations have been used to analyse CSA's performance in comparison to that of PSO and the differential evolution algorithm, two additional optimization methods (DEA). The findings favour CSA above the other two approaches.

In order to manage congestion in a market-based power system, Nagi et al. [47] introduced a PSO-based method for determining the optimal location and size of a single unified power flow controller (UPFC). The cost curves for the generators are smooth quadratic functions thanks to the technique. The effects of load fluctuation on the optimization issue are included into the model with the use of a typical load duration curve (LDC). While the Newton-Raphson solution reduces the mismatch of the power flow equations, the PSO method is used to distribute the near-optimal GenCos and the ideal placement and size of UPFC. The effect of UPFC on congestion levels in the RTS 24-bus test system is analysed using simulation results (without/with the line flow limits, before and after the compensation). Both the new PSO technique and the more traditional sequential quadratic programming (SQP) method are used to run simulations and then compare the outcomes to each other.

In order to enhance the dynamic stability of the power system, Kumar and Ramaiah [48] recommended the use of the Firefly Algorithm (FA) and the Cuckoo Search (CS) algorithm, both of which are dependent on the proper placement and capacity of UPFC. The searching efficiency, random reduction, and complexity of these algorithms have all been significantly enhanced.

Constraints on the dynamic stability of the system, such as voltage, power loss, actual power, and reactive power, are influenced by the generator fault. The UPFC is best placed along the line of greatest power loss, which is determined by the FA method. Utilizing the improved capacity of the UPFC, which was achieved by cost-effective optimization using the CS method, the compromised location parameters and dynamic stability requirements are brought back within safe bounds. The damaged area's obtained UPFC capacity has been pinpointed, and the system's power flow has been studied.

The UPFC for an actual 380 kV, 400 km, double-circuit tie transmission line linking the central and western networks in the Kingdom of Saudi Arabia (KSA) has been studied by Arif et al. [49]. The UPFC for the actual system is optimally sized using GA methodology, and its allocation is maximized using this method as well. Additionally, the effects of the UPFC on the current protection system are evaluated, and workable alternatives to addressing these issues are provided. The issue is formulated in MATLAB/SIMULINK, and then the optimal parameters and placement of the UPFC are found. The performance of the interconnection system in terms of voltage profile and stability margin is simulated, and the findings are shown, debated, and ultimately recommendations are made for improvement.

In order to increase dynamic stability, Reddy et al. [50] presented a hybrid method based on the best placement and size of UPFC. Since the generator outage influences the power flow restrictions such power loss, voltage, real and reactive power flow, the largest power loss bus is located at the best spot for repairing the UPFC. The Artificial Bees Colony (ABC) method was used to identify the best site. The GSA optimizes the amount of UPFC needed to restore the initial operating state based on the amounts of the violated power flow. The performance of this work is assessed through comparisons using several methodologies, including ABC and GSA, and it is implemented in the MATLAB/simulink platform. The comparative findings show how effective this strategy is and validate its ability to resolve the issue.

At order to manage transmission line congestion, Thippana et al. [51] suggested a method for placing IPFC in the best location possible based on the disparity line usage factor (DLUF) and firefly algorithm (FA)-based optimal tuning. The difference in the mega voltage ampere (MVA) consumption of each line linked to the same bus is calculated by DLUF. The lines with the highest DLUF are where the IPFC is located. The results of using this strategy on an IEEE 30-bus system have been reported and examined. A multi-objective

function made up of active power loss, total voltage variations, security margin, and installed IPFC capacity is optimized for the IPFC at the suggested site using FA. Additionally, genetic algorithms are used to tune IPFC. The outcomes have been contrasted with FA's for various loading scenarios.

Amarendra et al. [52] have suggested a method for determining IPFC's ideal placement within the power system. Both LR and ABC optimization tools are utilized. The technique is based on the FACTS devices' installation and power generating expenses. Optimal IPFC parameter values and generating unit dispatch are also determined using this approach. Results indicate that placing IPFC at the best possible place increases the system's dependability and load margin.

A novel method for determining where in a transmission system FACTS devices should be installed has been presented by Zhang et al. [53]. Congestion is managed by congestion relief and congestion cost. They use an RGA optimization strategy to address the congestion issue. Analytical Hierarchy Process (AHP) using fuzzy sets is used to evaluate the RGA fitness function.

A biogeography-based optimization technique was published by Das et al [54] to address the challenging economic emission load dispatch issues of thermal generators in power networks. For case studies, several emission chemicals including NOX, SOX, and COX are taken into consideration. When resolving issues with economic emission load dispatch, the technique takes into account the operational limit restriction and the limitation on power demand equality. The geographical distribution of living things is the subject of biogeography. Biogeographic mathematical models explain how species form, how they move from one environment to another, and how they become extinct. Here, it will be explained how to address economic emission load dispatch issues using biogeography-based optimization. This method primarily uses the two processes of migration and mutation to get the global optimum.

A hybrid approach for improved voltage stability and ensured optimum power flow with FACTS device installation has been put forward by Mahapatra et al. [55]. By strategically positioning the TCSC controller, the performance of the hybrid Improved Gravitational Search algorithm (IGSA) and Firefly algorithm (FA) is examined. The technique is put into practise using the MATLAB working environment, and IEEE 30 bus transmission systems are used to assess the voltage stability and power flow security. The best outcomes produced are contrasted with those found in the literature, and

the better performance of the algorithm is shown by its low cost of production, decreased actual power losses, and capacity to maintain voltage stability.

According to Kyomugisha et al. [56] the voltage stability problem in today's power systems is a problem related to the framework constraints and voltage fall. FACTS is an example of a modern system prepared to more effectively regulate the receptive power flow. Given the evolutionary process, this research suggests a programmed FACTS device distribution handle. The model aims to increase the power systems' voltage stability. The results showed that the suggested method improved voltage stability in benchmarks using the IEEE framework and that it outperformed alternative probabilistic and heuristic optimization methods.

In light of the actual power execution record (Severity list) in the power system network, Abrishambaf et al. [57] advise that the Unified Power flow Controller be located as efficiently as possible. The conduct of the UPFC is overhauled in the regulation of active power, reactive power, and voltage profile using the two-voltage source (Power infusion) model. To reduce the amount of fuel used both with and without the use of the Unified Power Controller, the Particle Swarm Optimization (PSO) approach has been used in this study. The suggested techniques' justifications and simulations on the IEEE 30 bus system are done for approval and correlation. The ideal distribution of the unified power flow controller may significantly improve the power framework's exhibitions.

Optimal Receptive Power Dispatch (ORPD), according to Nikam [58], is described as the minimizing of active power transmission errors and mean voltage deviation by regulating various control components while meeting certain adjust and divergence requirements. The suggested CKHA is developed and successfully tested on the industry-standard IEEE 30-bus test control system. Two different types of FACTS controllers specifically, a thyristor-controlled arrangement capacitor and a thyristor-controlled stage shifter are installed in the models of the investigated power systems. Finally, to supplement the adaptability of the suggested CKHA approach, reenactment is expanded to various wide scale control system models, such as the IEEE 57-bus and IEEE 118-bus test control structures.

Kumar et al. [59] proposed an improved solution for active power conditioner (APC) arrangement and scaling to improve power quality in appropriation frameworks by using the enhanced discrete firefly algorithm



(IDFA). The goal of a multi-objective optimization problem is to improve voltage profile, reduce voltage add-on symphonic twisting, and increase venture cost. The suggested algorithm's execution on the IEEE 16- and 69-bus test frameworks using Matlab programming is authorized. The findings are compared with those of the conventional discrete firefly method, genetic algorithm, and discrete particle swarm optimization. The analysis of the data showed that, among other techniques, the suggested IDFA is the best one for determining the ideal size and position of the APC in dispersion frameworks.

Jayabarathi et al. [60] looked at how UPFC may increase the transient stability of a two-area power system. The efficiency of UPFC in improving the system's transient stability is shown through simulation results.

Peddakapu et al. [61] looked at how to use TCSC to increase the transient stability of a two-area power system. The simulation results show how effectively TCSC improves transient stability when the performance of TCSC is compared to that of other FACTS devices.

Using a STATic synchronous COMpensator (STATCOM), a static synchronous series compensator (SSSC), and a unified power flow controller, Galvani et al. [62] have implemented and explored the aforementioned control technique to dampen unwanted electromechanical oscillations in the power system (UPFC). The impact of several disturbances on a single-machine infinite-bus power system was investigated. The data gathered demonstrates the devices' usefulness and durability in maintaining power grid stability.

An overview of control techniques for power system security evaluation employing FACTS devices to coordinate various loads in an interconnected power system nearing a severe emergency situation has been addressed by Wang et al. [63]. In addition to regulating the flow of electricity, FACTS controllers may improve the reliability of the power grid. With this strategy, even if a small number of FACTS devices fail, the island will not experience a complete supply disruption.

The optimum number and placement of FACTS devices have been reported by Pham et al. [64], who use a Modified Shuffled Frog Leaping Algorithm. The UPFC decoupled model is used to increase system loadability within the constraints of the transmission lines' capacity and the required voltage. In the proposed procedure, both the placement and the settings of UPFCs are optimized concurrently.

According to Majidi et al. [65] research, a hybrid optimization technique based on FACTS is necessary to achieve optimum power flow. They take into account the active power transmission loss, the active power flow execution file in the transmission lines, and the voltage contrast across bus execution files as the goal functions of power flow.

An advanced and flexible FACTS controller candidate was the interline power flow controller, as suggested by Mugiira [66]. In a power grid setup, IPFC was used in a number of transmission lines. Power injection modelling was integrated with the Newton-Raphson (NR) power flow approach for effect evaluation of IPFC settings. It was shown that by using optimal IPFC settings, power losses may be kept to a minimum.

## **2.5 SUMMARY**

Based on the Literature survey, the following research gaps have been identified: The proper placement of FACTS devices to strengthen the safety of the electrical grid is the subject of a lot of study. However, the places are selected explicitly according to the contingency rating in all the works. That is to say, the route with the greatest severity index gets prioritized. However, in reality, any of the ranking lines may be significantly impacted by a single contingency condition. Therefore, all the rated lines are supplied as input parameters to the algorithms employed in this study with this consideration in mind.

The RGA with Simulated Binary Crossover (SBX) and non-uniform Polynomial mutation has not been used to the suggested power system challenges, despite the fact that there are numerous research articles on optimum allocation problems using Evolutionary Algorithms. In this study, these recombination operators are applied with RGA, and the algorithm parameters are tweaked and set by several iterations of solving the benchmark issues. Because of this, you may be certain that the algorithm will consistently provide optimal results. Once the algorithms have determined the best places and configurations, the cost of the device may be estimated. One of the restrictions taken into account in this study is the price of the gadget. Incorporating FACTS devices into power systems has been the focus of many researchers, but there is still a need for further in-depth study that may lead to a variety of trustworthy solutions that can meet the needs of utilities while also bolstering power system security and increasing loadability.

Transmission lines' capacity to transmit was boosted by conventional line compensating techniques. FACTS' primary goal is to increase the lines' actual transmission capacity and regulate power flow. Because of the way their voltage source converters are set up, FACTS devices are able to adapt to both immediate and long-term changes in the system by independently regulating voltage, impedance, and angle, or by controlling the flow of actual and reactive power. FACTS controllers, especially converter kinds with multiple power flow control capabilities, have dramatically altered the landscape of power distribution and transmission. FACTS devices have the potential to significantly improve the functioning of a power system by overcoming some of the conventional restrictions, as shown by both economic analysis and practical considerations.

## **CHAPTER 3**

### **OPTIMAL LOCATION AND SIZING OF FACTS DEVICES USING PSO AND SSA ALGORITHM**

#### **3.1 OBJECTIVE**

Due to rising load demands and complications, today's electrical power systems often run near to their maximum load-ability point. As a result, utilities and power system operators' primary objectives include preventing voltage breakdown and ensuring the stability of the power system. Flexible AC transmission systems (FACTS) are cutting-edge technologies that can increase power system stability, improve voltage profile, and raise real power transfer by controlling various power system parameters like impedance, voltage, and angle. Nevertheless, to maximize benefits and effectively control power flow, FACTS must be allocated and sized in the power system network. The Particle Swarm Optimization (PSO) algorithm and Squirrel Search Algorithm (SSA) is used in this chapter to provide a strategy for allocating and sizing FACTS devices in the best possible way. The shunt VAR compensator (SVC), the static compensator (STATCOM), and the thyristor controlled series compensator (TCSC) are the three kinds of FACTS devices that are chosen. To determine the best rating for these devices, PSO with the goal of reducing actual power losses and voltage variations is used. The IEEE 30 bus test system is used to implement the approach. Real power losses have significantly decreased as a result, and the voltage profile has improved.

#### **3.2 INTRODUCTION**

Due to the rising need for electrical energy, the cost-effective, dependable, and efficient conveyance of large amounts of electricity has been explored for a decade. For electrical operators, transferring a lot of electricity to satisfy load demand is a challenging task.

Growing the network and adding additional transmission lines often encounters cost challenges and is thus not always a practical option. Usually,

Power plants are far from where power is required, so electricity must be transmitted through long transmission lines. This causes a lot of problems with power transfer, such as voltage collapse, frequency collapse, and reactive power flows. The amount of power being transferred is constrained by these problems. However, the aforementioned issues can be resolved by regulating power flow. Power transfer capability can be improved and transmission lines can be used to their full potential if voltage, current, angle, or impedance can be controlled in real time in some case. Historically, reactive assistance was provided by electromechanical devices to enhance voltage profile and boost actual power flow. These, however, are ineffective and unable to be started regularly. The advance of technology Solid-state technologies are used in Flexible AC Transmission Systems (FACTS), which can control the flow of electricity by controlling the voltage, current, angle, and impedance of the transmission line. FACTS can be used to improve the flow of real power and reduce real power losses and voltage change. These devices consist of a thyristor controlled series compensator (TCSC), a static Var compensator (SVC), a unified power flow controller, a static compensator (STATCOM), etc. in FACTS. A general classification of FACTS is depicted in figure 3.1.

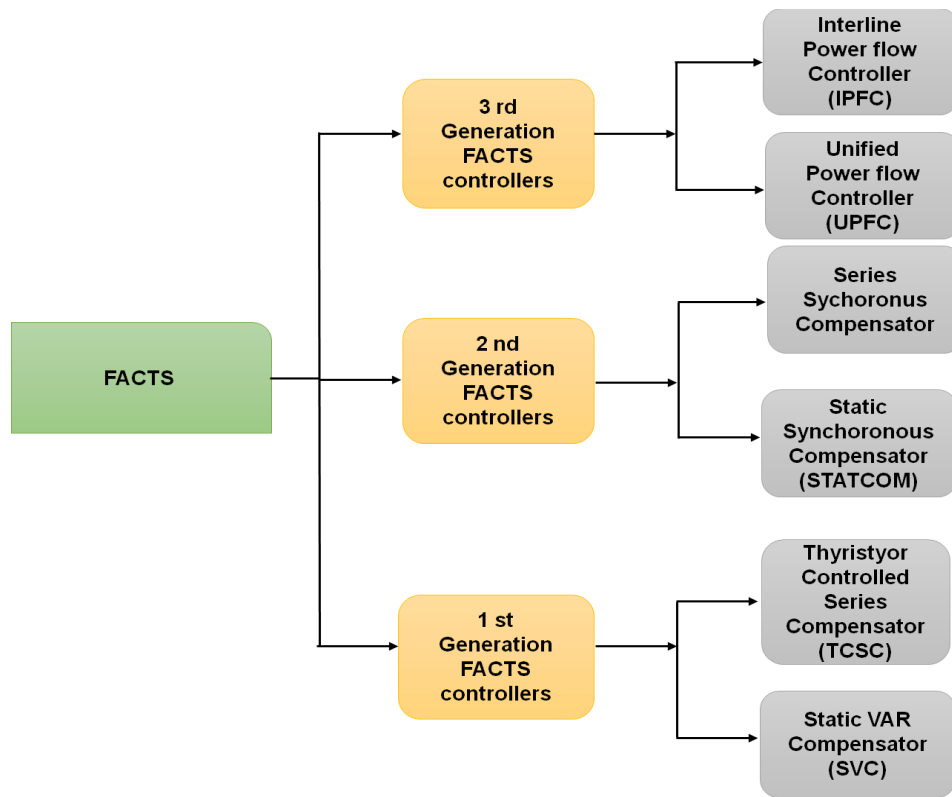


**Figure 3.1: General classification of FACTS**

Each FACTS modifies a separate power system parameter to enhance electrical power flow. FACTS may increase power transfer efficiency and voltage stability by managing the corresponding parameters, which also helps to decrease actual power losses, voltage variations, and transmission line congestion. FACTS may increase power transfer efficiency and voltage stability by managing the corresponding parameters, which also helps to decrease actual power losses, voltage variations, and transmission line congestion. The optimum allocation and size of FACTS are required because to the high installation costs. Due to financial and environmental constraints, building additional power production units and transmission connections to boost electricity generation is not feasible. The efficient and secure functioning of power systems depends on good reactive power flow control, which might also increase system performance. Results reduce energy losses, decrease in reactive power production, boost reactive power reserves, and enhance voltage profiles. Notable FACTS recognized for its rapid reaction and low cost is the

TCSC. As a result, optimizing the size and location of TCSC devices is crucial for enhancing the performance of contemporary power systems. In this research, weak buses and lines are first identified in order to find the optimal placements for FACTS and the optimal sizes FACTS sizes using particle swarm optimization (PSO) and Squirrel Search Algorithm (SSA). We consider three different types of FACTS devices such as SVC, TCSC, and STATCOM... Additionally, the static models of SVC, STATCOM, and TCSC are taken into consideration here.

### 3.3 OPTIMAL POWER FLOW

#### 3.3.1 Objective functions

A multi-objective function is taken into account while looking for a location and size for the SVC that minimizes active power loss and reactive power loss and voltage deviation..

##### Minimize the active power loss

Supply and demand should be balanced by the power equality constraint. Total system demand plus power losses [67], which may be calculated by (3.1),

$$\sum_{l=1}^{NG} PG_i = \sum_{l=1}^{NB} PD_i + P_{losses} \dots \dots \dots (3.1)$$

$PG_i$  - unit I's active power generation.

$PD_i$  - load on the bus for active power.

##### Minimize the Reactive power loss:

The power equality constraint should force supply and demand into stability. Power losses plus total system demand [67], which may be computed by equation (3.2).

$$\sum_{l=1}^{NG} QG_i = \sum_{l=1}^{NB} QD_i + Q_{losses} \dots \dots \dots (3.2)$$

$QG_i$  - unit I's reactive power generation.

$QD_i$  - load on the bus for reactive power.

**Voltage Deviation:**

The voltage improvement index for a power system is defined as the deviation



of voltage magnitude of each and every bus from unity.[68] Thus, for a given system, The voltage improvement index is defined as

$$VD = \sum_{i=1}^n \left(1 - \frac{V_i}{V_{iref}}\right)^2 \dots\dots\dots (3.2)$$

Where n is the number of buses,  $V_{ref}$  is the reference voltage at bus I and  $V_i$  is the actual voltage at bus i.

### Multi objective optimization function [67]:

$$\text{Min } F = w_1 \frac{P_{loss}}{P_{loss_{base}}} + w_2 \frac{Q_{loss}}{Q_{loss_{base}}} + w_3 \times VD$$

Where  $P_{loss}$  and  $Q_{loss}$  are the active and reactive power losses with compensating devices;  $P_{loss_{base}}$  and  $Q_{loss_{base}}$  are the active and reactive power loss without compensating devices

Where  $w_1$   $w_2$   $w_3$  are the weightage factors on active power loss and reactive power loss and Voltage deviation.

### Operational constraints

The following restrictions are taken into account since the goal of using SVC is to regulate system variables such line real and reactive power flows and bus voltages.

### Power Flow balance equations

Each node must maintain a balance between its active and reactive powers. Power balance with relation to a bus may be written as equation [68] (3.3 & 3.4):

$$P_{Gi} - P_{Li} = V_i \sum_{j=1}^b [V_j [G'_{ij} \sin(\delta_i - \delta_j) - B'_{ij} \sin(\delta_i - \delta_j)]] \dots\dots\dots (3.3)$$

$$Q_{Gi} - Q_{Li} = V_i \sum_{j=1}^b [V_j [G'_{ij} \sin(\delta_i - \delta_j) - B'_{ij} \sin(\delta_i - \delta_j)]] \dots\dots\dots (3.4)$$

Where  $P_{Li}$  and  $Q_{Li}$  = load active and reactive powers at node i,

$P_{Gi}$  and  $Q_{Gi}$  = generated active and reactive powers,

The actual and hypothetical components of element  $Y'_{ij}$  of the  $[Y'_{bb}]$  matrix are represented by the conductance,  $G'_k$  and susceptance,  $B'_k$ , which were modified when the SVC was first introduced.

### Power loss limit

A limiting number,  $S_{l \max}$ , which reflects the thermal limit of the line or transformer in steady-state operation, must not be exceeded by the apparent power transferred by a branch  $l$ , in equation [68] (3.5).

$$S_l \leq S_{l \max} \quad \dots\dots\dots(3.5)$$

### Limits of generators:

$$\begin{aligned} P_{gi, \min} \leq P_{gi} \leq P_{gi, \max} \quad i = 1, \dots\dots\dots, N_G \\ Q_{gi, \min} \leq Q_{gi} \leq Q_{gi, \max} \quad i = 1, \dots\dots\dots, N_G \\ V_{gi, \min} \leq V_{gi} \leq V_{gi, \max} \quad i = 1, \dots\dots\dots, N_G \quad \dots\dots\dots(3.6) \end{aligned}$$

### Limits of reactive power compensators:

$$Q_{Ci, \min} \leq Q_{Ci} \leq Q_{Ci, \max} \quad i = 1, \dots\dots\dots, N_C \quad \dots\dots\dots(3.7)$$

### Limits of voltage magnitude for load buses[68]:

$$V_{Li, \min} \leq V_{Li} \leq V_{Li, \max} \quad i = 1, \dots\dots\dots, N_{pq} \quad \dots\dots\dots(3.8)$$

### Power limits of transmission line:

$$S_{Li, \min} \leq S_{Li} \leq S_{Li, \max} \quad i = 1, \dots\dots\dots, N_{tl} \quad \dots\dots\dots(3.9)$$

## 3.3 Thyristor Controlled Series Compensator

The TCSC focuses on certain dynamical issues in transmission systems. The TCSC addresses certain dynamical challenges in transmission systems. When big systems are connected, it first increases the damping ratio. Second, it eliminates Sub Synchronous Resonance (SSR) glitches; TCSC is capable of high-speed switching mechanisms for transmission power flow, allowing for load expansion of current transmission systems and quick power flow readjustment in a variety of situations.

Inside of its rating range, the TCSC controls steady-state power flow. The setup of TTCSC is shown in figure 3.2.

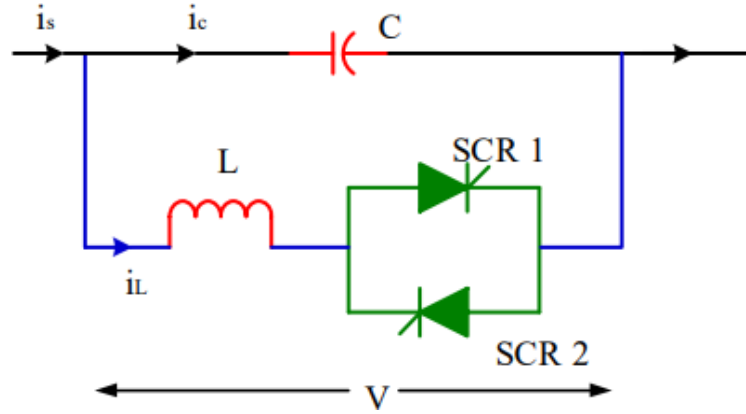


**Figure 3.2 Configuration of a TCSC**

### 3.4.1 Modeling of TCSC

By altering the transmission line's reactance, the TCSC functions as an inductive or capacitive compensator. Figure 3.3 depicts the TCSC equal circuit. By altering transmission line reactance, TCSC is shown. Because of this, the compensation values range from  $-0.8 X_{line}$  to  $0.2 X_{line}$ , as shown below.

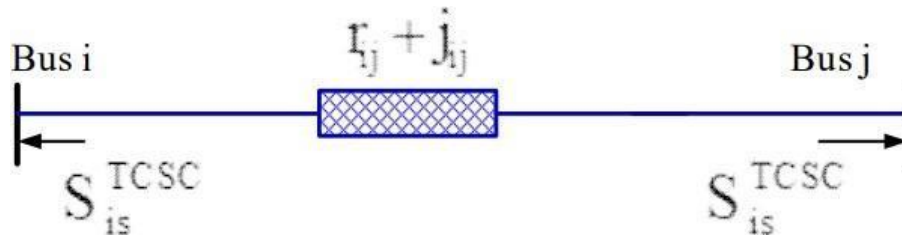


**Figure 3.3 Equivalent TCSC structure**

$$X_{ij} = X_{line} + X_{TCSC}$$

(3.10)

$$X_{TCSC} = \gamma_{TCSC} + X_{line}$$

(3.11)

Where,  $X_{line}$  = reactance of transmission line

$\gamma_{TCSC}$  = compensation factor of TCSC.

### 3.4.1 STATIC VAR COMPENSATOR

#### 3.4.1 SVC Equivalent Susceptance Model

The creation of quick SVCs in the early 1970s was made feasible by advancements in power electronics technology and control techniques. The

SVC is made up of banks of capacitors and reactors that are shunt linked, with quick control action provided by thyristor switching circuits.

The SVC may be seen as a changeable shunt reactance for operational purposes that automatically adapts to the operational circumstances of the system. The equivalent SVC pulls capacitive or inductive current from the network depending on the reactance type of the equivalent SVC, which may be either capacitive or inductive. Given that the associated SVC's equivalent reactance is appropriately low.

At the SVC connection point, the voltage magnitude may be adjusted and regulated. Thyristor switched capacitor and thyristor controlled reactor or fix capacitor and thyristor controlled reactor are the two most common configurations for continuously controlled SVC. Both setups may be represented similarly for steady-state analysis.

#### **3.4.2 Modeling of SVC**

The SVC was formerly modelled as a generator operating within bounds behind an inductive reactance in the SVC model used for power flow analysis. This reactance, or the slope  $X_{st}$  of the SVC, shows the SVC voltage regulation feature. For the sake of voltage regulation, a simpler formulation assumes that the SVC slope is zero. The SVC slope is assumed to be zero for voltage regulation in a simplified approximation. As long as the Static Var Compensator is running within parameters, this assumption could be fine, but if the SVC is operating near to its reactive limitations, it might result in serious mistakes. Figure 3.4 depicts the voltage current characteristic of SVC.

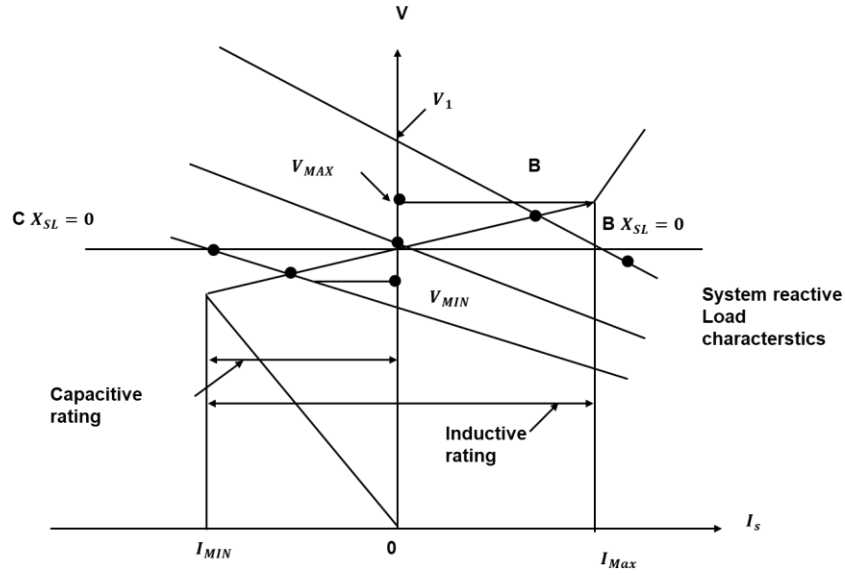


**Figure 3.4 Voltage- Current Characteristics of SVC**

When low loading situations are taken into account, the system's higher characteristics are shown. The generator will transgress the point  $B_{K_{SL}=0}$ , which is its minimal reactive limit, if the slope is assumed to be zero.

However, if the SVC slope which is shown by point B is taken into account, the generator will work well within bounds.

By connecting the generator to an auxiliary bus that is inductively linked to the high-voltage bus with a reactance that is equal to the per-unit slope of the SVC slope, the SVC characteristic may be expressed. In contrast to the high-voltage bus, the auxiliary bus is shown as a PV type bus. The generator representation deviates from reality when it acts outside of the bounds. It is important in these circumstances to switch the SVC representation to a fixed reactive Susceptance. Accurate findings are produced by this generator-susceptibility combination model. However, the quantity of buses needed varies between the two representations. In contrast to the fixed Susceptance, which only utilizes one bus, the generator employs two or three buses.

The current drawn and reactive power injected by the SVC can be expressed as  $I_{SVC} = jB_{SVC} * V$

$$Q_{SVC} = -jB_{SVC} * V^2$$

### 3.4.3 Modelling of STATCOM

A shunt compensating device called a STATCOM is used to alter transmission voltage and reactive power. The actual power exchange between the system and the STATCOM device may be disregarded in an ideal steady state analysis, and only the reactive power can be transferred between the system and the control device. Figure 3.5 shows the similar circuit for STATCOM.

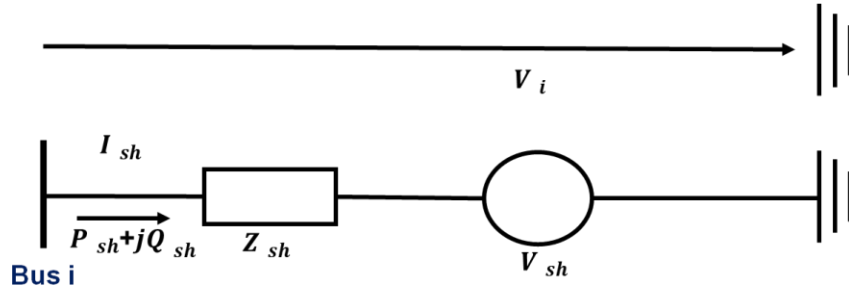


**Figure 3.5 Similar circuit for STATCOM**

It is assumed in the source that harmonics produced by the STATCOM are disregarded and the system, together with the STATCOM, is three-phase stable. A programmable significant frequency positive sequence voltage source  $V_{sh}$  may therefore be used to reliably indicate the STATCOM. The power flow constraints are,

$$P_{sh} = V_i^2 g_{sh} - V_i V_h \left( g_{sh} \cos(\theta_i - \theta_{sh}) + b_{sh} \sin(\theta_i - \theta_{sh}) \right) \quad (3.12)$$

$$Q_{sh} = -V_i^2 b_{sh} - V_i V_h \left( g_{sh} \sin(\theta_i - \theta_{sh}) - b_{sh} \cos(\theta_i - \theta_{sh}) \right) \quad (3.13)$$

Where,  $g_{sh} + jb_{sh} = 1/Z_{sh}$

The operating limit of the Static Compensator (STATCOM) is the real power exchange through the DC-link as,

$$PE = (V_{sh} I^*)_{s\neq 0} \quad (3.14)$$

Where

$$Re(V_{sh} I^*)^2 g_{sh} - V_i V_h \left( g_{sh} \sin(\theta_i - \theta_{sh}) - b_{sh} \cos(\theta_i - \theta_{sh}) \right)$$

In reactive power control mode, reactive power is controlled by the

reactive power injection reference provided by STATCOM. Such a control constraint is defined as follows in equation (3.15):

$$Q_{sh} - Q_{sh}^{spec} = 0 \dots\dots\dots (3.15)$$

$Q_{sh}^{spec}$ - Reactive power injection control reference.

### 3.5 FACTS optimal allocation

To enhance power transfer efficiency and voltage profile, FACTS devices regulate various transmission line parameters such as voltage, current, angle, and impedance. However, the optimum location of these devices is necessary to use them to their greatest capacity. The potential advantages of FACTS are limited by poor placement, which also increases the cost.

### 3.6 Particle swarm optimization

PSO is a heuristic method. It is a technique that is stochastic, self-adaptive, and population based. This approach introduces a swarm of particles and then updates their velocities and positions depending on their fitness rating. As a result, each particle repeatedly achieves the optimal global location. Particle velocities are regulated by inertia weights. The processes for determining appropriate SVC, STATCOM, and TCSC size for PSO are as follows.

#### Stage 1: Receiving the power system data and initialize PSO

Power system line and bus data are supplied in the first stage, and PSO is initialised. There are limits on the number of particles, the number of iterations, and the initial inertial weights. In addition, specific search spaces for TCSC, SVC, and STATCOM sizes are provided. Limits for TCSCs, SVCs, and STATCOM's size are determined by the search space. Random initialization is used for particle size and velocity. SVC, STATCOM, and TCSC-sized particles are present here.

#### Stage 2: Fitness function evaluation

The Newton Raphson power flow technique is used to compute load flow, and FACTS devices are connected at their optimum positions as defined by their respective indices.

The goal function also known as the fitness function for each particle is then assessed.

### Stage 3: $P_{best}$ and $G_{best}$ evaluation

$P_{best}$  stands for the personal best of each particle, which is the objective function's minimum value for that particle over all iterations.  $G_{best}$ , on the other hand, refers to the minimal fitness function value among all particles and stands for global best.  $Q_{best}$  and  $G_{best}$  are updated after each iterations by comparing them to the values from the preceding iteration.

$$P_{best_p^{i+1}} = \begin{cases} X_p^{i+1} & f_p^{i+1} \leq f_p^i \\ P_{best_p^i} & f_p^{i+1} \geq f_p^i \end{cases} \quad (3.19)$$

Where 'p' stands for particle and  $f_i$  is the fitness value of the particle at iteration i. Similarly,  $H_{best}$  is updated in each iteration as follows:

$$G_{best^{i+1}} = \begin{cases} P_{best_p^{i+1}} & f_p^{i+1} \leq f_p^i \\ G_{best_p^i} & f_p^{i+1} \geq f_p^i \end{cases} \quad (3.20)$$

### Stage 4: Revise your position and velocity.

After revising  $Q_{best}$  and  $P_{best}$  values, each particle velocity is modified to guide it to the optimal position. The following formula is used to update velocity:

$$V_i^{k+1} = w \times v_i^k + c1 \times rand_1 \times (Pbest_i^k - s_i^k) + c2 \times rand_2 \times (Gbest_i^k - s_i^k) \quad (3.21)$$

A random integer between [0, 1] is used for  $rand_1$  and  $rand_2$ , and  $k$  is the iteration number. The acceleration coefficients for the particle are [1, 2] for  $c_2$  and  $c_1$  respectively.  $W$  is the inertial weight, and the following formula is used to change its value after each iteration.

$$w = \frac{w_{max} - w_{mi}}{iter_{max}} \times iter \quad (3.22)$$

The positions of the particles are updated when each particle's velocity has been revised.

$$S_i^{k+1} = S_i^k + V_i^{k+1} \quad (3.23)$$



The flowchart for the PSO algorithm is depicted in figure 3.6.

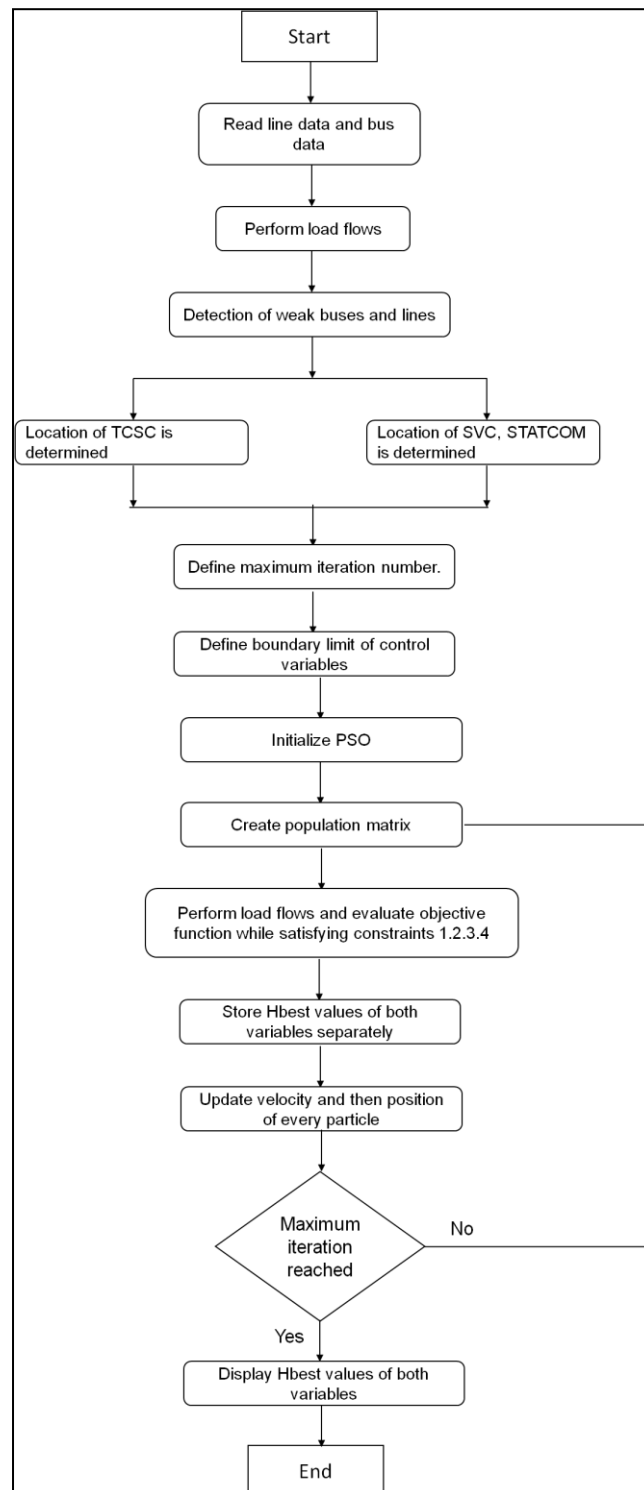


**Figure 3.6: Flowchart of PSO algorithm**

### 3.7 SQUIRREL SEARCH ALGORITHM

Based on the gliding behavior of squirrels, this algorithm was developed. Instead of flying, they choose the unusual kind of mobility known as "gliding," which is seen in figure 3.7 and allows them to go great distances quickly and

effectively. Figure 3.8 depicts the standard SSA's process.



**Figure 3.7 Flying squirrel landing on a tree**

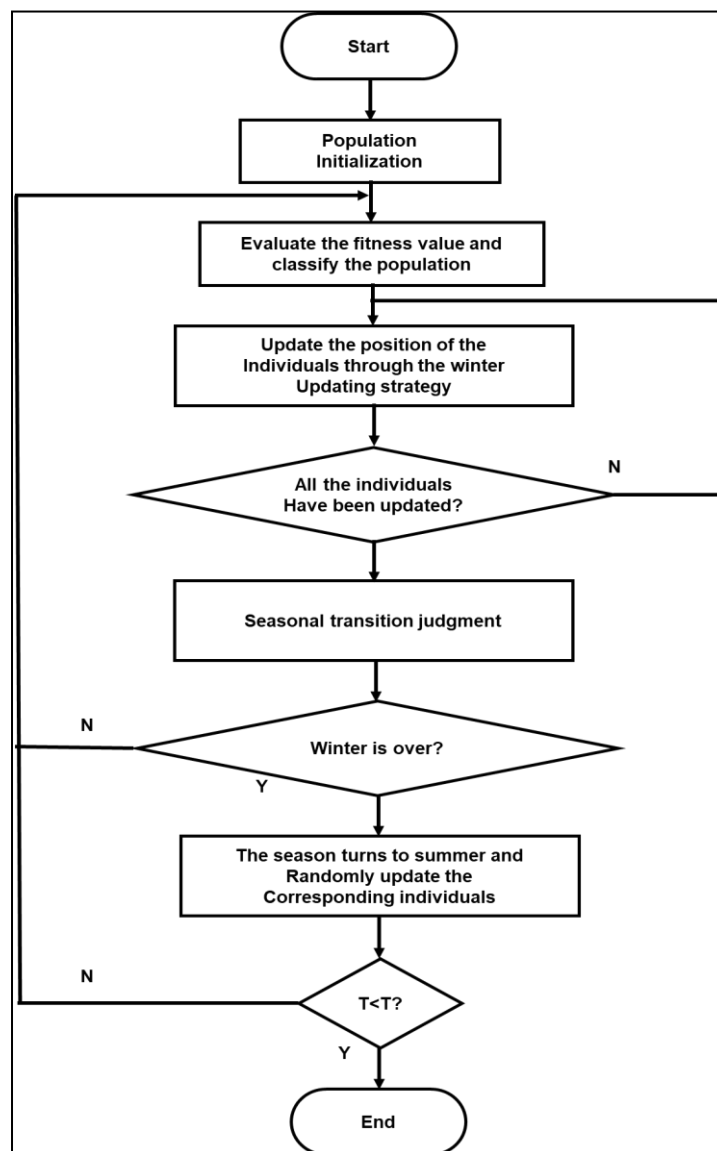


**Figure 3.8 Standard squirrel search algorithm's process**

## Initialize the Population

The upper and lower boundaries of the search space are  $FS_U$  and  $FS_L$ , assuming that the population size is  $N$ .  $N$  people are generated at random using equation (3.24):

$$FS_i = FS_L + r(1, D) \times (FS_U - FS_L) \dots\dots\dots (3.24)$$

$FS_i = i^{\text{th}}$  individual,

$i = 1. N$ ,

$D$  = dimension of the problem,

rand = random number between 0 and 1.

## Classify the Population

SSA stipulates that there must be a single squirrel at each tree, thus if the total number of squirrels is  $N$ , there must be  $N$  trees in the forest. Let's use the minimization issue as an example. One hickory tree and  $N_{fs}$  ( $1 < N_{fs} < \infty$ ) acorn trees are present in every  $N$  tree; all other trees are regular trees without any food. The acorn tree comes in second position as the greatest source of food for squirrels, after the hickory tree. Depending on the varied issues,

$N_{fs}$  may vary. Individuals found in hickory trees ( $F_h$ ), individuals found in acorn trees ( $F_a$ ), and individuals found in regular trees ( $F_n$ ) are classified according to the population's fitness ratings in ascending order ( $F_n$ ). The person with the lowest fitness value is designated as  $F_h$ , followed by people with fitness values ranging from 2 to  $N_{fs} + 1$ , and the remaining individuals are designated as  $F_n$ . The destination of  $F_a$  is  $F_h$  in order to locate the most advantageous food source, whereas the destinations of  $F_n$  are chosen at random as either  $F_a$  or  $F_h$ .

## Update the Position

The people glide to the acorn or hickory trees to update their places. Equations (3.25) and (3.26), which represent the particular updating formulas, are as follows:

$$\begin{cases} FS_i^{t+1} = FS_i^t + d_g \times G_c \times (F_h^t - FS_i^t) & \text{if } r > P_{dp} \\ \text{random location} & \text{otherwise} \end{cases} \quad (3.25)$$

$$FS^{t+1}_i = FS^t_i + d_g \times G_c \times \begin{cases} -FS^t_{ai} & \text{if } r > P_{dp} \\ random\ location & \text{otherwise} \end{cases} \quad (3.26)$$

$P_{dp}$  = predator appearance probability

T = current iteration,

$G_c$  = constant with the value of 1.9,

R = random number between 0 and 1.

If  $r > P_{dp}$  then, there being no threat, the squirrels are secure as they go through the forest in search of food.  $r \leq P_{dp}$ , the appearance of predators forces the squirrels to focus on fewer activities, puts them in danger, and causes unpredictable positional relocation.  $d_g$  = gliding distance which can be calculated by equation (3.27).

$$d_g = \frac{h_g}{\tan(\varphi) \times sf} \quad \dots\dots\dots (3.27)$$

sf = constant valued 18,

$h_g$  = constant valued 8,

$\tan(\varphi)$  = gliding angle which can be calculated by equation (3.28):

$$\tan(\varphi) = \frac{D}{L} \quad \dots\dots\dots (3.28)$$

L = lift force,

D = drag force which can be calculated by calculated by equations (3.29) and (3.30), respectively

$$D = \frac{1}{2\rho V^2 SC_D} \quad \dots\dots\dots (3.29)$$

$$L = \frac{1}{2\rho V^2 SC_L} \quad \dots\dots\dots (3.30)$$

The constants,  $\rho$ , V, S, and  $C_D$  are  $1.204 \text{ kg m}^{-3}$ ,  $5.25 \text{ ms}^{-1}$ ,  $154 \text{ cm}^2$ , and 0.6, respectively.  $r$ , is a random integer between 0.675 and 1.5.

### Seasonal Transition Judgement and Random Updating

Each cycle must start with all of the population in winter according to the normal SSA. After all the people have been updated, equations (3.31) and (3.32) are used to determine if the season changes:

$$S^t_c = \sqrt{\sum_{k=1}^D (F^t_{ai} - F^t_{h,k})^2} \quad i = 1, 2, \dots, N_{fs} \quad \dots\dots\dots (3.31)$$

$$S_{min} = \frac{10e^{-6}}{(365)^{t/(T/2.5)}} \quad \dots\dots\dots (3.32)$$

T= maximum number of iteration

If  $S_c^t < S_{min}$ , the season remains unaltered except from the end of winter and the transition to summer. All gliders to  $F_h$  remain at the updated location when the season changes to summer, whereas all gliders to  $F_a$  who do not encounter predators move to a new site according to equation (3.33):

$$FS_i^{t+1}new = FS_L + Le'(n) \times (FS_U - FS_L) \dots\dots\dots (3.33)$$

The random walk model known as  $Le'vy$  has steps that follow the  $Le'vy$  distribution and may be computed using equation (3.34):

$$Le'(x) = 0.01 \times \frac{r_a \times \sigma}{|r_b|^\beta} \dots\dots\dots (3.34)$$

, is a constant with the value 1.5, and  $\sigma$  can be computed using equation (3.35):

$$\sigma = \frac{\Gamma(1+\beta) \times \sin(\frac{\pi\beta}{2})}{\Gamma(\frac{\beta}{2}) \times \beta \times 2^{\frac{\beta-1}{2}}} \dots\dots\dots (3.35)$$

where  $\Gamma(x) = (x-1)!$

For a balanced diet, squirrels decide to consume acorn nuts in the summer and hickory nuts in the winter. They consume one acorn just before the environment temperature drops, which swiftly provides them with their daily energy needs. They start looking for the best winter food sources in order to reduce their excursions in the cold and conserve them for a longer period of time. They move between acorn and hickory trees while looking for food, instead of staying still in either one. Algorithm 3.1 represents the implementation process for squirrel search algorithm.

---

**Algorithm: 3.1 Squirrel Search Algorithm**

---

**Step 1:** Define input parameters i.e., number of flying squirrels, dimension, maximum number of iterations, gliding constant  $G_c$ , density of air  $p$ , lift coefficient  $C_L$ , drag coefficient  $C_D$ , Speed  $V$ , height  $h_g$ ,

**Step 2:** Generate random locations for  $q$  number of flying squirrels using following equation

$$SS_i = SS_L + (0,1) \times (SS_u - SS_l)$$

Where  $SS_l$  and  $SS_u$  are lower and upper bounds respectively of  $i^{th}$  flying squirrel in  $j^{th}$  dimension and  $U(0, 1)$  is a uniformly distributed random number in the  $f$  range  $[0, 1]$ .

**Step 3:** Evaluate fitness of each flying squirrel's location.

**Step 4:** Sort the locations of flying squirrels based on their fitness value.

**Step5:** Declare the flying squirrels on hickory nut tree, acorn nut tree and normal trees i.e., Best value will be of that flying squirrel located at hickory nut tree, then next three fit values of flying squirrels will be on acorn trees and then remaining will be on normal trees.

**Step 6:** Select randomly some flying squirrels which are on normal trees move towards hickory nut tree and the remaining will move towards acorn nuts trees.

While (stopping criteria is not satisfied)

For m=1 to  $q^1$

$q^1 =$

*total number of flying squirrels on acorn tree, proceed towards hickory trees)*

If  $R1 > 0.1$

$$SS_{at}^{m+1} = SS_{at}^m + d_g \times G_c \times (SS_{nt}^m - SS_{at}^m)$$

Else

$SS_{at}^{m+1} = \text{Random location will be allocated}$

End

End

For m=1 to

$q^2(q^2 =$

*total number of flying squirrels on common trees and proceed towards acorn tree*

$$SS_{at}^{m+1} = SS_{at}^m + d_g \times G_c \times (SS_{nt}^m - SS_{at}^m)$$

End

End

For m=1 to

$q^3(q^3 =$

*total number of flying squirrels on common trees and proceed towards acorn tree*

If  $R1 > 0.1$

$$SS_{at}^{m+1} = SS_{at}^m + d_g \times G_c \times (SS_{nt}^m - SS_{at}^m)$$

Else

$SS_{at}^{m+1} = \text{Random location will be allocated}$

End

End

End

**Step 7:** Calculate seasonal constant  $S_c$  and  $S_{min}$  using equations

$$\left( \overline{SS_c^t} - \sqrt{\sum_{k=1}^u SS_{at,k}^t - SS_{ht,k}^t} \right) ; S_{min} = \frac{10aE^{-6}}{(365)^{\frac{t}{(tm/2.5)}}}$$

Where  $t = 1, 2, 3$

**Step 8:** Check whether the seasonal monitoring condition ( $S_c^t < S_{min}$ ) is

satisfied and randomly relocate squirrels using equation

$$SS_L + Levy(n) \times (SS_U - SS_L)$$

$$\text{Where, } L(x) = 0.01 \times \frac{r_1}{|r_2|^{1/a}} \times y$$

$r_1$  and  $r_2$  are random numbers in the range of (0,1) and

$$y = \left( \frac{(1+a) \times \sin(0.5\pi\alpha)}{2 \times a \times 2} \right)^{\frac{1}{0.5(a-1)}}$$

Where,  $a$  is a constant value = 1.5

**Step9:** Update the minimum value of seasonal constant ( $S_{min}$ ) by making  $m = m + 1$  and go to step 3.

**Step 10:** If the stopping criteria ( $ite < ite_{mix}$ ) is satisfied algorithm will be stop.

**Step 11:** The location of flying squirrel on hickory nut tree is final optimal solution.

---

### 3.8 SUMMARY

In this chapter, a PSO and SSA is suggested. The whole process is evaluated on a typical IEEE-30 bus system, and the findings show that the technique suggested may efficiently handle the OPF issue in a power system. Following a comparison of the OPF results with and without FACTS controllers, TCSC, SVC, and STATCOM, it was found that installing TCSC improved power system performance and reduced the goal functions under consideration to their best values.

## **CHAPTER 4**

### **SIMULATION RESULT AND EXPERIMENTAL ANALYSIS**

#### **4.1 SIMULATION RESULT**

The affect of placement of FACTS is verified by taking the IEEE 30 BUS system load flow results is used for verification purposes. The code has been done on MATLAB platform. The FACTS devices can absorb reactive power and inject reactive power in the power system.

The placement of FACTS devices not only reduces the active power loss and reactive power loss but also increase the utilization of the existing power network thereby increase the power transfer capacity

The IEEE-30 bus system was employed in the power flow study, which was simulated using the MATLAB tool. Figure 4.1 depicts the IEEE -30 bus system modeling. A simulated model of the IEEE-30 bus system is shown in figure 4.1. Furthermore, all input data such as PQ load data, branch data, power generation data, PV generator data, transformer tap setting data, model of IEEE-30 bus, and so on are included.



## 4.2 EXPERIMENTAL ANALYSIS

### 4.2.1 WITHOUT FACTS DEVICES

The OPF issues were resolved in order to construct the proposed PSO and SSA on the IEEE-30 bus system. The specifics are provided below.

**Table 4.1:** Load flow results of IEEE 30 BUS system without FACTS devices.

| Bus No | Voltage magnitude (PU) | Phase angle (in degree) |
|--------|------------------------|-------------------------|
| 1      | 1.06                   | 0                       |
| 2      | 1.043                  | -5.5053                 |
| 3      | 1.0294                 | -8.1604                 |
| 4      | 1.0224                 | -9.8455                 |
| 5      | 1.01                   | -14.3429                |
| 6      | 1.0218                 | -11.5516                |
| 7      | 1.0093                 | -13.2208                |
| 8      | 1.0227                 | -12.2986                |
| 9      | 1.0772                 | -14.5286                |
| 10     | 1.0719                 | -16.0626                |
| 11     | 1.1217                 | -14.5286                |
| 12     | 1.0913                 | -15.4432                |
| 13     | 1.1213                 | -15.4432                |
| 14     | 1.0758                 | -16.2651                |
| 15     | 1.0704                 | -16.3129                |
| 16     | 1.0761                 | -15.9577                |
| 17     | 1.068                  | -16.2257                |
| 18     | 1.0589                 | -16.8989                |
| 19     | 1.0552                 | -17.0474                |
| 20     | 1.0587                 | -16.8551                |
| 21     | 1.0583                 | -16.564                 |
| 22     | 1.0628                 | -16.3886                |
| 23     | 1.0583                 | -16.5756                |
| 24     | 1.0504                 | -16.735                 |
| 25     | 1.0405                 | -16.2874                |
| 26     | 1.0232                 | -16.6883                |
| 27     | 1.0427                 | -15.7663                |
| 28     | 1.0196                 | -12.1609                |
| 29     | 1.0232                 | -16.9499                |
| 30     | 1.012                  | -17.7985                |

**Table 4.2:** Load flow results without FACTS devices

| Bus No       | Generation |            | Load       |            |
|--------------|------------|------------|------------|------------|
|              | $P_g$ (PU) | $Q_g$ (PU) | $P_l$ (PU) | $Q_l$ (PU) |
| 1            | 2.6238     | -0.2159    | 0          | 0          |
| 2            | 0.4        | 0.         | 0.217      | 0.127      |
| 3            | 0          | 0          | 0.024      | 0.012      |
| 4            | 0          | 0          | 0.076      | 0.016      |
| 5            | 0          | 0          | 0.942      | 0.19       |
| 6            | 0          | 0          | 0          | 0          |
| 7            | 0          | 0          | 0.228      | 0.109      |
| 8            | 0          | 0.4        | 0.3        | 0.3        |
| 9            | 0          | 0          | 0          | 0          |
| 10           | 0          | 0          | 0.058      | 0.02       |
| 11           | 0          | 0.24       | 0          | 0          |
| 12           | 0          | 0          | 0.122      | 0.075      |
| 13           | 0          | 0.24       | 0          | 0          |
| 14           | 0          | 0          | 0.062      | 0.016      |
| 15           | 0          | 0          | 0.082      | 0.025      |
| 16           | 0          | 0          | 0.035      | 0.018      |
| 17           | 0          | 0          | 0.09       | 0.058      |
| 18           | 0          | 0          | 0.035      | 0.009      |
| 19           | 0          | 0          | 0.095      | 0.035      |
| 20           | 0          | 0          | 0.022      | 0.007      |
| 21           | 0          | 0          | 0.175      | 0.112      |
| 22           | 0          | 0          | 0          | 0          |
| 23           | 0          | 0          | 0.032      | 0.016      |
| 24           | 0          | 0          | 0.087      | 0.067      |
| 25           | 0          | 0          | 0          | 0          |
| 26           | 0          | 0          | 0.035      | 0.023      |
| 27           | 0          | 0          | 0          | 0          |
| 28           | 0          | 0          | 0          | 0          |
| 29           | 0          | 0          | 0.024      | 0.009      |
| 30           | 0          | 0          | 0.106      | 0.019      |
| <b>Total</b> | 3.0238     | 0.6641     | 2.847      | 1.267      |

**Table 4.3:** Line losses without FACTS devices.

| Line No.     | From<br>BUS | To<br>BUS | Active power<br>loss(PU) | Reactive power<br>loss(PU) |
|--------------|-------------|-----------|--------------------------|----------------------------|
| 1            | 1           | 2         | 0.0548                   | 0.1057                     |
| 2            | 1           | 3         | 0.0286                   | 0.0728                     |
| 3            | 2           | 4         | 0.0112                   | -0.0053                    |
| 4            | 3           | 4         | 0.0079                   | 0.0137                     |
| 5            | 2           | 5         | 0.0297                   | 0.0805                     |
| 6            | 2           | 6         | 0.0208                   | 0.0231                     |
| 7            | 4           | 6         | 0.0059                   | 0.0113                     |
| 8            | 5           | 7         | 0.0012                   | -0.0179                    |
| 9            | 6           | 7         | 0.0037                   | -0.0061                    |
| 10           | 6           | 8         | 0.0011                   | -0.0055                    |
| 11           | 6           | 9         | 0                        | 0.0197                     |
| 12           | 6           | 10        | 0                        | 0.0131                     |
| 13           | 9           | 11        | 0                        | 0.0095                     |
| 14           | 9           | 10        | 0                        | 0.0078                     |
| 15           | 4           | 12        | 0                        | 0.0447                     |
| 16           | 12          | 13        | 0                        | 0.0064                     |
| 17           | 12          | 14        | 0.0007                   | 0.0015                     |
| 18           | 12          | 15        | 0.0022                   | 0.0043                     |
| 19           | 12          | 16        | 0.0006                   | 0.0013                     |
| 20           | 14          | 15        | 0.0001                   | 0.0001                     |
| 21           | 16          | 17        | 0.0002                   | 0.0004                     |
| 22           | 15          | 18        | 0.0005                   | 0.0009                     |
| 23           | 18          | 19        | 0.0001                   | 0.0001                     |
| 24           | 19          | 20        | 0.0001                   | 0.0003                     |
| 25           | 10          | 20        | 0.0007                   | 0.0016                     |
| 26           | 10          | 17        | 0.0001                   | 0.0003                     |
| 27           | 10          | 21        | 0.0014                   | 0.003                      |
| 28           | 10          | 22        | 0.0003                   | 0.0006                     |
| 29           | 21          | 23        | 0                        | 0                          |
| 30           | 15          | 23        | 0.0003                   | 0.0007                     |
| 31           | 22          | 24        | 0.0005                   | 0.0008                     |
| 32           | 23          | 24        | 0.0001                   | 0.0002                     |
| 33           | 24          | 25        | 0.0002                   | 0.0004                     |
| 34           | 25          | 26        | 0.0004                   | 0.0006                     |
| 35           | 25          | 27        | 0.0002                   | 0.0004                     |
| 36           | 27          | 28        | 0                        | 0.0113                     |
| 37           | 27          | 29        | 0.0008                   | 0.0016                     |
| 38           | 27          | 30        | 0.0016                   | 0.0029                     |
| 39           | 29          | 30        | 0.0003                   | 0.0006                     |
| 40           | 8           | 28        | 0                        | -0.0446                    |
| 41           | 6           | 28        | 0.0005                   | -0.0116                    |
| <b>Total</b> |             |           | <b>0.1768</b>            | <b>0.3512</b>              |

#### 4.2.2 PSO STATCOM

Table 4.4 represents the PSO STATCOM results

**Table 4.4:** Voltage magnitude and Phase angle after placement of STATCOM

| Bus No | Case:1 $w_1=1$ , $w_2=0$ $w_3=0$ |                         | Case:2 $w_1=1/3$ $w_2=1/3$ $w_3=1/3$ |                         |
|--------|----------------------------------|-------------------------|--------------------------------------|-------------------------|
|        | Voltage magnitude (PU)           | Phase angle (in degree) | Voltage magnitude (PU)               | Phase angle (in degree) |
| 1      | 1.06                             | 0                       | 1.06                                 | 0                       |
| 2      | 1.0787                           | -4.2992                 | 1.0381                               | -5.4923                 |
| 3      | 1.0768                           | -6.032                  | 1.0106                               | -7.9474                 |
| 4      | 1.0792                           | -7.3599                 | 0.9996                               | -9.6013                 |
| 5      | 1.0716                           | -11.2978                | 1.0048                               | -14.5483                |
| 6      | 1.0864                           | -8.6044                 | 0.9991                               | -11.4284                |
| 7      | 1.074                            | -10.0548                | 0.9936                               | -13.245                 |
| 8      | 1.0927                           | -9.5292                 | 0.9998                               | -12.2113                |
| 9      | 1.1488                           | -10.4026                | 1.0365                               | -14.7238                |
| 10     | 1.1439                           | -11.8562                | 1.0214                               | -16.4663                |
| 11     | 1.1959                           | -10.4026                | 1.0826                               | -14.7238                |
| 12     | 1.1676                           | -12.0636                | 1.0154                               | -15.3606                |
| 13     | 1.212                            | -12.0636                | 1.0475                               | -15.3606                |
| 14     | 1.1522                           | -12.702                 | 1.0037                               | -16.3242                |
| 15     | 1.1471                           | -12.3729                | 1.0026                               | -16.5069                |
| 16     | 1.1514                           | -12.1517                | 1.0104                               | -16.1358                |
| 17     | 1.1413                           | -12.1288                | 1.0126                               | -16.591                 |
| 18     | 1.1347                           | -12.8427                | 0.9963                               | -17.2538                |
| 19     | 1.1303                           | -12.9433                | 0.9961                               | -17.4705                |
| 20     | 1.133                            | -12.7252                | 1.0016                               | -17.2815                |
| 21     | 1.1331                           | -12.0619                | 1.0037                               | -16.9707                |
| 22     | 1.1371                           | -10.6121                | 1.0123                               | -16.8008                |
| 23     | 1.1339                           | -11.9531                | 1.0027                               | -16.9661                |
| 24     | 1.1078                           | -9.9598                 | 1                                    | -17.1553                |
| 25     | 1.1147                           | -10.2405                | 0.9993                               | -16.7024                |
| 26     | 1.0995                           | -10.5412                | 0.9813                               | -17.1376                |
| 27     | 1.111                            | -11.1049                | 1.0076                               | -16.1505                |
| 28     | 1.0876                           | -8.8039                 | 0.9953                               | -12.0759                |
| 29     | 1.0933                           | -12.3408                | 0.9874                               | -17.4198                |
| 30     | 1.0829                           | -13.2312                | 0.9757                               | -18.3318                |

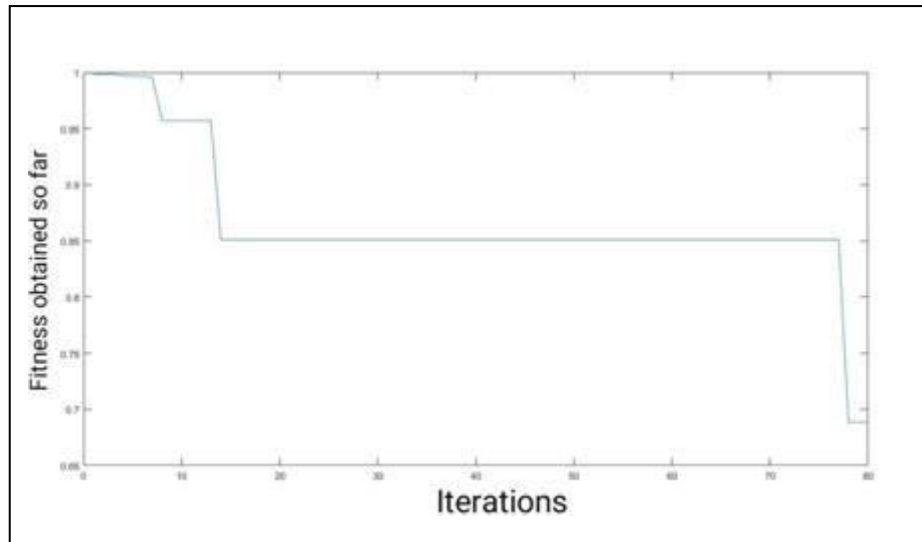


**Figure 4.1 Convergence curve case 1 of STATCOM**

**Iteration at convergence:88**

**Table 4.5: PSO STATCOM Case 1**

|                                     |                        |
|-------------------------------------|------------------------|
| Size of STATCOM                     | 88.24 MVA <sub>r</sub> |
| Location of Bus No                  | 24                     |
| Objective function without STATCOM  | 1.4865                 |
| Active power loss without STATCOM   | 0.1768(pu)             |
| Reactive power loss without STATCOM | 0.3513(pu)             |
| Active power loss with STATCOM      | 0.1219(pu)             |
| Reactive power loss with STATCOM    | 0.1035(pu)             |
| Objective function with STATCOM     | 0.6884                 |

**Table 4.6:** Line losses after placing STATCOM for Case1

| SL No.       | From Bus | To Bus | Active power loss (pu) | Reactive power loss (pu) |
|--------------|----------|--------|------------------------|--------------------------|
| 1            | 1        | 2      | 0.0355                 | 0.0458                   |
| 2            | 1        | 3      | 0.0161                 | 0.0193                   |
| 3            | 2        | 4      | 0.0057                 | -0.0256                  |
| 4            | 3        | 4      | 0.0052                 | 0.0051                   |
| 5            | 2        | 5      | 0.0196                 | 0.0341                   |
| 6            | 2        | 6      | 0.0113                 | -0.0097                  |
| 7            | 4        | 6      | 0.0039                 | 0.003                    |
| 8            | 5        | 7      | 0.0016                 | -0.0194                  |
| 9            | 6        | 7      | 0.0032                 | -0.0099                  |
| 10           | 6        | 8      | 0.0022                 | -0.003                   |
| 11           | 6        | 9      | 0                      | 0.013                    |
| 12           | 6        | 10     | 0                      | 0.0084                   |
| 13           | 9        | 11     | 0                      | 0.0106                   |
| 14           | 9        | 10     | 0                      | 0.0079                   |
| 15           | 4        | 12     | 0                      | 0.0359                   |
| 16           | 12       | 13     | 0                      | 0.0141                   |
| 17           | 12       | 14     | 0.0006                 | 0.0013                   |
| 18           | 12       | 15     | 0.0014                 | 0.0028                   |
| 19           | 12       | 16     | 0.0005                 | 0.0011                   |
| 20           | 14       | 15     | 0.0002                 | 0.0002                   |
| 21           | 16       | 17     | 0.0002                 | 0.0004                   |
| 22           | 15       | 18     | 0.0004                 | 0.0009                   |
| 23           | 18       | 19     | 0.0001                 | 0.0001                   |
| 24           | 19       | 20     | 0.0002                 | 0.0003                   |
| 25           | 10       | 20     | 0.0007                 | 0.0017                   |
| 26           | 10       | 17     | 0.0001                 | 0.0004                   |
| 27           | 10       | 21     | 0.0007                 | 0.0015                   |
| 28           | 10       | 22     | 0.0017                 | 0.0036                   |
| 29           | 21       | 23     | 0.0001                 | 0.0002                   |
| 30           | 15       | 23     | 0.0005                 | 0.001                    |
| 31           | 22       | 24     | 0.0026                 | 0.004                    |
| 32           | 23       | 24     | 0.0032                 | 0.0066                   |
| 33           | 24       | 25     | 0.0001                 | 0.0002                   |
| 34           | 25       | 26     | 0.0003                 | 0.0005                   |
| 35           | 25       | 27     | 0.0006                 | 0.0011                   |
| 36           | 27       | 28     | 0                      | 0.0055                   |
| 37           | 27       | 29     | 0.0009                 | 0.0016                   |
| 38           | 27       | 30     | 0.0017                 | 0.0032                   |
| 39           | 29       | 30     | 0.0004                 | 0.0007                   |
| 40           | 8        | 28     | 0.0003                 | -0.0499                  |
| 41           | 6        | 28     | 0.0001                 | -0.0151                  |
| <b>Total</b> |          |        | <b>0.1219</b>          | <b>0.1035</b>            |

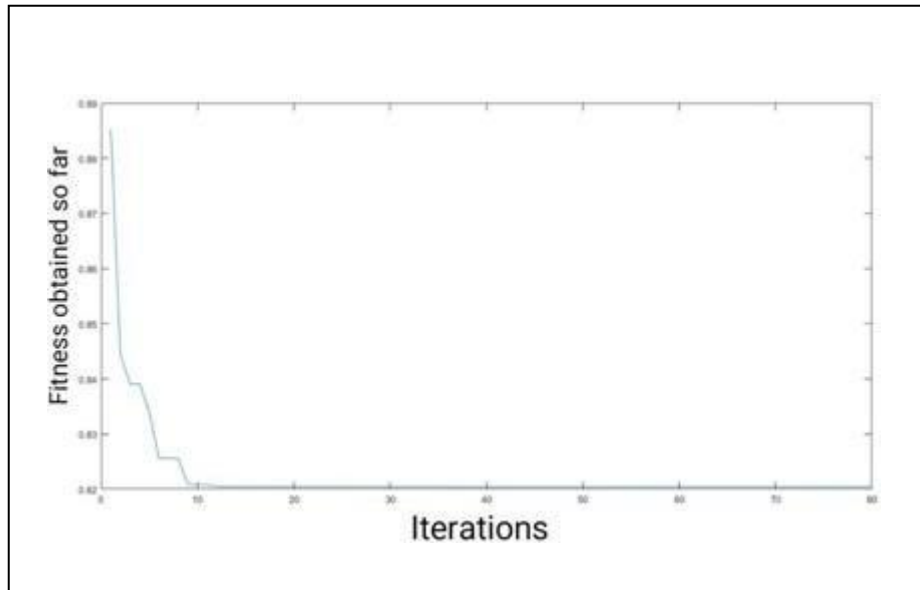


**Figure 4.2 Convergence Curve Case 2 Iteration at convergence:11**

Figure 4.6 depicts the STATCOM convergence curve. A quick-acting device known as a STATCOM may regulate voltage at the point of connection to a power grid by either delivering or absorbing reactive current. It is in the category of FACTS devices. The STATCOM case 2 ( $w_1=w_2=w_3=1/3$ ) is shown in Table 4.7

**Table 4.7: PSO STATCOM Case 2**

|                                    |                       |
|------------------------------------|-----------------------|
| Size of STATCOM                    | 39.33MVA <sub>r</sub> |
| Location of Bus No                 | 12                    |
| Objective function without STATCOM | 1.4865                |
| Active power loss without STATCOM  | 0.1768(pu)            |
| Reactive power loss with STATCOM   | 0.3513(pu)            |
| Active power loss with STATCOM     | 0.1321(pu)            |
| Reactive power loss with STATCOM   | 0.3295(pu)            |
| Objective function with STATCOM    | 1.0944                |

**Table 4.8:** Line losses after placing STATCOM for Case 2

| SL No.       | From Bus | To Bus | Active power loss(pu) | Reactive power loss(pu) |
|--------------|----------|--------|-----------------------|-------------------------|
| 1            | 1        | 2      | 0.00503               | 0.1075                  |
| 2            | 1        | 3      | 0.0286                | 0.0736                  |
| 3            | 2        | 4      | 0.0611                | -0.0028                 |
| 4            | 3        | 4      | 0.0079                | 0.0141                  |
| 5            | 2        | 5      | 0.0380                | 0.0858                  |
| 6            | 2        | 6      | 0.0231                | 0.0259                  |
| 7            | 4        | 6      | 0.0065                | 0.0137                  |
| 8            | 5        | 7      | 0.0019                | -0.0156                 |
| 9            | 6        | 7      | 0.0037                | -0.0055                 |
| 10           | 6        | 8      | 0.0012                | -0.0049                 |
| 11           | 6        | 9      | 0                     | 0.0079                  |
| 12           | 6        | 10     | 0                     | 0.0148                  |
| 13           | 9        | 11     | 0                     | 0.0102                  |
| 14           | 9        | 10     | 0                     | 0.011                   |
| 15           | 4        | 12     | 0                     | 0.0017                  |
| 16           | 12       | 13     | 0                     | 0.0073                  |
| 17           | 12       | 14     | 0.0004                | 0.0013                  |
| 18           | 12       | 15     | 0.0018                | 0.0035                  |
| 19           | 12       | 16     | 0.0001                | 0.0009                  |
| 20           | 14       | 15     | 0                     | 0                       |
| 21           | 16       | 17     | 0.0005                | 0.0003                  |
| 22           | 15       | 18     | 0.0004                | 0.0008                  |
| 23           | 18       | 19     | 0                     | 0.0001                  |
| 24           | 19       | 20     | 0.0002                | 0.0005                  |
| 25           | 10       | 20     | 0.0011                | 0.0024                  |
| 26           | 10       | 17     | 0.0003                | 0.0008                  |
| 27           | 10       | 21     | 0.0050                | 0.0043                  |
| 28           | 10       | 22     | 0.0001                | 0.0006                  |
| 29           | 21       | 23     | 0                     | 0                       |
| 30           | 15       | 23     | 0.0001                | 0.0003                  |
| 31           | 22       | 24     | 0.0005                | 0.0008                  |
| 32           | 23       | 24     | 0                     | 0.0001                  |
| 33           | 24       | 25     | 0.0001                | 0.0001                  |
| 34           | 25       | 26     | 0.0001                | 0.0007                  |
| 35           | 25       | 27     | .0002                 | 0.0006                  |
| 36           | 27       | 28     | 0                     | 0.0143                  |
| 37           | 27       | 29     | 0.0009                | 0.0032                  |
| 38           | 27       | 30     | 0.001                 | 0.0007                  |
| 39           | 29       | 30     | 0.00002               | 0.0032                  |
| 40           | 8        | 28     | 0                     | -0.0425                 |
| 41           | 6        | 28     | 0.0006                | -0.0107                 |
| <b>Total</b> |          |        | 0.1321                | 0.3295                  |



### 4.2.3 PSO TCSC

It is used to control active power flow in transmission lines to set levels within the electrical system. TCSC variants include controlled reactors connected in parallel to capacitor bank sections. The fundamental frequency capacitive reactance may be smoothly controlled across a broad range thanks to this combination. Following table represents the cases of TCSC.

**Table 4.9:** Voltage magnitude and Phase angle after placement of TCSC

| Bus No | Case:1 $w_1=1, w_2=0, w_3=0$ |                         | Case:2 $w_1=1/3, w_2=1/3, w_3=1/3$ |                         |
|--------|------------------------------|-------------------------|------------------------------------|-------------------------|
|        | Voltage magnitude (pu)       | Phase angle (in degree) | Voltage magnitude (pu)             | Phase angle (in degree) |
| 1      | 1.06                         | 0                       | 1.06                               | 0                       |
| 2      | 1.043                        | -5.5053                 | 1.043                              | -4.0632                 |
| 3      | 1.0146                       | -8.1604                 | 1.0294                             | -3.289                  |
| 4      | 1.0114                       | -9.8455                 | 1.0224                             | -6.0806                 |
| 5      | 1.01                         | -14.3429                | 1.01                               | -12.2327                |
| 6      | 1.0086                       | -11.5516                | 1.0218                             | -8.3909                 |
| 7      | 1.0014                       | -13.2208                | 1.0093                             | -10.4949                |
| 8      | 1.0093                       | -12.2986                | 1.0227                             | -9.1588                 |
| 9      | 0.9936                       | -14.5286                | 1.0772                             | -12.0348                |
| 10     | 0.9737                       | -16.0626                | 1.0719                             | -13.9861                |
| 11     | 1.0416                       | -14.5286                | 1.1217                             | -12.0348                |
| 12     | 0.9686                       | -15.4432                | 1.0913                             | -12.8744                |
| 13     | 1.0021                       | -15.4432                | 1.1213                             | -12.8744                |
| 14     | 0.956                        | -16.2651                | 1.0758                             | -13.9179                |
| 15     | 0.9546                       | -16.3129                | 1.0704                             | -14.095                 |
| 16     | 0.9629                       | -15.9577                | 1.0761                             | -13.6817                |
| 17     | 0.9647                       | -16.2257                | 1.068                              | -14.1408                |
| 18     | 0.9478                       | -16.8989                | 1.0589                             | -14.8959                |
| 19     | 0.9474                       | -17.0474                | 1.0552                             | -15.1213                |
| 20     | 0.9531                       | -16.8551                | 1.0587                             | -14.9052                |
| 21     | 0.9549                       | -16.564                 | 1.0583                             | -14.549                 |
| 22     | 0.9631                       | -16.3886                | 1.0628                             | -14.3414                |
| 23     | 0.9538                       | -16.5756                | 1.0583                             | -14.5461                |
| 24     | 0.9489                       | -16.735                 | 1.0504                             | -14.7068                |
| 25     | 0.9457                       | -16.2874                | 1.0405                             | -14.172                 |
| 26     | 0.9266                       | -16.6883                | 1.0232                             | -14.6588                |
| 27     | 0.9529                       | -15.7663                | 1.0427                             | -13.5401                |
| 28     | 1.0051                       | -12.1609                | 1.0196                             | -9.0252                 |
| 29     | 0.9314                       | -16.9499                | 1.0232                             | -14.962                 |
| 30     | 0.919                        | -17.7985                | 1.012                              | -15.9879                |

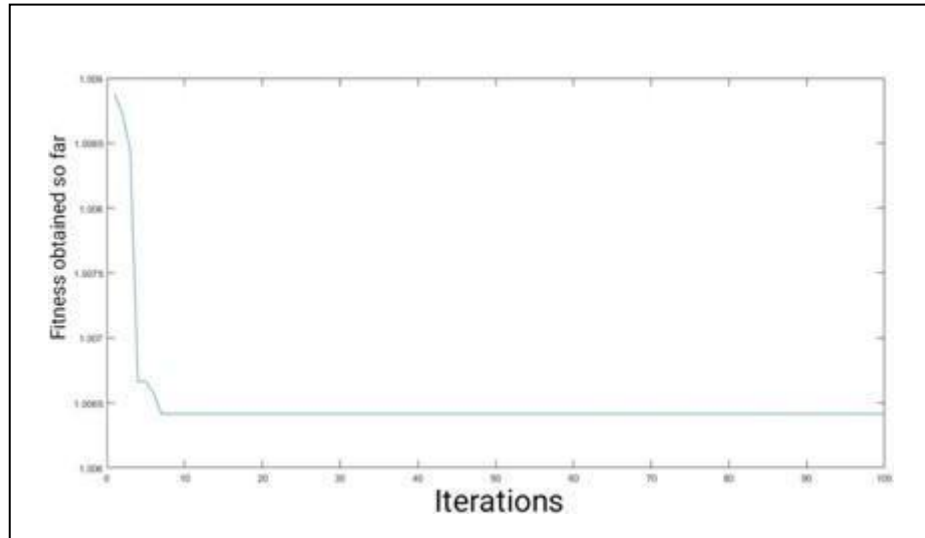


**Figure 4.3: Convergence Curve Case 1 .Iterations at convergence:9**

**Table 4.10 PSO TCSC Case 1**

|                                  |            |
|----------------------------------|------------|
| Size of TCSC                     | 0.0239MVar |
| Location of Line number          | 2          |
| Objective function without TCSC  | 1.4865     |
| Active power loss without TCSC   | 0.1768(pu) |
| Reactive power loss without TCSC | 0.3513(pu) |
| Active power loss with TCSC      | 0.1295(pu) |
| Reactive power loss with TCSC    | 0.2475(pu) |
| Objective function with TCSC     | 0.9947     |

**Table 4.11:** Line losses after placing TCSC for Case1

| SL. No.      | From Bus | To bus | Active power loss (pu) | Reactive power loss (pu) |
|--------------|----------|--------|------------------------|--------------------------|
| 1            | 1        | 2      | 0.0103                 | 0.0324                   |
| 2            | 1        | 3      | 0.0224                 | 0.0154                   |
| 3            | 2        | 4      | 0.0039                 | -0.0271                  |
| 4            | 3        | 4      | 0.0203                 | 0.0496                   |
| 5            | 2        | 5      | 0.0255                 | 0.063                    |
| 6            | 2        | 6      | 0.012                  | -0.0029                  |
| 7            | 4        | 6      | 0.0108                 | 0.0283                   |
| 8            | 5        | 7      | 0.003                  | -0.0131                  |
| 9            | 6        | 7      | 0.0051                 | -0.0015                  |
| 10           | 6        | 8      | 0.0012                 | -0.0051                  |
| 11           | 6        | 9      | 0                      | 0.0193                   |
| 12           | 6        | 10     | 0                      | 0.0163                   |
| 13           | 9        | 11     | 0                      | 0.011                    |
| 14           | 9        | 10     | 0                      | 0.0138                   |
| 15           | 4        | 12     | 0                      | 0.0528                   |
| 16           | 12       | 13     | 0                      | 0.008                    |
| 17           | 12       | 14     | 0.0001                 | 0.0015                   |
| 18           | 12       | 15     | 0.006                  | 0.0038                   |
| 19           | 12       | 16     | 0.0004                 | 0.0009                   |
| 20           | 14       | 15     | 0                      | 0                        |
| 21           | 16       | 17     | 0.0001                 | 0.0003                   |
| 22           | 15       | 18     | 0.0004                 | 0.0008                   |
| 23           | 18       | 19     | 0                      | 0.0001                   |
| 24           | 19       | 20     | 0.0003                 | 0.0005                   |
| 25           | 10       | 20     | 0.0012                 | 0.0026                   |
| 26           | 10       | 17     | 0.0003                 | 0.0009                   |
| 27           | 10       | 21     | 0.0023                 | 0.0049                   |
| 28           | 10       | 22     | 0.0004                 | 0.0008                   |
| 29           | 21       | 23     | 0                      | 0                        |
| 30           | 15       | 23     | 0.0001                 | 0.0002                   |
| 31           | 22       | 24     | 0.0006                 | 0.001                    |
| 32           | 23       | 24     | 0                      | 0.0001                   |
| 33           | 24       | 25     | 0.0001                 | 0.0002                   |
| 34           | 25       | 26     | 0.0005                 | 0.0008                   |
| 35           | 25       | 27     | 0.0003                 | 0.0006                   |
| 36           | 27       | 28     | 0                      | 0.0155                   |
| 37           | 27       | 29     | 0.001                  | 0.0019                   |
| 38           | 27       | 30     | 0.0019                 | 0.0036                   |
| 39           | 29       | 30     | 0.0004                 | 0.0007                   |
| 40           | 8        | 28     | 0                      | -0.0433                  |
| 41           | 6        | 28     | 0.0006                 | -0.0111                  |
| <b>Total</b> |          |        | 0.1295                 | 0.2475                   |

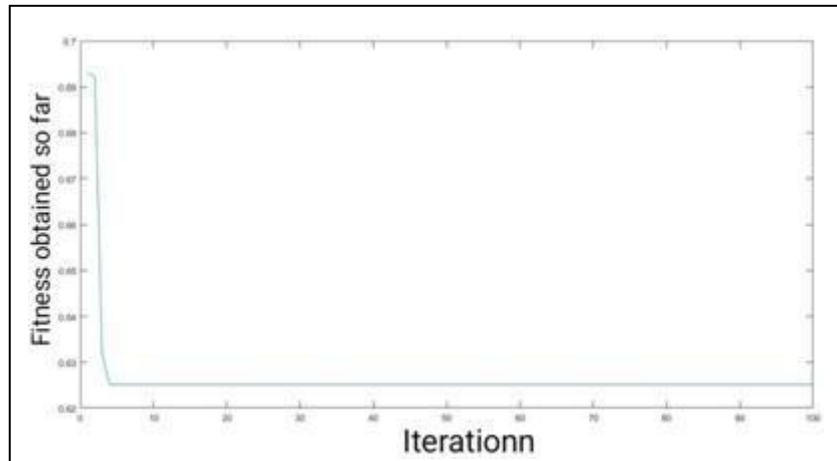


**Fig 4.4: Convergence curve case 2 .Iteration at convergence:8**

**Table 4.10: TCSC Case 2**

|                                  |             |
|----------------------------------|-------------|
| Size of TCSC                     | 0.0931 MVar |
| Location of line No              | 2           |
| Objective function without TCSC  | 1.4865      |
| Active power loss without TCSC   | 0.1768(pu)  |
| Reactive power loss without TCSC | 0.3513(pu)  |
| Active power loss with TCSC      | 0.1754(pu)  |
| Reactive power loss with TCSC    | 0.2491(pu)  |
| Objective function with TCSC     | 0.6251      |

The TCSC convergence curve for case 1 ( $w_1 = 1$  and  $w_2=w_3= 0$ ) is shown in figure 4.3. Figure 4.4 depicts the TCSC convergence curve for case 2, with  $w_1$  and  $w_2$  and  $w_3$  both equal to 0.333 The objective function's value is shown against the computing time required for minimization along the convergence curve.

**Table 4.11:** Line losses after placing TCSC for Case 2

| SL. No. | From Bus | To bus | Active power loss (pu) | Reactive power loss (pu) |
|---------|----------|--------|------------------------|--------------------------|
| 1       | 1        | 2      | 0.0303                 | 0.0324                   |
| 2       | 1        | 3      | 0.0724                 | 0.0154                   |
| 3       | 2        | 4      | 0.0039                 | -0.0271                  |
| 4       | 3        | 4      | 0.0203                 | 0.0496                   |
| 5       | 2        | 5      | 0.0255                 | 0.063                    |
| 6       | 2        | 6      | 0.012                  | -0.0029                  |
| 7       | 4        | 6      | 0.0108                 | 0.0283                   |
| 8       | 5        | 7      | 0.003                  | -0.0131                  |
| 9       | 6        | 7      | 0.0051                 | -0.0015                  |
| 10      | 6        | 8      | 0.0012                 | -0.0051                  |
| 11      | 6        | 9      | 0                      | 0.0193                   |
| 12      | 6        | 10     | 0                      | 0.0163                   |
| 13      | 9        | 11     | 0                      | 0.011                    |
| 14      | 9        | 10     | 0                      | 0.0138                   |
| 15      | 4        | 12     | 0                      | 0.0528                   |
| 16      | 12       | 13     | 0                      | 0.008                    |
| 17      | 12       | 14     | 0.0007                 | 0.0015                   |
| 18      | 12       | 15     | 0.0019                 | 0.0038                   |
| 19      | 12       | 16     | 0.0004                 | 0.0009                   |
| 20      | 14       | 15     | 0                      | 0                        |
| 21      | 16       | 17     | 0.0001                 | 0.0003                   |
| 22      | 15       | 18     | 0.0004                 | 0.0008                   |
| 23      | 18       | 19     | 0                      | 0.0001                   |
| 24      | 19       | 20     | 0.0003                 | 0.0005                   |
| 25      | 10       | 20     | 0.0012                 | 0.0026                   |
| 26      | 10       | 17     | 0.0003                 | 0.0009                   |
| 27      | 10       | 21     | 0.0023                 | 0.0049                   |
| 28      | 10       | 22     | 0.0004                 | 0.0008                   |
| 29      | 21       | 23     | 0                      | 0                        |
| 30      | 15       | 23     | 0.0001                 | 0.0002                   |
| 31      | 22       | 24     | 0.0006                 | 0.001                    |
| 32      | 23       | 24     | 0                      | 0.0001                   |
| 33      | 24       | 25     | 0.0001                 | 0.0002                   |
| 34      | 25       | 26     | 0.0005                 | 0.0008                   |
| 35      | 25       | 27     | 0.0003                 | 0.0006                   |
| 36      | 27       | 28     | 0                      | 0.0155                   |
| 37      | 27       | 29     | 0.001                  | 0.0019                   |
| 38      | 27       | 30     | 0.0019                 | 0.0036                   |
| 39      | 29       | 30     | 0.0004                 | 0.0007                   |
| 40      | 8        | 28     | 0                      | -0.0433                  |
| 41      | 6        | 28     | 0.0006                 | -0.0111                  |
| Total   |          |        | 0.1754                 | 0.2491                   |

#### 4.2.4 PSO SVC

**Table 4.12:** Bus Voltages and phase angle after Placement of SVC

| Bus No | Case:1 $w_1=1, w_2=0, w_3=0$ |                         | Case:2 $w_1=1/3, w_2=1/3, w_3=1/3$ |                         |
|--------|------------------------------|-------------------------|------------------------------------|-------------------------|
|        | Voltage magnitude (PU)       | Phase angle (in degree) | Voltage magnitude (PU)             | Phase angle (in degree) |
| 1      | 1.0600                       | 0                       | 1.06                               | 0                       |
| 2      | 1.0430                       | -5.5053                 | 1.043                              | -5.4821                 |
| 3      | 1.0339                       | -8.1604                 | 1.0399                             | -8.3134                 |
| 4      | 1.0279                       | -9.8455                 | 1.0352                             | -10.0226                |
| 5      | 1.0100                       | -14.3429                | 1.01                               | -14.2363                |
| 6      | 1.0279                       | -11.5516                | 1.0342                             | -11.6565                |
| 7      | 1.0129                       | -13.2208                | 1.0166                             | -13.2355                |
| 8      | 1.0290                       | -12.2986                | 1.0353                             | -12.3846                |
| 9      | 1.0917                       | -14.5286                | 1.1017                             | -14.4552                |
| 10     | 1.0911                       | -16.0626                | 1.1031                             | -15.8737                |
| 11     | 1.1357                       | -14.5286                | 1.1453                             | -14.4552                |
| 12     | 1.1065                       | -15.4432                | 1.14                               | -15.5645                |
| 13     | 1.1361                       | -15.4432                | 1.185                              | -15.5645                |
| 14     | 1.0929                       | -16.2651                | 1.1218                             | -16.3064                |
| 15     | 1.0889                       | -16.3129                | 1.1134                             | -16.2685                |
| 16     | 1.0931                       | -15.9577                | 1.1177                             | -15.9188                |
| 17     | 1.0866                       | -16.2257                | 1.1025                             | -16.0658                |
| 18     | 1.0778                       | -16.8989                | 1.0981                             | -16.7568                |
| 19     | 1.0744                       | -17.0474                | 1.0922                             | -16.8617                |
| 20     | 1.0778                       | -16.8551                | 1.0942                             | -16.6638                |
| 21     | 1.0823                       | -16.564                 | 1.0921                             | -16.38                  |
| 22     | 1.0825                       | -16.3886                | 1.0939                             | -16.1963                |
| 23     | 1.0825                       | -16.5756                | 1.0928                             | -16.4027                |
| 24     | 1.0707                       | -16.735                 | 1.0813                             | -16.5394                |
| 25     | 1.0561                       | -16.2874                | 1.0651                             | -16.0861                |
| 26     | 1.0391                       | -16.6883                | 1.0483                             | -16.4683                |
| 27     | 1.0552                       | -15.7663                | 1.0632                             | -15.5769                |
| 28     | 1.0264                       | -12.1609                | 1.0329                             | -12.2448                |
| 29     | 1.0360                       | -16.9499                | 1.0442                             | -16.7145                |
| 30     | 1.0249                       | -17.7985                | 1.0332                             | -17.529                 |

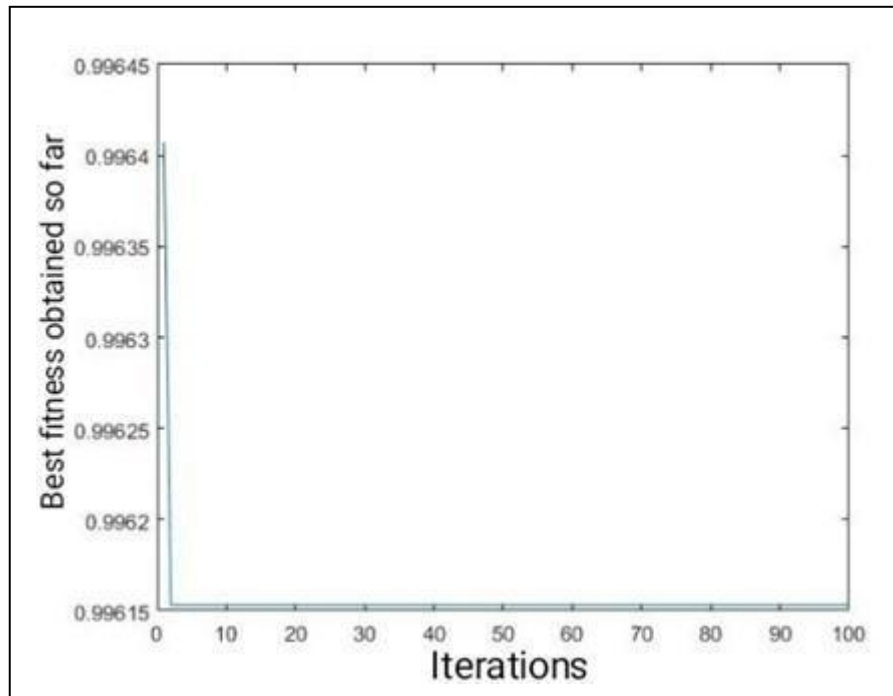


**Figure 4.5 Convergence Curve Case 1 Iteration at convergence:6**

**Table 4.13 PSO SVC Case 1**

|                                 |                       |
|---------------------------------|-----------------------|
| Size of svc                     | 5.05 MVA <sub>r</sub> |
| Location of Bus No              | 29                    |
| Objective function without SVC  | 1.4865                |
| Active power loss without SVC   | 0.1768(pu)            |
| Reactive power loss without SVC | 0.3513(pu)            |
| Active power loss with SVC      | 0.1761(pu)            |
| Reactive power loss with SVC    | 0.2362(pu)            |
| Objective function with SVC     | 0.9962                |

**Table 4.14:** Line losses after placing SVC for Case1

| SL. No.      | From bus | To bus | Active power loss (pu) | Reactive power loss (pu) |
|--------------|----------|--------|------------------------|--------------------------|
| 1            | 1        | 2      | 0.0546                 | 0.1051                   |
| 2            | 1        | 3      | 0.0288                 | 0.0733                   |
| 3            | 2        | 4      | 0.0112                 | -0.0052                  |
| 4            | 3        | 4      | 0.0079                 | 0.0138                   |
| 5            | 2        | 5      | 0.0294                 | 0.0795                   |
| 6            | 2        | 6      | 0.021                  | 0.0236                   |
| 7            | 4        | 6      | 0.006                  | 0.0114                   |
| 8            | 5        | 7      | 0.0011                 | -0.0182                  |
| 9            | 6        | 7      | 0.0038                 | -0.006                   |
| 10           | 6        | 8      | 0.0011                 | -0.0056                  |
| 11           | 6        | 9      | 0                      | 0.0225                   |
| 12           | 6        | 10     | 0                      | 0.0142                   |
| 13           | 9        | 11     | 0                      | 0.0093                   |
| 14           | 9        | 10     | 0                      | 0.0074                   |
| 15           | 4        | 12     | 0                      | 0.0435                   |
| 16           | 12       | 13     | 0                      | 0.0062                   |
| 17           | 12       | 14     | 0.0007                 | 0.0014                   |
| 18           | 12       | 15     | 0.0019                 | 0.0038                   |
| 19           | 12       | 16     | 0.0006                 | 0.0012                   |
| 20           | 14       | 15     | 0                      | 0                        |
| 21           | 16       | 17     | 0.0001                 | 0.0003                   |
| 22           | 15       | 18     | 0.0004                 | 0.0009                   |
| 23           | 18       | 19     | 0.0001                 | 0.0001                   |
| 24           | 19       | 20     | 0.0001                 | 0.0003                   |
| 25           | 10       | 20     | 0.0007                 | 0.0015                   |
| 26           | 10       | 17     | 0.0001                 | 0.0003                   |
| 27           | 10       | 21     | 0.0011                 | 0.0023                   |
| 28           | 10       | 22     | 0.0003                 | 0.0006                   |
| 29           | 21       | 23     | 0                      | -0.1129                  |
| 30           | 15       | 23     | 0.0002                 | 0.0004                   |
| 31           | 22       | 24     | 0.0005                 | 0.0007                   |
| 32           | 23       | 24     | 0.0002                 | 0.0004                   |
| 33           | 24       | 25     | 0.0004                 | 0.0007                   |
| 34           | 25       | 26     | 0.0004                 | 0.0006                   |
| 35           | 25       | 27     | 0.0002                 | 0.0004                   |
| 36           | 27       | 28     | 0                      | 0.0105                   |
| 37           | 27       | 29     | 0.0008                 | 0.0015                   |
| 38           | 27       | 30     | 0.0015                 | 0.0029                   |
| 39           | 29       | 30     | 0.0003                 | 0.0006                   |
| 40           | 8        | 28     | 0                      | -0.0451                  |
| 41           | 6        | 28     | 0.0005                 | -0.0119                  |
| <b>Total</b> |          |        | 0.1761                 | 0.2362                   |



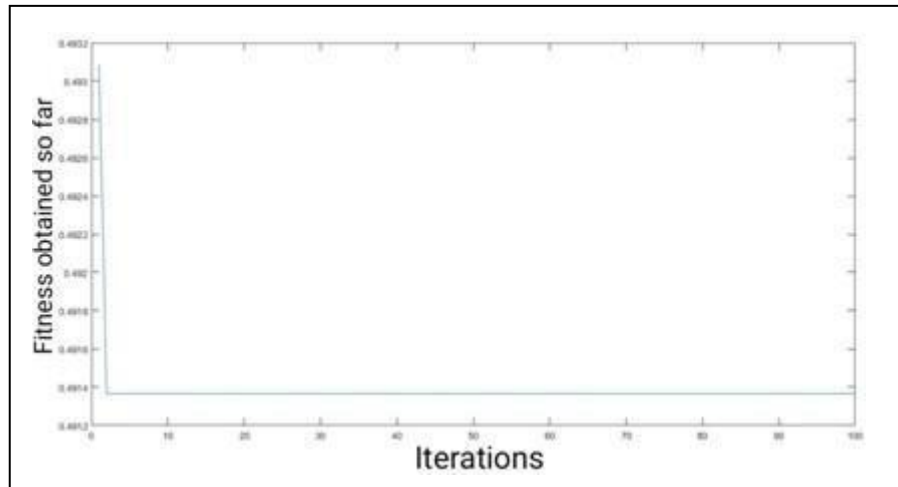


**Figure 4.6:** Convergence Curve Case 2.Iteration at Convergence:5

**Table 4.14: PSO SVC Case 2**

|                                 |                       |
|---------------------------------|-----------------------|
| Size of SVC                     | 11.58MVA <sub>r</sub> |
| Location of Bus No              | 16                    |
| Objective function without SVC  | 1.4865                |
| Active power loss without SVC   | 0.1768(pu)            |
| Reactive power loss without SVC | 0.3513(pu)            |
| Active power loss with SVC      | 0.1765(pu)            |
| Reactive power loss with SVC    | 0.0961(pu)            |
| Objective function with SVC     | 0.4914                |

. A FACTS device called a SVC is used for shunt compensation to keep the magnitude of the bus voltage constant. To continually adjust for changes in reactive power loads, SVC controls bus voltage. The SVC convergence curve for case 1 with  $w_1 = 1$  and  $w_2=w_3= 0$  is shown in figure 4.5. Figure 4.6 depicts the SVC convergence curve for case 2, with  $w_1$ ,  $w_2$  and  $w_3$  equal to 0.33.

**Table 4.16:** Line losses after placing SVC for Case 2

| SL. No.      | From bus | To bus | Active power loss (pu) | Reactive power loss (pu) |
|--------------|----------|--------|------------------------|--------------------------|
| 1            | 1        | 2      | 0.0243                 | 0.1044                   |
| 2            | 1        | 3      | 0.0193                 | 0.0751                   |
| 3            | 2        | 4      | 0.0117                 | -0.0042                  |
| 4            | 3        | 4      | 0.008                  | 0.014                    |
| 5            | 2        | 5      | 0.0291                 | 0.0783                   |
| 6            | 2        | 6      | 0.0212                 | 0.0241                   |
| 7            | 4        | 6      | 0.0056                 | 0.0098                   |
| 8            | 5        | 7      | 0.0011                 | -0.0183                  |
| 9            | 6        | 7      | 0.004                  | -0.0057                  |
| 10           | 6        | 8      | 0.0011                 | -0.0058                  |
| 11           | 6        | 9      | 0                      | 0.0228                   |
| 12           | 6        | 10     | 0                      | 0.0138                   |
| 13           | 9        | 11     | 0                      | 0.0091                   |
| 14           | 9        | 10     | 0                      | 0.0068                   |
| 15           | 4        | 12     | 0                      | 0.0496                   |
| 16           | 12       | 13     | 0                      | -0.2559                  |
| 17           | 12       | 14     | 0.0008                 | 0.0017                   |
| 18           | 12       | 15     | 0.0028                 | 0.0055                   |
| 19           | 12       | 16     | 0.0011                 | 0.0022                   |
| 20           | 14       | 15     | 0.0002                 | 0.0002                   |
| 21           | 16       | 17     | 0.0005                 | 0.0011                   |
| 22           | 15       | 18     | 0.0006                 | 0.0012                   |
| 23           | 18       | 19     | 0.0001                 | 0.0002                   |
| 24           | 19       | 20     | 0.0001                 | 0.0002                   |
| 25           | 10       | 20     | 0.0006                 | 0.0012                   |
| 26           | 10       | 17     | 0.0001                 | 0.0001                   |
| 27           | 10       | 21     | 0.0011                 | 0.0024                   |
| 28           | 10       | 22     | 0.0003                 | 0.0007                   |
| 29           | 21       | 23     | 0                      | 0                        |
| 30           | 15       | 23     | 0.0009                 | 0.0017                   |
| 31           | 22       | 24     | 0.0005                 | 0.0008                   |
| 32           | 23       | 24     | 0.0002                 | 0.0004                   |
| 33           | 24       | 25     | 0.0004                 | 0.0008                   |
| 34           | 25       | 26     | 0.0004                 | 0.0006                   |
| 35           | 25       | 27     | 0.0002                 | 0.0004                   |
| 36           | 27       | 28     | 0                      | 0.0097                   |
| 37           | 27       | 29     | 0.0008                 | 0.0015                   |
| 38           | 27       | 30     | 0.0015                 | 0.0028                   |
| 39           | 29       | 30     | 0.0003                 | 0.0006                   |
| 40           | 8        | 28     | 0                      | -0.0457                  |
| 41           | 6        | 28     | 0.0005                 | -0.0121                  |
| <b>Total</b> |          |        | 0.1394                 | 0.0961                   |

## 4.2.5 SSA STATCOM

**Table 4.17:** Voltage magnitude and Phase angle

| Bus No | Case:1 $w_1=1$ , $w_2=0$ $w_3=0$ |                         | Case:2 $w_1=1/3$ , $w_2=1/3$ $w_3=1/3$ |                         |
|--------|----------------------------------|-------------------------|--|-------------------------|
|        | Voltage magnitude (PU)           | Phase angle (in degree) | Voltage magnitude ( PU)                | Phase angle (in degree) |
| 1      | 1.06                             | 0                       | 1.06                                   | 0                       |
| 2      | 1.043                            | -5.4861                 | 1.043                                  | -5.5053                 |
| 3      | 1.0378                           | -8.2638                 | 1.0294                                 | -8.1604                 |
| 4      | 1.0326                           | -9.9641                 | 1.0224                                 | -9.8455                 |
| 5      | 1.01                             | -14.2578                | 1.01                                   | -14.3429                |
| 6      | 1.0332                           | -11.6743                | 1.0218                                 | -11.5516                |
| 7      | 1.0161                           | -13.2551                | 1.0093                                 | -13.2208                |
| 8      | 1.0344                           | -12.4055                | 1.0227                                 | -12.2986                |
| 9      | 1.1046                           | -14.5996                | 1.0772                                 | -14.5286                |
| 10     | 1.1082                           | -16.074                 | 1.0719                                 | -16.0626                |
| 11     | 1.1481                           | -14.5996                | 1.1217                                 | -14.5286                |
| 12     | 1.1196                           | -15.3256                | 1.0913                                 | -15.4432                |
| 13     | 1.1488                           | -15.3256                | 1.1213                                 | -15.4432                |
| 14     | 1.1074                           | -16.1414                | 1.0758                                 | -16.2651                |
| 15     | 1.1046                           | -16.2812                | 1.0704                                 | -16.3129                |
| 16     | 1.1079                           | -15.8853                | 1.0761                                 | -15.9577                |
| 17     | 1.1031                           | -16.2015                | 1.068                                  | -16.2257                |
| 18     | 1.0942                           | -16.8401                | 1.0589                                 | -16.8989                |
| 19     | 1.0911                           | -16.9848                | 1.0552                                 | -17.0474                |
| 20     | 1.0946                           | -16.8079                | 1.0587                                 | -16.8551                |
| 21     | 1.1042                           | -16.7811                | 1.0583                                 | -16.564                 |
| 22     | 1.0997                           | -16.4112                | 1.0628                                 | -16.3886                |
| 23     | 1.1025                           | -16.7545                | 1.0583                                 | -16.5756                |
| 24     | 1.0879                           | -16.7788                | 1.0504                                 | -16.735                 |
| 25     | 1.0694                           | -16.2152                | 1.0405                                 | -16.2874                |
| 26     | 1.0526                           | -16.5944                | 1.0232                                 | -16.6883                |
| 27     | 1.0659                           | -15.6397                | 1.0427                                 | -15.7663                |
| 28     | 1.0324                           | -12.2751                | 1.0196                                 | -12.1609                |
| 29     | 1.047                            | -16.7714                | 1.0232                                 | -16.9499                |
| 30     | 1.036                            | -17.5815                | 1.012                                  | -17.7985                |

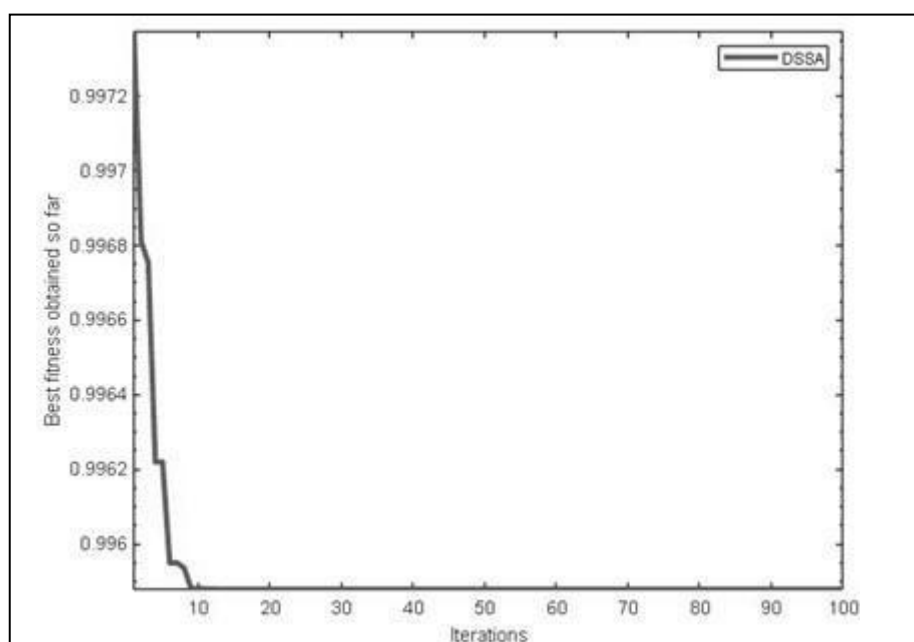


**Figure 4.7:** Convergence Curve Case 1 Iteration at Convergence:9

**Table 4.18:** SSA STATCOM Case 1

|                                     |             |
|-------------------------------------|-------------|
| Size of STATCOM                     | 21.63 MVar  |
| Location of Bus No                  | 21          |
| Objective function without STATCOM  | 1.4865      |
| Active power loss without STATCOM   | 0.1768(pu)  |
| Reactive power loss without STATCOM | 0.3513(pu)  |
| Active power loss with STATCOM      | 0.0785(pu)  |
| Reactive power loss with STATCOM    | 0.03016(pu) |
| Objective function with STATCOM     | 0.9993      |

**Table 4.19:** Line losses after placing STATCOM for Case 1

| SL. No.      | From Bus | To bus | Active power loss (pu) | Reactive power loss (pu) |
|--------------|----------|--------|------------------------|--------------------------|
| 1            | 1        | 2      | 0.0146                 | 0.0137                   |
| 2            | 1        | 3      | 0.0095                 | 0.0199                   |
| 3            | 2        | 4      | 0.0046                 | 0.0169                   |
| 4            | 3        | 4      | 0.0025                 | 0.0072                   |
| 5            | 2        | 5      | 0.015                  | 0.0232                   |
| 6            | 2        | 6      | 0.0081                 | 0.0245                   |
| 7            | 4        | 6      | 0.0027                 | 0.0093                   |
| 8            | 5        | 7      | 0.0008                 | 0.002                    |
| 9            | 6        | 7      | 0.0035                 | 0.0106                   |
| 10           | 6        | 8      | 0.0005                 | 0.0016                   |
| 11           | 6        | 9      | 0                      | 0.009                    |
| 12           | 6        | 10     | 0                      | 0.0087                   |
| 13           | 9        | 11     | 0                      | 0.0316                   |
| 14           | 9        | 10     | 0                      | 0.0137                   |
| 15           | 4        | 12     | 0                      | 0.0199                   |
| 16           | 12       | 13     | 0                      | 0.0169                   |
| 17           | 12       | 14     | 0.0018                 | 0.0038                   |
| 18           | 12       | 15     | 0.0025                 | 0.0049                   |
| 19           | 12       | 16     | 0.0005                 | 0.001                    |
| 20           | 14       | 15     | 0.0009                 | 0.0008                   |
| 21           | 16       | 17     | 0.0001                 | 0.0003                   |
| 22           | 15       | 18     | 0.0004                 | 0.0008                   |
| 23           | 18       | 19     | 0.0001                 | 0.0001                   |
| 24           | 19       | 20     | 0.0002                 | 0.0005                   |
| 25           | 10       | 20     | 0.001                  | 0.0022                   |
| 26           | 10       | 17     | 0.0002                 | 0.0006                   |
| 27           | 10       | 21     | 0.0023                 | 0.0049                   |
| 28           | 10       | 22     | 0.0006                 | 0.0013                   |
| 29           | 21       | 23     | 0                      | 0.0001                   |
| 30           | 15       | 23     | 0.0002                 | 0.0004                   |
| 31           | 22       | 24     | 0.001                  | 0.0015                   |
| 32           | 23       | 24     | 0.0002                 | 0.0004                   |
| 33           | 24       | 25     | 0.0006                 | 0.0011                   |
| 34           | 25       | 26     | 0.0005                 | 0.0007                   |
| 35           | 25       | 27     | 0.0002                 | 0.0003                   |
| 36           | 27       | 28     | 0                      | 0.0138                   |
| 37           | 27       | 29     | 0.0009                 | 0.0018                   |
| 38           | 27       | 30     | 0.0018                 | 0.0034                   |
| 39           | 29       | 30     | 0.0004                 | 0.0007                   |
| 40           | 8        | 28     | 0.0001                 | 0.0004                   |
| 41           | 6        | 28     | 0.0002                 | 0.0009                   |
| <b>Total</b> |          |        | 0.0785                 | 0.3016                   |

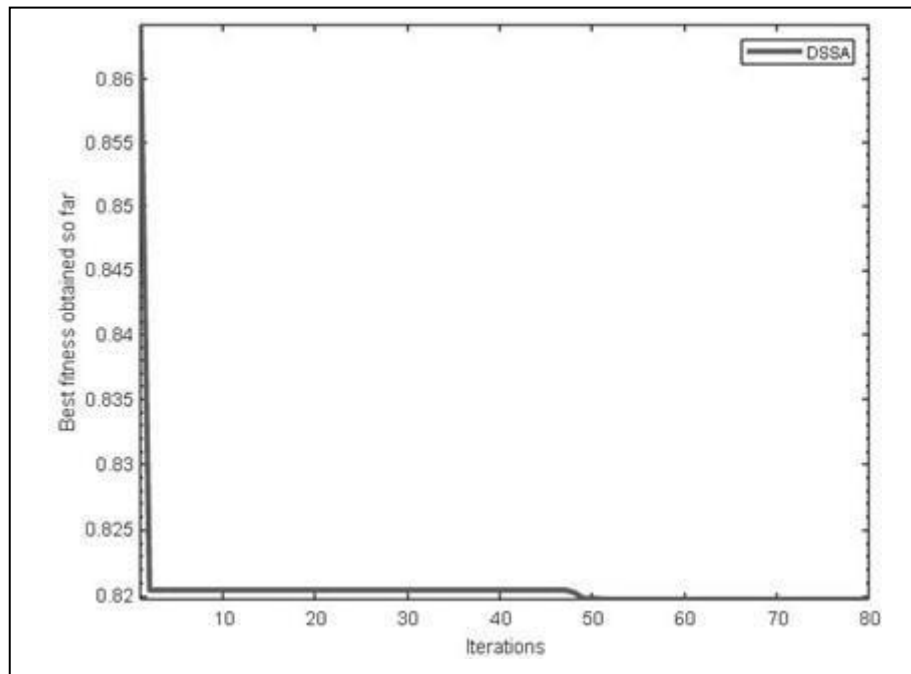


**Figure 4.9:** Convergence Curve Case 2  
Iteration at convergence:50

**Table 4.8:** SSA STATCOM Case 2

|                                     |            |
|-------------------------------------|------------|
| Size of STATCOM                     | 33.92 MVar |
| Location of Bus No                  | 24         |
| Objective function without STATCOM  | 1.4865     |
| Active power loss without STATCOM   | 0.1768(pu) |
| Reactive power loss without STATCOM | 0.3513(pu) |
| Active power loss with STATCOM      | 0.1088(pu) |
| Reactive power loss with STATCOM    | 0.2512(pu) |
| Objective function with STATCOM     | 0.8197     |

The voltage at the point of connection to a power grid may be controlled by a quick-acting device known as a STATCOM by either supplying or absorbing reactive current. The FACTS devices category includes it. The STATCOM convergence curve for case 1 with  $w_1 = 1$  and  $w_2=w_3=0$  is shown in figure 4.7. Figure 4.8 depicts the STATCOM convergence curve for case 2, with  $w_1$ ,  $w_2$  and  $w_3$  equal to 0.33. The STATCOM cases 1 and 2 are shown in Tables

4.19 and 4.21.

**Table 4.21:** Line losses after placing STATCOM for Case 2

| SL. No.      | From bus | To Bus | Active power loss (pu) | Reactive power loss (pu) |
|--------------|----------|--------|------------------------|--------------------------|
| 1            | 1        | 2      | 0.0548                 | 0.1057                   |
| 2            | 1        | 3      | 0.0286                 | 0.0728                   |
| 3            | 2        | 4      | 0.0112                 | -0.0053                  |
| 4            | 3        | 4      | 0.0079                 | 0.0137                   |
| 5            | 2        | 5      | 0.0297                 | 0.0805                   |
| 6            | 2        | 6      | 0.0208                 | 0.0231                   |
| 7            | 4        | 6      | 0.0059                 | 0.0113                   |
| 8            | 5        | 7      | 0.0012                 | -0.0179                  |
| 9            | 6        | 7      | 0.0037                 | -0.0061                  |
| 10           | 6        | 8      | 0.0011                 | -0.0055                  |
| 11           | 6        | 9      | 0                      | 0.0197                   |
| 12           | 6        | 10     | 0                      | 0.0131                   |
| 13           | 9        | 11     | 0                      | 0.0095                   |
| 14           | 9        | 10     | 0                      | 0.0078                   |
| 15           | 4        | 12     | 0                      | 0.0447                   |
| 16           | 12       | 13     | 0                      | 0.0064                   |
| 17           | 12       | 14     | 0.0007                 | 0.0015                   |
| 18           | 12       | 15     | 0.0022                 | 0.0043                   |
| 19           | 12       | 16     | 0.0006                 | 0.0013                   |
| 20           | 14       | 15     | 0.0001                 | 0.0001                   |
| 21           | 16       | 17     | 0.0002                 | 0.0004                   |
| 22           | 15       | 18     | 0.0005                 | 0.0009                   |
| 23           | 18       | 19     | 0.0001                 | 0.0001                   |
| 24           | 19       | 20     | 0.0001                 | 0.0003                   |
| 25           | 10       | 20     | 0.0007                 | 0.0016                   |
| 26           | 10       | 17     | 0.0001                 | 0.0003                   |
| 27           | 10       | 21     | 0.0014                 | 0.003                    |
| 28           | 10       | 22     | 0.0003                 | 0.0006                   |
| 29           | 21       | 23     | 0                      | 0                        |
| 30           | 15       | 23     | 0.0003                 | 0.0007                   |
| 31           | 22       | 24     | 0.0005                 | 0.0008                   |
| 32           | 23       | 24     | 0.0001                 | 0.0002                   |
| 33           | 24       | 25     | 0.0002                 | 0.0004                   |
| 34           | 25       | 26     | 0.0004                 | 0.0006                   |
| 35           | 25       | 27     | 0.0002                 | 0.0004                   |
| 36           | 27       | 28     | 0                      | 0.0113                   |
| 37           | 27       | 29     | 0.0008                 | 0.0016                   |
| 38           | 27       | 30     | 0.0016                 | 0.0029                   |
| 39           | 29       | 30     | 0.0003                 | 0.0006                   |
| 40           | 8        | 28     | 0                      | -0.0446                  |
| 41           | 6        | 28     | 0.0005                 | -0.0116                  |
| <b>Total</b> |          |        | 0.1088                 | 0.2512                   |

#### 4.2.6 SSA TCSC

**Table 4.22:** Voltage magnitude and phase angle

| Bus No | Case:1 $w_1=1$ , $w_2=w_3=0$ |                         | Case:2 $w_1=1/3$ , $w_2=1/3$ $w_3=1/3$ |                         |
|--------|------------------------------|-------------------------|--|-------------------------|
|        | Voltage magnitude (PU)       | Phase angle (in degree) | Voltage magnitude (PU)                 | Phase angle (in degree) |
| 1      | 1.06                         | 0                       | 1.06                                   | 0                       |
| 2      | 1.043                        | -5.2013                 | 1.043                                  | -4.0264                 |
| 3      | 1.0287                       | -7.2165                 | 1.0147                                 | -3.2489                 |
| 4      | 1.0218                       | -9.104                  | 1.0117                                 | -6.068                  |
| 5      | 1.01                         | -13.8826                | 1.01                                   | -12.1283                |
| 6      | 1.0214                       | -10.915                 | 1.0144                                 | -8.3578                 |
| 7      | 1.0091                       | -12.6559                | 1.0049                                 | -10.4291                |
| 8      | 1.0224                       | -11.6622                | 1.0153                                 | -9.1142                 |
| 9      | 1.0765                       | -13.8757                | 1.0682                                 | -11.2864                |
| 10     | 1.071                        | -15.4021                | 1.062                                  | -12.7986                |
| 11     | 1.121                        | -13.8757                | 1.1131                                 | -11.2864                |
| 12     | 1.0906                       | -14.7499                | 1.0812                                 | -11.9803                |
| 13     | 1.1206                       | -14.7499                | 1.1115                                 | -11.9803                |
| 14     | 1.0751                       | -15.5785                | 1.0657                                 | -12.8489                |
| 15     | 1.0696                       | -15.6311                | 1.0602                                 | -12.9312                |
| 16     | 1.0753                       | -15.2783                | 1.066                                  | -12.5828                |
| 17     | 1.0671                       | -15.5597                | 1.0579                                 | -12.9319                |
| 18     | 1.058                        | -16.2257                | 1.0486                                 | -13.5715                |
| 19     | 1.0544                       | -16.379                 | 1.045                                  | -13.7487                |
| 20     | 1.0578                       | -16.1887                | 1.0485                                 | -13.5662                |
| 21     | 1.0573                       | -15.8985                | 1.0481                                 | -13.2842                |
| 22     | 1.0617                       | -15.7248                | 1.0526                                 | -13.1279                |
| 23     | 1.0573                       | -15.9083                | 1.0481                                 | -13.2878                |
| 24     | 1.0491                       | -16.0654                | 1.0399                                 | -13.4763                |
| 25     | 1.0394                       | -15.635                 | 1.0307                                 | -13.0864                |
| 26     | 1.0222                       | -16.0367                | 1.0133                                 | -13.495                 |
| 27     | 1.0418                       | -15.1239                | 1.0334                                 | -12.596                 |
| 28     | 1.0191                       | -11.5228                | 1.012                                  | -8.9683                 |
| 29     | 1.0224                       | -16.3096                | 1.0138                                 | -13.8014                |
| 30     | 1.0111                       | -17.1596                | 1.0024                                 | -14.6661                |



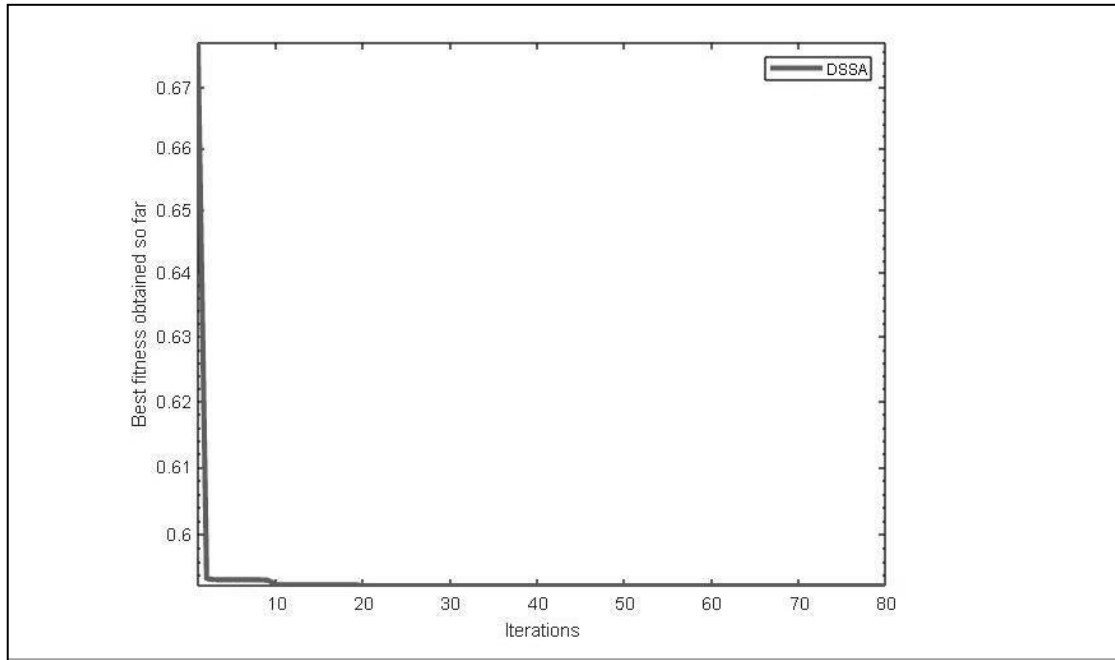


**Figure 4.10: Convergence Curve Case 1 Iteration at convergence:15**

**Table 4.23 SSA TCSC Case 1**

|                                  |             |
|----------------------------------|-------------|
| Size of TCSC                     | 0.0248 MVar |
| Location of line number          | 2           |
| Objective function without TCSC  | 1.4865      |
| Active power loss without TCSC   | 0.1768(pu)  |
| Reactive power loss without TCSC | 0.3513(pu)  |
| Active power loss with TCSC      | 0.1557(pu)  |
| Reactive power loss with TCSC    | 0.3241(pu)  |
| Objective function with TCSC     | 0.9947      |

**Table 4.24:** Line losses after placing TCSC for Case1

| SL. No.      | From Bus | To Bus | Active power loss (pu) | Reactive power loss(pu) |
|--------------|----------|--------|------------------------|-------------------------|
| 1            | 1        | 2      | 0.0291                 | 0.0886                  |
| 2            | 1        | 3      | 0.0353                 | 0.0695                  |
| 3            | 2        | 4      | 0.0092                 | -0.0112                 |
| 4            | 3        | 4      | 0.0097                 | 0.0191                  |
| 5            | 2        | 5      | 0.0287                 | 0.0763                  |
| 6            | 2        | 6      | 0.0186                 | 0.0167                  |
| 7            | 4        | 6      | 0.0067                 | 0.0139                  |
| 8            | 5        | 7      | 0.0014                 | -0.0173                 |
| 9            | 6        | 7      | 0.004                  | -0.0053                 |
| 10           | 6        | 8      | 0.0011                 | -0.0055                 |
| 11           | 6        | 9      | 0                      | 0.0194                  |
| 12           | 6        | 10     | 0                      | 0.013                   |
| 13           | 9        | 11     | 0                      | 0.0095                  |
| 14           | 9        | 10     | 0                      | 0.0077                  |
| 15           | 4        | 12     | 0                      | 0.0454                  |
| 16           | 12       | 13     | 0                      | 0.0064                  |
| 17           | 12       | 14     | 0.0007                 | 0.0015                  |
| 18           | 12       | 15     | 0.0022                 | 0.0044                  |
| 19           | 12       | 16     | 0.0006                 | 0.0014                  |
| 20           | 14       | 15     | 0.0001                 | 0.0001                  |
| 21           | 16       | 17     | 0.0002                 | 0.0004                  |
| 22           | 15       | 18     | 0.0005                 | 0.0009                  |
| 23           | 18       | 19     | 0.0001                 | 0.0001                  |
| 24           | 19       | 20     | 0.0001                 | 0.0003                  |
| 25           | 10       | 20     | 0.0007                 | 0.0016                  |
| 26           | 10       | 17     | 0.0001                 | 0.0002                  |
| 27           | 10       | 21     | 0.0014                 | 0.003                   |
| 28           | 10       | 22     | 0.0003                 | 0.0007                  |
| 29           | 21       | 23     | 0                      | 0                       |
| 30           | 15       | 23     | 0.0003                 | 0.0007                  |
| 31           | 22       | 24     | 0.0005                 | 0.0008                  |
| 32           | 23       | 24     | 0.0001                 | 0.0002                  |
| 33           | 24       | 25     | 0.0002                 | 0.0004                  |
| 34           | 25       | 26     | 0.0004                 | 0.0006                  |
| 35           | 25       | 27     | 0.0002                 | 0.0003                  |
| 36           | 27       | 28     | 0                      | 0.0112                  |
| 37           | 27       | 29     | 0.0008                 | 0.0016                  |
| 38           | 27       | 30     | 0.0016                 | 0.0029                  |
| 39           | 29       | 30     | 0.0003                 | 0.0006                  |
| 40           | 8        | 28     | 0                      | -0.0445                 |
| 41           | 6        | 28     | 0.0005                 | -0.0116                 |
| <b>Total</b> |          |        | 0.1557                 | 0.3241                  |

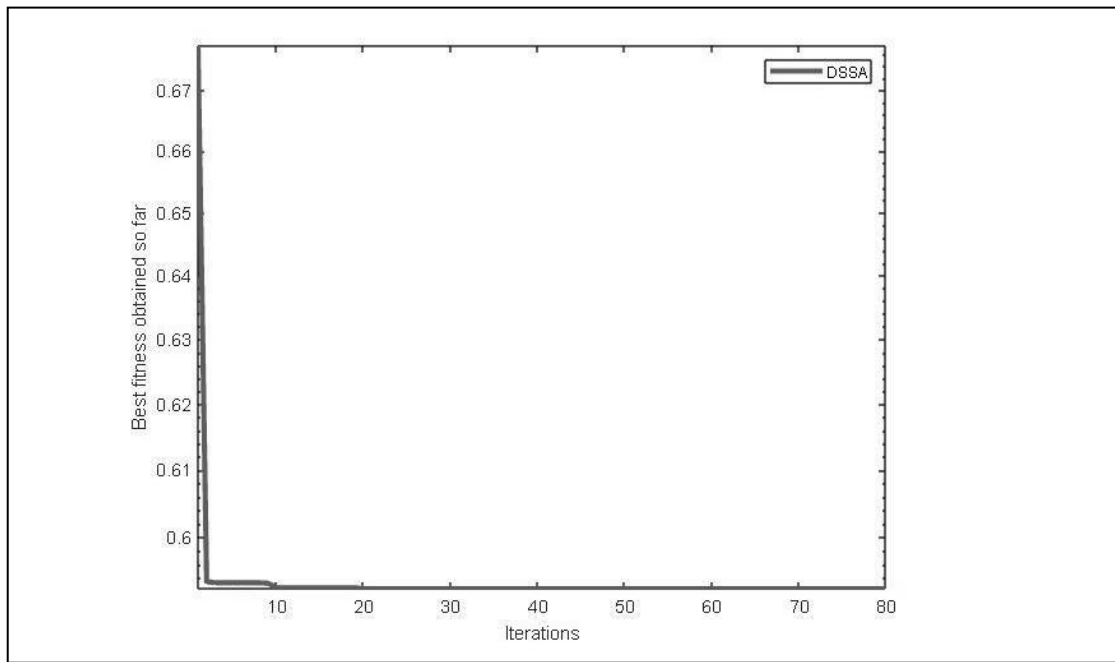


**Figure 4.11:** Convergence Curve Case 2. Iteration at convergence: 16

**Table 4.25:** SSA TCSC Case 2

|                                  |             |
|----------------------------------|-------------|
| Size of TCSC                     | 0.0939 MVar |
| Location of Bus No               | 2           |
| Objective function without TCSC  | 1.4865      |
| Active power loss without TCSC   | 0.1768(pu)  |
| Reactive power loss without TCSC | 0.3513(pu)  |
| Active power loss with TCSC      | 0.1560(pu)  |
| Reactive power loss with TCSC    | 0.2170(pu)  |
| Objective function with TCSC     | 0.59245     |

**Table 4.26:** Line losses after placing TCSC for Case 2

| SL. No.      | From Bus | To bus | Active power loss (pu) | Reactive power loss (pu) |
|--------------|----------|--------|------------------------|--------------------------|
| 1            | 1        | 2      | 0.03                   | 0.0315                   |
| 2            | 1        | 3      | 0.033                  | 0.0159                   |
| 3            | 2        | 4      | 0.004                  | -0.0268                  |
| 4            | 3        | 4      | 0.0204                 | 0.0501                   |
| 5            | 2        | 5      | 0.0251                 | 0.0615                   |
| 6            | 2        | 6      | 0.0116                 | -0.0045                  |
| 7            | 4        | 6      | 0.0106                 | 0.0275                   |
| 8            | 5        | 7      | 0.0027                 | -0.0139                  |
| 9            | 6        | 7      | 0.0051                 | -0.0016                  |
| 10           | 6        | 8      | 0.0011                 | -0.0053                  |
| 11           | 6        | 9      | 0                      | 0.0185                   |
| 12           | 6        | 10     | 0                      | 0.0124                   |
| 13           | 9        | 11     | 0                      | 0.0097                   |
| 14           | 9        | 10     | 0                      | 0.0075                   |
| 15           | 4        | 12     | 0                      | 0.0488                   |
| 16           | 12       | 13     | 0                      | 0.0065                   |
| 17           | 12       | 14     | 0.0008                 | 0.0016                   |
| 18           | 12       | 15     | 0.0024                 | 0.0046                   |
| 19           | 12       | 16     | 0.0007                 | 0.0015                   |
| 20           | 14       | 15     | 0.0001                 | 0.0001                   |
| 21           | 16       | 17     | 0.0002                 | 0.0005                   |
| 22           | 15       | 18     | 0.0005                 | 0.001                    |
| 23           | 18       | 19     | 0.0001                 | 0.0001                   |
| 24           | 19       | 20     | 0.0001                 | 0.0003                   |
| 25           | 10       | 20     | 0.0007                 | 0.0015                   |
| 26           | 10       | 17     | 0.0001                 | 0.0002                   |
| 27           | 10       | 21     | 0.0014                 | 0.003                    |
| 28           | 10       | 22     | 0.0003                 | 0.0007                   |
| 29           | 21       | 23     | 0                      | 0                        |
| 30           | 15       | 23     | 0.0004                 | 0.0008                   |
| 31           | 22       | 24     | 0.0005                 | 0.0008                   |
| 32           | 23       | 24     | 0.0001                 | 0.0002                   |
| 33           | 24       | 25     | 0.0002                 | 0.0003                   |
| 34           | 25       | 26     | 0.0004                 | 0.0006                   |
| 35           | 25       | 27     | 0.0002                 | 0.0003                   |
| 36           | 27       | 28     | 0                      | 0.0113                   |
| 37           | 27       | 29     | 0.0008                 | 0.0016                   |
| 38           | 27       | 30     | 0.0016                 | 0.003                    |
| 39           | 29       | 30     | 0.0003                 | 0.0006                   |
| 40           | 8        | 28     | 0                      | -0.0439                  |
| 41           | 6        | 28     | 0.0005                 | -0.0115                  |
| <b>Total</b> |          |        | 0.1560                 | 0.2170                   |

#### 4.2.7 SSA SVC

**Table 4.27:** Bus voltage and phase angle after placement of SVC

| Bus No | Case:1 $w_1=1, w_2=0, w_3=0$ |                         | Case:2 $w_1=1/3, w_2=1/3, w_3=1/3$ |                         |
|--------|------------------------------|-------------------------|------------------------------------|-------------------------|
|        | Voltage magnitude (PU)       | Phase angle (in degree) | Voltage magnitude (PU)             | Phase angle (in degree) |
| 1      | 1.06                         | 0                       | 1.06                               | 0                       |
| 2      | 1.043                        | -5.4937                 | 1.043                              | -5.4936                 |
| 3      | 1.0339                       | -8.214                  | 1.0343                             | -8.2214                 |
| 4      | 1.0279                       | -9.9069                 | 1.0284                             | -9.9156                 |
| 5      | 1.01                         | -14.295                 | 1.01                               | -14.3015                |
| 6      | 1.0279                       | -11.6141                | 1.0262                             | -11.5855                |
| 7      | 1.0129                       | -13.2361                | 1.0119                             | -13.2224                |
| 8      | 1.029                        | -12.3526                | 1.0271                             | -12.3262                |
| 9      | 1.0917                       | -14.5598                | 1.0822                             | -14.5358                |
| 10     | 1.0911                       | -16.0599                | 1.0773                             | -16.0549                |
| 11     | 1.1357                       | -14.5598                | 1.1265                             | -14.5358                |
| 12     | 1.1065                       | -15.3778                | 1.0971                             | -15.4538                |
| 13     | 1.1361                       | -15.3778                | 1.1269                             | -15.4538                |
| 14     | 1.0929                       | -16.1974                | 1.0816                             | -16.266                 |
| 15     | 1.0889                       | -16.2977                | 1.0761                             | -16.31                  |
| 16     | 1.0931                       | -15.9134                | 1.0818                             | -15.9576                |
| 17     | 1.0866                       | -16.2048                | 1.0735                             | -16.2182                |
| 18     | 1.0778                       | -16.8649                | 1.0645                             | -16.8873                |
| 19     | 1.0744                       | -17.009                 | 1.0609                             | -17.0327                |
| 20     | 1.0778                       | -16.8238                | 1.0642                             | -16.8415                |
| 21     | 1.0823                       | -16.6654                | 1.0638                             | -16.5528                |
| 22     | 1.0825                       | -16.3963                | 1.0682                             | -16.3784                |
| 23     | 1.0825                       | -16.686                 | 1.0638                             | -16.565                 |
| 24     | 1.0707                       | -16.7613                | 1.0558                             | -16.7223                |
| 25     | 1.0561                       | -16.2475                | 1.0457                             | -16.2751                |
| 26     | 1.0391                       | -16.6364                | 1.0285                             | -16.672                 |
| 27     | 1.0552                       | -15.6951                | 1.0477                             | -15.7569                |
| 28     | 1.0264                       | -12.2191                | 1.024                              | -12.1898                |
| 29     | 1.036                        | -16.8503                | 1.0283                             | -16.929                 |
| 30     | 1.0249                       | -17.6779                | 1.0172                             | -17.7691                |

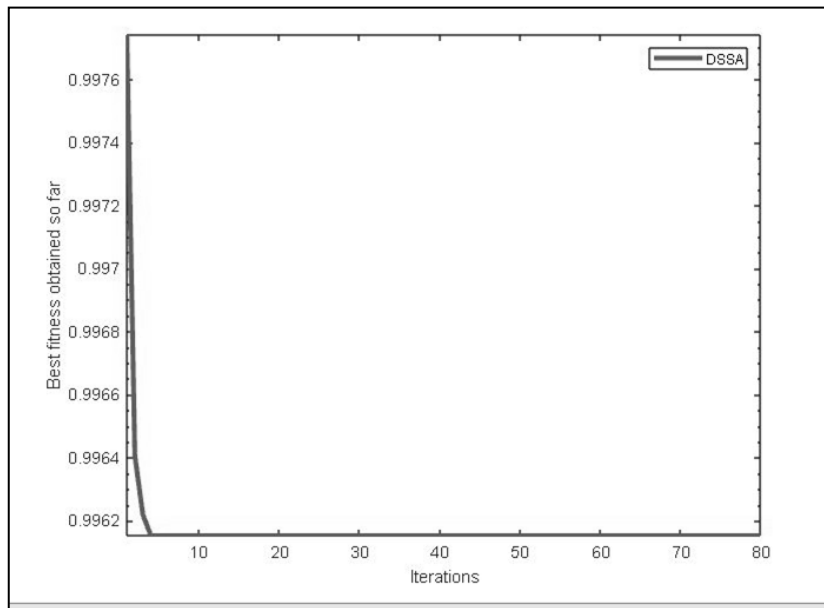


**Figure 4.12:** Convergence Curve Case 1 Iterations at convergence:10

**Table 4.28:** SSA SVC Case 1

|                                 |            |
|---------------------------------|------------|
| Size of SVC                     | 5.05 MVar  |
| Location of Bus No              | 29         |
| Objective function without SVC  | 1.4865     |
| Active power loss without SVC   | 0.1768(pu) |
| Reactive power loss without SVC | 0.3513(pu) |
| Active power loss with SVC      | 0.1557(pu) |
| Reactive power loss with SVC    | 0.3240(pu) |
| Objective function with SVC     | 0.9962     |

**Table 4.29:** Line losses after placing SVC for Case 1

| SL. No.      | From Bus | To bus | Active power loss (pu) | Reactive power loss (pu) |
|--------------|----------|--------|------------------------|--------------------------|
| 1            | 1        | 2      | 0.0346                 | 0.1051                   |
| 2            | 1        | 3      | 0.0288                 | 0.0733                   |
| 3            | 2        | 4      | 0.0112                 | -0.0052                  |
| 4            | 3        | 4      | 0.0079                 | 0.0138                   |
| 5            | 2        | 5      | 0.0294                 | 0.0795                   |
| 6            | 2        | 6      | 0.021                  | 0.0236                   |
| 7            | 4        | 6      | 0.006                  | 0.0114                   |
| 8            | 5        | 7      | 0.0011                 | -0.0182                  |
| 9            | 6        | 7      | 0.0038                 | -0.006                   |
| 10           | 6        | 8      | 0.0011                 | -0.0056                  |
| 11           | 6        | 9      | 0                      | 0.0225                   |
| 12           | 6        | 10     | 0                      | 0.0142                   |
| 13           | 9        | 11     | 0                      | 0.0093                   |
| 14           | 9        | 10     | 0                      | 0.0074                   |
| 15           | 4        | 12     | 0                      | 0.0435                   |
| 16           | 12       | 13     | 0                      | 0.0062                   |
| 17           | 12       | 14     | 0.0007                 | 0.0014                   |
| 18           | 12       | 15     | 0.0019                 | 0.0038                   |
| 19           | 12       | 16     | 0.0006                 | 0.0012                   |
| 20           | 14       | 15     | 0                      | 0                        |
| 21           | 16       | 17     | 0.0001                 | 0.0003                   |
| 22           | 15       | 18     | 0.0004                 | 0.0009                   |
| 23           | 18       | 19     | 0.0001                 | 0.0001                   |
| 24           | 19       | 20     | 0.0001                 | 0.0003                   |
| 25           | 10       | 20     | 0.0007                 | 0.0015                   |
| 26           | 10       | 17     | 0.0001                 | 0.0003                   |
| 27           | 10       | 21     | 0.0011                 | 0.0023                   |
| 28           | 10       | 22     | 0.0003                 | 0.0006                   |
| 29           | 21       | 23     | 0                      | -0.1129                  |
| 30           | 15       | 23     | 0.0002                 | 0.0004                   |
| 31           | 22       | 24     | 0.0005                 | 0.0007                   |
| 32           | 23       | 24     | 0.0002                 | 0.0004                   |
| 33           | 24       | 25     | 0.0004                 | 0.0007                   |
| 34           | 25       | 26     | 0.0004                 | 0.0006                   |
| 35           | 25       | 27     | 0.0002                 | 0.0004                   |
| 36           | 27       | 28     | 0                      | 0.0105                   |
| 37           | 27       | 29     | 0.0008                 | 0.0015                   |
| 38           | 27       | 30     | 0.0015                 | 0.0029                   |
| 39           | 29       | 30     | 0.0003                 | 0.0006                   |
| 40           | 8        | 28     | 0                      | -0.0451                  |
| 41           | 6        | 28     | 0.0005                 | -0.0119                  |
| <b>Total</b> |          |        | 0.1557                 | 0.3240                   |

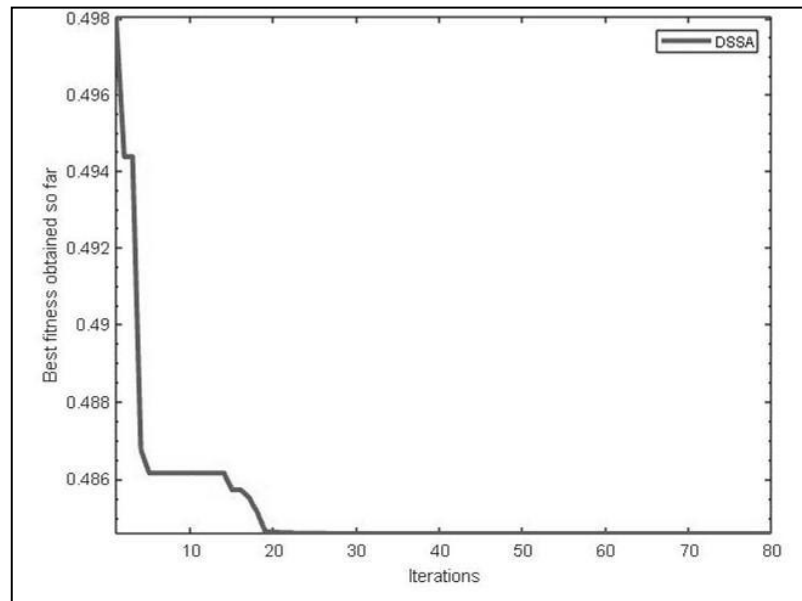


**Figure 4.13:** Convergence Curve Case 2 Iteration at convergence:30

**Table 4.30:** SSA SVC Case 2

|                                 |            |
|---------------------------------|------------|
| Size of SVC                     | 10.59 MVr  |
| Location of Bus No              | 3          |
| Objective function without SVC  | 1.4865     |
| Active power loss without SVC   | 0.1768(pu) |
| Reactive power loss without SVC | 0.3513(pu) |
| Active power loss with SVC      | 0.1667(pu) |
| Reactive power loss SVC         | 0.1338(pu) |
| Objective function with SVC     | 0.448865   |



**Table 4.31:** Line losses after placing SVC for Case 2

| SL. No.      | From Bus | To bus | Active power loss (pu) | Reactive power loss (pu) |
|--------------|----------|--------|------------------------|--------------------------|
| 1            | 1        | 2      | 0.0446                 | 0.105                    |
| 2            | 1        | 3      | 0.0288                 | 0.0735                   |
| 3            | 2        | 4      | 0.0113                 | -0.2197                  |
| 4            | 3        | 4      | 0.0079                 | 0.0138                   |
| 5            | 2        | 5      | 0.0295                 | 0.0797                   |
| 6            | 2        | 6      | 0.0209                 | 0.0233                   |
| 7            | 4        | 6      | 0.0058                 | 0.0106                   |
| 8            | 5        | 7      | 0.0011                 | -0.0181                  |
| 9            | 6        | 7      | 0.0038                 | -0.0061                  |
| 10           | 6        | 8      | 0.0011                 | -0.0056                  |
| 11           | 6        | 9      | 0                      | 0.0197                   |
| 12           | 6        | 10     | 0                      | 0.0131                   |
| 13           | 9        | 11     | 0                      | 0.0094                   |
| 14           | 9        | 10     | 0                      | 0.0077                   |
| 15           | 4        | 12     | 0                      | 0.0443                   |
| 16           | 12       | 13     | 0                      | 0.0064                   |
| 17           | 12       | 14     | 0.0007                 | 0.0015                   |
| 18           | 12       | 15     | 0.0022                 | 0.0043                   |
| 19           | 12       | 16     | 0.0006                 | 0.0013                   |
| 20           | 14       | 15     | 0.0001                 | 0.0001                   |
| 21           | 16       | 17     | 0.0002                 | 0.0004                   |
| 22           | 15       | 18     | 0.0005                 | 0.0009                   |
| 23           | 18       | 19     | 0.0001                 | 0.0001                   |
| 24           | 19       | 20     | 0.0001                 | 0.0003                   |
| 25           | 10       | 20     | 0.0007                 | 0.0015                   |
| 26           | 10       | 17     | 0.0001                 | 0.0002                   |
| 27           | 10       | 21     | 0.0014                 | 0.003                    |
| 28           | 10       | 22     | 0.0003                 | 0.0006                   |
| 29           | 21       | 23     | 0                      | 0                        |
| 30           | 15       | 23     | 0.0003                 | 0.0007                   |
| 31           | 22       | 24     | 0.0005                 | 0.0008                   |
| 32           | 23       | 24     | 0.0001                 | 0.0002                   |
| 33           | 24       | 25     | 0.0002                 | 0.0004                   |
| 34           | 25       | 26     | 0.0004                 | 0.0006                   |
| 35           | 25       | 27     | 0.0002                 | 0.0004                   |
| 36           | 27       | 28     | 0                      | 0.0111                   |
| 37           | 27       | 29     | 0.0008                 | 0.0016                   |
| 38           | 27       | 30     | 0.0015                 | 0.0029                   |
| 39           | 29       | 30     | 0.0003                 | 0.0006                   |
| 40           | 8        | 28     | 0                      | -0.0449                  |
| 41           | 6        | 28     | 0.0005                 | -0.0118                  |
| <b>Total</b> |          |        | 0.1667                 | 0.1338                   |

#### 4.2.8 COMPARISON

**Table 4.32:** Comparisons for results obtained from both algorithms for STATCOM

| PARAMETRS                                | PSO    |         | SSA    |        |
|--|--------|---------|--------|--------|
|  | CASE 1 | CASE 2  | CASE 1 | CASE 2 |
| Size (in MVar)                           | 88.24  | 39.33   | 21.63  | 33.92  |
| Location of bus no                       | 24     | 12      | 21     | 24.0   |
| Objective function without STATCOM       | 1.4865 | 1.4865  | 1.4865 | 1.4865 |
| Active power loss without STATCOM (pu)   | 0.1768 | 0.1768  | 0.1768 | 0.1768 |
| Reactive power loss without STATCOM (pu) | 0.3513 | 0.3513  | 0.3513 | 0.3513 |
| Active power loss with STATCOM (pu)      | 0.1219 | 0.1321  | 0.0785 | 0.1088 |
| Reactive power loss with STATCOM (pu)    | 0.1030 | 0.3295  | 0.3016 | 0.2512 |
| Objective function with STATCOM          | 0.6884 | 1.00944 | 0.9993 | 0.8197 |

**Table 4.33:** Comparisons for results obtained from both algorithms for TCSC

| PARAMETRS                             | PSO    |        | SSA    |         |
|---------------------------------------|--------|--------|--------|---------|
|                                       | CASE 1 | CASE 2 | CASE 1 | CASE 2  |
| Size (MVar)                           | 0.0239 | 0.0931 | 0.0248 | 0.0939  |
| Location of line no                   | 02     | 02     | 02     | 02      |
| Objective function without TCSC       | 1.4865 | 1.4865 | 1.4865 | 1.4865  |
| Active power loss without TCSC (pu)   | 0.1768 | 0.1768 | 0.1768 | 0.1768  |
| Reactive power loss without TCSC (pu) | 0.3513 | 0.3513 | 0.3513 | 0.3513  |
| Active power loss with TCSC (pu)      | 0.1295 | 0.1754 | 0.1557 | 0.1560  |
| Reactive power loss with TCSC (pu)    | 0.2475 | 0.2491 | 0.3241 | 0.2170  |
| Objective function with TCSC          | 0.9947 | 0.6251 | 0.9947 | 0.59245 |

**Table 4.34:** Comparisons for results obtained from both algorithms for SVC

| PARAMETRS                            | PSO    |        | SSA    |        |
|--------------------------------------|--------|--------|--------|--------|
|                                      | CASE 1 | CASE 2 | CASE 1 | CASE 2 |
| Size                                 | 5.05   | 11.58  | 5.05   | 10.59  |
| Location of bus no                   | 29     | 16     | 29     | 03     |
| Objective function without SVC       | 1.4865 | 1.4865 | 1.4865 | 1.4865 |
| Active power loss without SVC (pu)   | 0.1768 | 0.1768 | 0.1768 | 0.1768 |
| Reactive power loss without SVC (pu) | 0.3513 | 0.3513 | 0.3513 | 0.3513 |
| Active power loss with SVC (pu)      | 0.1761 | 0.1765 | 0.1557 | 0.1676 |
| Reactive power loss with SVC (pu)    | 0.2362 | 0.0961 | 0.3240 | 0.1338 |
| Objective function with SVC          | 0.9962 | 0.4914 | 0.9962 | 0.4488 |

#### 4.2.9 SUMMARY

This chapter examines the effectiveness of PSO and SSA in terms of the optimal placement and size for series (TCSC) and shunt compensating devices (SVC, STATCOM) in a power system. It has been shown how to use the FACTS device to minimize the active power losses and reactive power losses. By strategically positioning the particle swarm optimization-based method and Squirrel Search Algorithm optimization-based method, it was possible to achieve the lowest voltage variation and active power loss and reactive power loss. The method is applied to the IEEE-30 bus system. The findings demonstrate an improvement in voltage profile and a considerable decrease in the overall actual power losses and reactive power losses of the system.

## **CHAPTER 5**

### **CONCLUSION AND FUTURE WORK**

#### **5.1 CONCLUSION**

The primary goal of the current thesis is to improve the steady state stability of the power system utilizing series FACTS devices, shunt FACTS devices by using the static synchronous compensator (STATCOM), SVC and the Thyristor Controlled series capacitor (TCSC)". In order to improve the steady state stability, the ideal quantity and placement of series capacitor along the line supplying a substantial load area have been identified. The majority of the work is based on the system's steady state performance; it was discovered during the review of the literature. However, the multifunctional modelling shown in the research does not accurately reflect the dynamics of the system, and the literature falls short in terms of the system's steady state performance. It has been noted in the literature that variable degree series compensation has not been used in the long transmission system, and additional research into the system behavior under varied degrees of compensation is necessary. The use of the shunt compensation FACTS devices for controlling voltage stability has not been explored much. Investigating the characteristics of both the shunt and series FACTS devices is necessary in light of their steady state behavior.

In this thesis, a PSO and SSA are used. The whole process is evaluated on a typical IEEE-30 bus system, and the findings show that the technique may efficiently handle the OPF issue in a power system. Following a comparison of the OPF results with and without FACTS controllers, TCSC, SVC, and STATCOM, it was found that installing FACTS devices improved power system performance and reduced the goal functions under consideration to their best values.

## 5.2 FUTURE WORK

In the future, the present work's scope may be extended to cover the following aspects:

- Optimal combination of series and shunt compensation devices may be determined to enhance steady-state stability limit of the system.
- The behavior of the optimally placed FACTS devices may be studied when there is any fault or unbalance or power swing in the system.
- The efficacy of the compensation devices may be further examined to solve several reliability and power quality issues.
- Additional study may be done on the system's dynamic and transient behavior to anticipate voltage stability.

## Reference

1. Grainger, J.J. and Stevenson Jr, W.D., "*Power system Analysis*", McGraw Hill Education, 7<sup>th</sup> Edition, 2017.
2. Padiyar, K.R., "*FACTS Controllers in Power Transmission and Distribution*", New Age International Publishers, 4<sup>th</sup> Edition 2007.
3. Hingorani, N.G. and Gyugyi, L., "*Understanding FACTS: Concepts and Technology of Flexible AC Transmission Systems*", Wiley-IEEE Press, 1<sup>st</sup> Edition, 1999.
4. Chorghade, A., *FACTS Devices for Reactive Power compensation and power flow control-Recent Trends*, International Conference on Industry 4.0 Technology, 14<sup>th</sup> Edition, 2020.
5. Shicong, M., Jianbo, G., Qing, H., Jian, Z., Mian, D., Zhao, Y., *Guide for voltage regulation and Reactive power compensation at 1000KV AC and above with IEEE P1860 standard*, International Conference on Power System Technology, 2014.
6. Das, S., Sen, D., Gupta, M., Shegaonkar, M., Acharjee, P., *Selection of most favorable devices in Transmission System*. International Conference on power energy, environment and intelligent control, 2018.
7. Chevalier, S.C. and Hines, P.D., 2018. *Mitigating the risk of voltage collapse using statistical measures from pmu data*. IEEE Transactions on Power Systems, 34(1), pp.120-128.
8. Małkowski, R., Izdebski, M. and Miller, P., 2020. *Adaptive algorithm of a tap-changer controller of the power transformer supplying the radial network reducing the risk of voltage collapse*. Energies, 13(20), p.5403.
9. Chinda, P.R. and Rao, R.D., 2022. *A binary particle swarm optimization approach for power system security enhancement*. International Journal of Electrical and Computer Engineering, 12(2), p.1929.
10. Ansari pour, R., Barati, H. and Ghasemi, A., 2022. *A chance-constrained optimization framework for transmission congestion management and frequency regulation in the presence of wind farms and energy storage systems*. Electric Power Systems Research, 213, p.108712.
11. Sewdien, V.N., Preece, R., Torres, J.R. and van der Meijden, M.A., 2018, October. *Evaluation of PV and QV based voltage stability analyses in converter dominated power*

- Systems*. In 2018 IEEE PES Asia-Pacific Power and Energy Engineering Conference (APPEEC) (pp. 161-165). IEEE.
12. Atchison, F., Rahman, M. and Cecchi, V., 2020, October. *Temperature-Dependent Power Transfer Capability of Transmission Systems under Uncertainty: An Affine-Arithmetic Approach*. In 2020 IEEE/PES Transmission and Distribution Conference and Exposition (T&D) (pp. 1-5). IEEE.
  13. Zhang, N., Jia, H., Hou, Q., Zhang, Z., Xia, T., Cai, X. and Wang, J., 2022. *Data-Driven Security and Stability Rule in High Renewable Penetrated Power System Operation*. Proceedings of the IEEE.
  14. Baadji, B., Bentarzi, H. and Bakdi, A., 2020. *Comprehensive learning bat algorithm for optimal coordinated tuning of power system stabilizers and static VAR compensator in power systems*. Engineering Optimization, 52(10), pp.1761-1779.
  15. Mohamed, A.A., Kamel, S., Hassan, M.H., Mosaad, M.I. and Aljohani, M., 2022. *Optimal Power Flow Analysis Based on Hybrid Gradient-Based Optimizer with Moth-Flame Optimization Algorithm Considering Optimal Placement and Sizing of FACTS/Wind Power*. Mathematics, 10(3), p.361.
  16. Kuthadi, K.K., Sridhar, N.D. and Kumar, C.H., 2022. *Optimal placement of FACTS devices for enhancing of transmission system performance using whale optimization algorithm*. International Journal on Interactive Design and Manufacturing (IJIDeM), pp.1-16.
  17. Rawat, M.S. and Tamta, R., 2018, November. *Optimal placement of TCSC and STATCOM for voltage stability enhancement in transmission network*. In 2018 5th IEEE Uttar Pradesh Section International Conference on Electrical, Electronics and Computer Engineering (UPCON) (pp. 1-6). IEEE.
  18. Dash, S.P., Subhashini, K.R. and Satapathy, J.K., 2020. *Optimal location and parametric settings of FACTS devices based on JAYA blended moth flame optimization for transmission loss minimization in power systems*. Microsystem Technologies, 26(5), pp.1543-1552.
  19. Birchfield, A.B., Xu, T. and Overbye, T.J., 2018. *Power flow convergence and reactive power planning in the creation of large synthetic grids*. IEEE Transactions on Power Systems, 33(6), pp.6667-6674.

20. Adetokun, B.B., Muriithi, C.M. and Ojo, J.O., 2020. *Voltage stability assessment and enhancement of power grid with increasing wind energy penetration*. International Journal of Electrical Power & Energy Systems, 120, p.105988.
21. Alhejji, A., Hussein, M.E., Kamel, S. and Alyami, S., 2020. *Optimal power flow solution with an embedded center-node unified power flow controller using an adaptive grasshopper optimization algorithm*. IEEE Access, 8, pp.119020-119037.
22. Raj, S. and Bhattacharyya, B., 2018. *Optimal placement of TCSC and SVC for reactive power planning using Whale optimization algorithm*. Swarm and Evolutionary Computation, 40, pp.131-143.
23. Jiang, P., Fan, Z., Feng, S., Wu, X., Cai, H. and Xie, Z., 2019. *Mitigation of power system forced oscillations based on unified power flow controller*. Journal of Modern Power Systems and Clean Energy, 7(1), pp.99-112.
24. Abdollahi, M., Candela, J.I., Tarraso, A., Elsharty, M.A. and Rakhshani, E., 2021. *Electromechanical design of synchronous power controller in grid integration of renewable power converters to support dynamic stability*. Energies, 14(8), p.2115.
25. Meena, A., Ali, S. and Mahela, O.P., 2018, September. *Power System Oscillations Damping During Faulty Events in the Presence of Linear Load*. In 2018 International Conference on Computing, Power and Communication Technologies (GUCON) (pp.126-131). IEEE.
26. Ahmed Taher, M., Kamel, S., Jurado, F. and Yu, J., 2022. *Optimal Locations and Sizes of Shunt FACT Devices for Enhancing Power System Loadability Using Improved Moth Flame Optimization*. Electric Power Components and Systems, pp.1-19.
27. Bhandakkar, A.A. and Mathew, L., 2021. *A novel MDA2LO technique for load flow analysis with hybrid power flow controller*. Journal of Ambient Intelligence and Humanized Computing, pp.1-15.
28. Singh, B., Tiwari, P. and Singh, S.N., 2018, November. *Enhancement of power system performances by optimally placed FACTS controllers by using different optimization techniques in distribution systems: A taxonomical review*. In 2018 5th IEEE Uttar Pradesh Section International Conference on Electrical, Electronics and Computer Engineering (UPCON) (pp. 1-7). IEEE.



29. Singh, B. and Kumar, R., 2020. *A comprehensive survey on enhancement of system performances by using different types of FACTS controllers in power systems with static and realistic load models*. Energy Reports, 6, pp.55-79.
30. Ahmad, A.A. and Sirjani, R., 2020. *Optimal placement and sizing of multi-type FACTS devices in power systems using metaheuristic optimisation techniques: An updated review*. Ain Shams Engineering Journal, 11(3), pp.611-628.
31. Gupta, S., Kumar, N. and Srivastava, L., 2021. *Solution of optimal power flow problem using sine-cosine mutation based modified Jaya algorithm: A Case Study*. Energy Sources, Part A: Recovery, Utilization, and Environmental Effects, pp.1-24.
32. El Hassan, M.A.A., Kamel, S., Ebeed, M. and Nasrat, L.S., 2018, December. *Power Injection Models of HVDC and UPFC: A Comparison*. In 2018 Twentieth International Middle East Power Systems Conference (MEPCON) (pp. 767-772). IEEE.
33. Qiu, Y., Wu, H., Song, Y. and Wang, J., 2018. *Global approximation of static voltage stability region boundaries considering generator reactive power limits*. IEEE Transactions on Power Systems, 33(5), pp.5682-5691.
34. Nomula, G. and Ganesh, S.N.V., 2019. *Optimal Power Flow Analysis Using Facts Devices*. Think India Journal, 22(22), pp.71-79.
35. Simon, S.P., Kumar, K.A., Sundareswaran, K., Nayak, P.S.R. and Padhy, N.P., 2020. *Impact and economic assessment on solar PV mirroring system—A feasibility report*. Energy Conversion and Management, 203, p.112222.
36. Hernández-Callejo, L., 2019. *A comprehensive review of operation and control, maintenance and lifespan management, grid planning and design, and metering in smart grids*. Energies, 12(9), p.1630.
37. Gupta, A., Sharma, K.K. and Kaur, G., 2022. *Integrated Electric Power Systems and Their Power Quality Issues*. Power Electronics for Green Energy Conversion, pp.29-65.
38. Martins, A.S.C., de Araujo, L.R. and Penido, D.R.R., 2022. *Sensibility Analysis with Genetic Algorithm to Allocate Distributed Generation and Capacitor Banks in Unbalanced Distribution Systems*. Electric Power Systems Research, 209, p.107962.
39. Khare, C.J., Verma, H.K. and Khare, V., 2021. *Optimal power generation and power flow control using artificial intelligence techniques*. In Renewable Energy Systems (pp. 607-631). Academic Press.

40. Basu, J.B., Dawn, S., Saha, P.K., Chakraborty, M.R. and Ustun, T.S., 2022. *A Comparative Study on System Profit Maximization of a Renewable Combined Deregulated Power System*. Electronics, 11(18), p.2857.
41. Nguyen, T.T. and Mohammadi, F., 2020. *Optimal placement of TCSC for congestion management and power loss reduction using multi-objective genetic algorithm*. Sustainability, 12(7), p.2813.
42. Akbari, E., Ghasemi, M., Gil, M., Rahimnejad, A. and Andrew Gadsden, S., 2022. *Optimal Power Flow via Teaching-Learning-Studying-Based Optimization Algorithm*. Electric Power Components and Systems, 49(6-7), pp.584-601.
43. Jordehi, A.R., 2019. *Optimisation of demand response in electric power systems, a review*. Renewable and sustainable energy reviews, 103, pp.308-319.
44. Morshed, M.J. and Fekih, A., 2019. *A probabilistic robust coordinated approach to stabilize power oscillations in DFIG-based power systems*. IEEE Transactions on Industrial Informatics, 15(10), pp.5599-5612.
45. Salkuti, S.R. and Kim, S.C., 2019. *Congestion management using multi-objective glowworm swarm optimization algorithm*. Journal of Electrical Engineering & Technology, 14(4), pp.1565-1575.
46. Radhakrishnan, G. and Gopalakrishnan, V., 2020. *Applications of internet of things (IOT) to improve the stability of a grid connected power system using interline power flow controller*. Microprocessors and Microsystems, 76, p.103038.
47. Nagi, Baldeep Singh, and Gagandeep Kaur. *"Congestion management in deregulated power systems: a review."* In 2018 International Conference on Advances in Computing, Communication Control and Networking (ICACCCN), pp. 806-813. IEEE, 2018.
48. Kumar, B.V. and Ramaiah, V., 2020. *Enhancement of dynamic stability by optimal location and capacity of UPFC: A hybrid approach*. Energy, 190, p.116464.
49. Arif, M., Ahmad, F., Kashyap, R., Abdel-Galil, T.K., Othman, M.M., El-Amin, I. and Al-Mubarak, A., 2019. *Evaluation of EHV and AC/DC technologies for integration of large- scale renewable generation in Saudi Arabian network*. IET Generation, Transmission & Distribution, 13(4), pp.575-581.

50. Reddy, K.M.K., Rao, A.K. and Rao, R.S., 2022. *An improved Grey Wolf algorithm for optimal placement of unified power flow controller*. Advances in Engineering Software, 173, p.103187.
51. Thippana, V.C., Parimi, A.M. and Karri, C., 2020, December. *Placement of IPFC for Power Loss Reduction in Transmission lines using Firefly Algorithm*. In 2020 IEEE 17th India Council International Conference (INDICON) (pp. 1-6). IEEE.
52. Amarendra, A., Srinivas, L.R. and Rao, R.S., 2020. *Identification of the best location and size of IPFC to optimize the cost and to improve the power system security using Firefly optimization algorithm*. Materials Today: Proceedings.
53. Zhang, X., Shi, D., Wang, Z., Zeng, B., Wang, X., Tomsovic, K. and Jin, Y., 2018. *Optimal allocation of series FACTS devices under high penetration of wind power within a market environment*. IEEE Transactions on power systems, 33(6), pp.6206-6217.
54. Das, D., Bhattacharya, A. and Ray, R.N., 2020. *Dragonfly algorithm for solving probabilistic economic load dispatch problems*. Neural Computing and Applications, 32(8), pp.3029-3045.
55. Mahapatra, S., Malik, N., Raj, S. and Srinivasan, M.K., 2022. *Constrained optimal power flow and optimal TCSC allocation using hybrid cuckoo search and ant lion optimizer*. International Journal of System Assurance Engineering and Management, 13(2), pp.721-734.
56. Kyomugisha, R., Muriithi, C.M. and Edimu, M., 2021. *Multiobjective optimal power flow for static voltage stability margin improvement*. Heliyon, 7(12), p.e08631.
57. Abrishambaf, O., Lezama, F., Faria, P. and Vale, Z., 2019. *Towards transactive energy systems: An analysis on current trends*. Energy Strategy Reviews, 26, p.100418.
58. Nikam, R.A., 2020. *A novel hybrid approach for optimal reactive power dispatch under unbalanced conditions*. Journal of Computational Mechanics, Power System and Control, 3(4).
59. Kumar, A., Singh, J. and Sadhu, P.K., 2019, November. *A review of wind power generation utilizing statcom technology*. In IOP Conference Series: Materials Science and Engineering (Vol. 691, No. 1, p. 012016). IOP Publishing.

60. Jayabarathi, T., Raghunathan, T. and Gandomi, A.H., 2018. *The bat algorithm, variants and some practical engineering applications: A review*. Nature-inspired algorithms and applied optimization, pp.313-330.
61. Peddakapu, K., Mohamed, M.R., Srinivasarao, P., Veerendra, A.S., Kishore, D.J.K. and Leung, P.K., 2021. *Review on automatic generation control strategies for stabilising the frequency deviations in multi-area power system*. International Journal of Ambient Energy, pp.1-24.
62. Galvani, S., Mohammadi-Ivatloo, B., Nazari-Heris, M. and Rezaeian-Marjani, S., 2021. *Optimal allocation of static synchronous series compensator (SSSC) in wind-integrated power system considering predictability*. Electric Power Systems Research, 191, p.106871.
63. Wang, C., Ju, P., Wu, F., Pan, X. and Wang, Z., 2022. *A systematic review on power system resilience from the perspective of generation, network, and load*. Renewable and Sustainable Energy Reviews, 167, p.112567.
64. Pham, Q.B., Sammen, S.S., Abba, S.I., Mohammadi, B., Shahid, S. and Abdulkadir, R.A., 2021. *A new hybrid model based on relevance vector machine with flower pollination algorithm for phycocyanin pigment concentration estimation*. Environmental Science and Pollution Research, 28(25), pp.32564-32579.
65. Majidi, M. and Zare, K., 2018. *Integration of smart energy hubs in distribution networks under uncertainties and demand response concept*. IEEE Transactions on Power Systems, 34(1), pp.566-574.
66. Mugiira Kinoti, E., 2018. *Optimal Selection and Location of FACTS Devices for Enhancement of Power Transfer Capability using Bee Algorithm* (Doctoral dissertation, JKUAT-PAUSTI).
67. Wais,D.S., Majeed,W.S., *The gravitational search algorithm for incorporating TCSC devices into the system for optimum power flow*, International Journal of Electrical and Computer Engineering, vol. 11, no. 6, 2021,pp 4678-4688.
68. Sirjani, R., Mohamed,A., Shareef,H., *Optimal placement and sizing of Static Var Compensators in power system using Improved Harmony Search Algorithm*,Academia.

## APENDIX

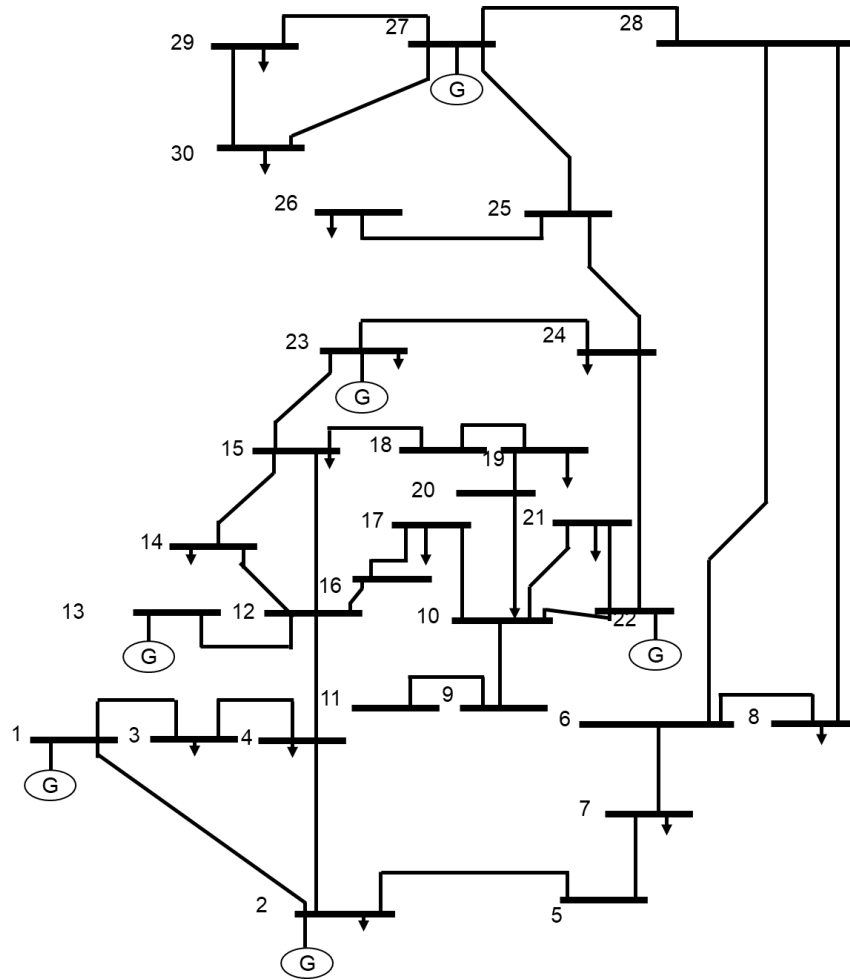


**Figure : IEEE -30 bus system modeling**

The system employs a base of 100 MVA power and comprises of 30 bus power. There are six producing units in this system; generating units 2, 13, 22, 23, and 27 operate as generator buses, while generating units 1 serves as a slack bus.

**TABLE: BUS DATA OF IEEE30 BUS SYSTEM**

| Bus No. | Bus type | Voltage Magnitude | Phase Angle | Generating     |                | Load           |                | Reactive power limit |                  |
|---------|----------|-------------------|-------------|----------------|----------------|----------------|----------------|----------------------|------------------|
|         |          |                   |             | P <sub>g</sub> | Q <sub>g</sub> | P <sub>l</sub> | Q <sub>l</sub> | Q <sub>max</sub>     | Q <sub>min</sub> |
| 1       | 1        | 1.06              | 0           | 0              | 0              | 0              | 0              | 0                    | 0                |
| 2       | 2        | 1.043             | 0           | 21.7           | 12.7           | 40             | 0              | -40                  | 50               |
| 3       | 3        | 1                 | 0           | 2.4            | 1.2            | 0              | 0              | 0                    | 0                |
| 4       | 3        | 1                 | 0           | 7.6            | 1.6            | 0              | 0              | 0                    | 0                |
| 5       | 2        | 1.01              | 0           | 94.2           | 19             | 0              | 0              | -40                  | 40               |
| 6       | 3        | 1                 | 0           | 0              | 0              | 0              | 0              | 0                    | 0                |
| 7       | 3        | 1                 | 0           | 22.8           | 10.9           | 0              | 0              | 0                    | 0                |
| 8       | 2        | 1.01              | 0           | 30             | 30             | 0              | 0              | -10                  | 40               |
| 9       | 3        | 1                 | 0           | 0              | 0              | 0              | 0              | 0                    | 0                |
| 10      | 3        | 1                 | 0           | 5.8            | 2              | 0              | 0              | 0                    | 0                |
| 11      | 2        | 1.082             | 0           | 0              | 0              | 0              | 0              | -6                   | 24               |
| 12      | 3        | 1                 | 0           | 12.2           | 7.5            | 0              | 0              | 0                    | 0                |
| 13      | 2        | 1.071             | 0           | 0              | 0              | 0              | 0              | -6                   | 24               |
| 14      | 3        | 1                 | 0           | 6.2            | 1.6            | 0              | 0              | 0                    | 0                |
| 15      | 3        | 1                 | 0           | 8.2            | 2.5            | 0              | 0              | 0                    | 0                |
| 16      | 3        | 1                 | 0           | 3.5            | 1.8            | 0              | 0              | 0                    | 0                |
| 17      | 3        | 1                 | 0           | 9              | 5.8            | 0              | 0              | 0                    | 0                |
| 18      | 3        | 1                 | 0           | 3.5            | 0.9            | 0              | 0              | 0                    | 0                |
| 19      | 3        | 1                 | 0           | 9.5            | 3.5            | 0              | 0              | 0                    | 0                |
| 20      | 3        | 1                 | 0           | 2.2            | 0.7            | 0              | 0              | 0                    | 0                |
| 21      | 3        | 1                 | 0           | 17.5           | 11.2           | 0              | 0              | 0                    | 0                |
| 22      | 3        | 1                 | 0           | 0              | 0              | 0              | 0              | 0                    | 0                |
| 23      | 3        | 1                 | 0           | 3.2            | 1.6            | 0              | 0              | 0                    | 0                |
| 24      | 3        | 1                 | 0           | 8.7            | 6.7            | 0              | 0              | 0                    | 0                |
| 25      | 3        | 1                 | 0           | 0              | 0              | 0              | 0              | 0                    | 0                |
| 26      | 3        | 1                 | 0           | 3.5            | 2.3            | 0              | 0              | 0                    | 0                |
| 27      | 3        | 1                 | 0           | 0              | 0              | 0              | 0              | 0                    | 0                |
| 28      | 3        | 1                 | 0           | 0              | 0              | 0              | 0              | 0                    | 0                |
| 29      | 3        | 1                 | 0           | 2.4            | 0.9            | 0              | 0              | 0                    | 0                |
| 30      | 3        | 1                 | 0           | 10.6           | 1.9            | 0              | 0              | 0                    | 0                |

**TABLE: LINE DATA OF IEEE30 BUS SYSTEM**

| <b>From bus</b> | <b>To bus</b> | <b>R (pu)</b> | <b>X (pu)</b> | <b>B (pu)</b> | <b>Tap Ratio</b> |
|-----------------|---------------|---------------|---------------|---------------|------------------|
| 1               | 2             | 0.0192        | 0.0575        | 0.0264        | 1                |
| 1               | 3             | 0.0452        | 0.1852        | 0.0204        | 1                |
| 2               | 4             | 0.057         | 0.1737        | 0.0184        | 1                |
| 3               | 4             | 0.0132        | 0.0379        | 0.0042        | 1                |
| 2               | 5             | 0.0472        | 0.1983        | 0.0209        | 1                |
| 2               | 6             | 0.0581        | 0.1763        | 0.0187        | 1                |
| 4               | 6             | 0.0119        | 0.0414        | 0.0045        | 1                |
| 5               | 7             | 0.046         | 0.116         | 0.0102        | 1                |
| 6               | 7             | 0.0267        | 0.082         | 0.0085        | 1                |
| 6               | 8             | 0.012         | 0.042         | 0.0045        | 1                |
| 6               | 9             | 0             | 0.208         | 0             | 0.978            |
| 6               | 10            | 0             | 0.556         | 0             | 0.969            |
| 9               | 11            | 0             | 0.208         | 0             | 1                |
| 9               | 10            | 0             | 0.11          | 0             | 1                |
| 4               | 12            | 0             | 0.256         | 0             | 0.932            |
| 12              | 13            | 0             | 0.14          | 0             | 1                |
| 12              | 14            | 0.1231        | 0.2559        | 0             | 1                |
| 12              | 15            | 0.0662        | 0.1304        | 0             | 1                |
| 12              | 16            | 0.0945        | 0.1987        | 0             | 1                |
| 14              | 15            | 0.221         | 0.1997        | 0             | 1                |
| 16              | 17            | 0.0824        | 0.1923        | 0             | 1                |
| 15              | 18            | 0.1073        | 0.2185        | 0             | 1                |
| 18              | 19            | 0.0639        | 0.1292        | 0             | 1                |
| 19              | 20            | 0.034         | 0.068         | 0             | 1                |
| 10              | 20            | 0.0936        | 0.209         | 0             | 1                |
| 10              | 17            | 0.0324        | 0.0845        | 0             | 1                |
| 10              | 21            | 0.0348        | 0.0749        | 0             | 1                |
| 10              | 22            | 0.0727        | 0.1499        | 0             | 1                |
| 21              | 23            | 0.0116        | 0.0236        | 0             | 1                |
| 15              | 23            | 0.1           | 0.202         | 0             | 1                |
| 22              | 24            | 0.115         | 0.179         | 0             | 1                |
| 23              | 24            | 0.132         | 0.27          | 0             | 1                |
| 24              | 25            | 0.1885        | 0.3292        | 0             | 1                |
| 25              | 26            | 0.2544        | 0.38          | 0             | 1                |
| 25              | 27            | 0.1093        | 0.2087        | 0             | 1                |
| 28              | 27            | 0             | 0.396         | 0             | 0.968            |
| 27              | 29            | 0.2198        | 0.4153        | 0             | 1                |
| 27              | 30            | 0.3202        | 0.6027        | 0             | 1                |
| 29              | 30            | 0.2399        | 0.4533        | 0             | 1                |
| 8               | 28            | 0.0636        | 0.2           | 0.0214        | 1                |
| 6               | 28            | 0.0169        | 0.0599        | 0.0065        | 1                |

